DEVELOPMENT OF NOVEL IMMOBILIZATION MATRICES VIA SURFACE MODIFICATION APPROACH FOR GLUCOSE DETECTION AND THEIR BIOSENSOR APPLICATIONS

A THESIS SUBMITTED TO
THE GRADUATE SCHOOL OF NATURAL AND APPLIED SCIENCES
OF
MIDDLE EAST TECHNICAL UNIVERSITY

BY

SEMA DEMİRCİ UZUN

IN PARTIAL FULFILLMENT OF THE REQUIREMENTS
FOR
THE DEGREE OF DOCTOR OF PHILOSOPHY
IN
POLYMER SCIENCE AND TECHNOLOGY

FEBRUARY 2014

Approval of the thesis

DEVELOPMENT OF NOVEL IMMOBILIZATION MATRICES *VIA* SURFACE MODIFICATION APPROACH FOR GLUCOSE DETECTION AND THEIR BIOSENSOR APPLICATIONS

submitted by **SEMA DEMİRCİ UZUN** in partial fulfillment of the requirements for the degree of **Doctor of Philosophy in Polymer Science and Technology Department, Middle East Technical University** by,

Prof. Dr. Canan Özgen

Dean, Graduate School of **Natural and Applied Sciences** _____

Prof. Dr. Teoman Tinçer

Head of Department, **Polymer Science and Technology Dept.** _____

Prof. Dr. Levent Toppare

Supervisor, **Chemistry Dept., METU** _____

Prof. Dr. Suna Timur

Co-Supervisor, **Biochemistry Dept., Ege University** _____

Examining Committee Members:

Prof. Dr. Cihangir Tanyeli _____
Chemistry Dept., METU

Prof. Dr. Levent K. Toppare** _____
Chemistry Dept., METU

Assoc. Prof. Dr. Yasemin Arslan Udum _____
Advanced Tech. Dept., Gazi University

Assoc. Prof. Dr. Ali Çırpan _____
Chemistry Dept., METU

Assist. Prof. Dr. Emren Nalbant Esentürk _____
Chemistry Dept., METU

Date: 07.02.2014

I hereby declare that all information in this document has been obtained and presented in accordance with academic rules and ethical conduct. I also declare that, as required by these rules and conduct, I have fully cited and referenced all material and results that are not original to this work.

Name, Last name: SEMA DEMİRCİ UZUN

Signature :

ABSTRACT

DEVELOPMENT OF NOVEL IMMOBILIZATION MATRICES
VIA SURFACE MODIFICATION APPROACH FOR GLUCOSE DETECTION
AND THEIR BIOSENSOR APPLICATIONS

Demirci Uzun, Sema

Ph. D., Department of Polymer Science and Technology

Supervisor: Prof. Dr. Levent Toppare

Co- Supervisor: Prof. Dr. Suna Timur

February 2014, 128 pages

Biosensors which include biorecognition element and the transducer are widely used devices in many research areas. In an electrochemical biosensor construction, immobilization of redox enzymes on conductive surfaces is a crucial step to obtain stable electrodes. The use of conducting polymers as appropriate immobilization matrices for biomolecules leads to the improvement of biosensors as economical tools for clinical and pharmaceutical analyses. In that manner, electrically conducting polymers can be deposited on an electrode surface as immobilization matrices for biomolecules to enhance stability, sensitivity and efficient electron transfer ability of biosensors. Also, electropolymerization enables easy control over the several properties such as morphology and thickness. Furthermore, their chemical functionalization offers a better microenvironment for biomolecules and electrochemical transduction of biological events.

In this thesis, it is aimed to create conducting polymer based new immobilization matrices providing high stability, sensitivity and electron transfer ability for glucose detection. Recently synthesized poly(2-(2,5-di(thiophen-2-yl)-1H-pyrrol-1-yl) (SNS) acetic acid) and 4-(4,7-di(thiophen-2-yl)-1H-benzo[d]imidazol-2- yl) benzaldehyde (BIBA) were electrochemically deposited on graphite electrodes. SNS acetic acid polymer was functionalized with lysine (Lys) amino acid and poly(amidoamine)

derivatives (PAMAM G2 and PAMAM G4) to investigate their matrix properties for biosensor applications. Glucose oxidase (GOx) was immobilized onto the modified surface as the model enzyme. X-Ray photoelectron spectroscopy (XPS) and atomic force microscopy (AFM) were used to report the surface properties of the matrices in each step of the biosensor construction. The biosensors were characterized in terms of their operational and storage stabilities and the kinetic parameters (K_m^{app} and I_{max}). Three new glucose biosensors revealed good stability, promising low detection limit and prolonged the shelf lives. The proposed biosensors were tested for glucose detection on real human blood serum samples.

To develop different immobilization matrices, glucose oxidase (GOx) was immobilized as a model enzyme on PBIBA polymer coated graphite electrode with the help of glutaraldehyde (GA). Besides non-modified PBIBA biosensor, other electrode surfaces were modified with gold nanorods (AuNRs) and single-walled carbon nano tubes (SWCNTs) to enhance sensitivity and electron transfer ability of desired biosensors. The surface characterization and morphology were investigated to confirm bioconjugation by X-ray photoelectron spectroscopy (XPS) and transmission electron microscopy (TEM) at each step of biosensor fabrication. Three new optimized biosensors show good linearity and low limit of detection (LOD) values. Kinetic parameters K_m^{app} and I_{max} were also determined for each biosensor. Furthermore, biosensors were tested for real samples.

Keywords: Conducting polymers, biosensors, glucose detection, surface modification, glucose oxidase.

ÖZ

GLUKOZ TAYİNİ İÇİN YENİ İMMOBİLİZASYON MATRİSLERİNİN YÜZEY MODİFİKASYONU YAKLAŞIMI İLE GELİŞTİRİLMESİ VE BİYOSENSÖR UYGULAMALARI

Demirci Uzun, Sema

Doktora, polimer Bilimi ve Teknolojisi Bölümü

Tez Yöneticisi: Prof. Dr. Levent Toppare

Ortak Tez Yöneticisi: Prof. Dr. Suna Timur

Şubat 2014, 128 sayfa

Biyotanıma elemanı ve transduser içeren biyosensörler birçok araştırma alanında yaygın olarak kullanılan cihazlardır. Elektrokimyasal biyosensör oluşturulmasında, redoks enzimlerinin iletken yüzeylere tutuklanması, kararlı elektrotlar elde etmek için önemli bir basamaktır. İletken polimerlerin biyomoleküller için uygun tutuklama yüzeyleri olarak kullanımları, biyosensörlerin klinik ve farmasötik analizler için ekonomik araçlar olarak geliştirilmesine öncülük etmektedir. Bu bağlamda, elektriksel iletken polimerler, biyomoleküllerin tutuklama matrisleri olarak biyosensörlerin kararlılığı, duyarlılığı ve etkin elektron transferi için elektrot yüzeylerine kaplanabilirler. Ayrıca elektropolimerizasyon morfoloji ve kalınlık gibi çeşitli yüzey özelliklerinin kolayca kontrol edilebilmesine olanak sağlamaktadır. Buna ek olarak, polimerlerin kimyasal olarak fonksiyonlandırılması biyomoleküller ve biyolojik olayların elektrokimyasal bilgi aktarımı için daha iyi bir mikro çevre sağlar.

Bu tezde, iletken polimer tabanlı yüksek kararlılık, duyarlılık ve elektron transferi saplayan yeni tutuklama yüzeylerinin üretilmesi amaçlanmıştır. Bu amaçla sentezlenen poli(2-(2,5-di(tiyofen-2-il)-1H-pirol-1-il) (SNS) asetik asit) ve 4-(4,7-

di(tiyofen-2-il)-1H-benzo[d]imidazol-2- il)benzaldehit (PBIBA) grafit elektrotlar üzerine elektrokimyasal olarak kaplandı. SNS asetik asit polimeri, biyosensör uygulamalarında matris özelliklerinin araştırılması için Lisin amino asidi ve PAMAM türevleri (PAMAM G2 ve PAMAM G4) ile fonksiyonlandırıldı. Glukoz oksidaz modifiye edilmiş yüzeyler üzerine model enzim olarak tutuklandı. X-Işını spektroskopisi ve atomik güç mikroskobu, biyosensör oluşturulmasındaki her basamakta yüzey özelliklerini belirlemek için kullanıldı. Biyosensörler operasyonel ve depolama kararlılığı ve kinetik parametreler açısından karakterize edildi. Üç yeni glukoz biyosensörü iyi kararlılık, umut verici düşük tayin limiti ve uzun raf ömrü gösterdi. Söz konusu biyosensörler insan kanı serum örneklerindeki glukoz tayini için test edildi.

Farklı tutuklama matrisleri geliştirmek için glukoz oksidaz glteraldehit yardımıyla model enzim olarak grafit elektrot yüzeyine kaplanan PBIBA üzerine tutuklandı. Fonksiyonlandırılmamış PBIBA'nın yanı sıra, diğer elektrot yüzeyleri hedeflenen biyosensörlerin duyarlılığı ve elektron transfer yeteneğini arttırmak için altın nano çubuklar ve tek duvarlı karbon nano tüplerle modifiye edildi. Biyobağlanmayı kanıtlamak için yüzey karakterizasyonu ve morfolojisi, biyosensör oluşturulmasının her basamağında X-ışını spektrofotometresi ve geçişli elektron mikroskobu ile incelendi. Üç yeni optimum elektrot iyi bir doğrusallık ve düşük tayin limiti gösterdi. Kinetik parametreler K_m^{app} ve I_{max} her bir biyosensör için belirlendi. Ayrıca biyosensörler gerçek örnekler için test edildi.

Anahtar Kelimeler: İletken polimerler, biyosensörler, glukoz tayini, yüzey modifikasyonu, glukoz oksidaz.

To My Precious Parents, Sister and Husband

ACKNOWLEDGMENTS

I would like to express my sincere appreciations to my supervisor Prof. Dr. Levent Toppare for his diligent guidance, advice, endless patience and enthusiasm for science. I am grateful to him not only scientific instructions but also his valuable contributions all steps of real life.

I would like to express my deepest gratitude to my co-advisor Prof. Dr. Suna Timur for her endless support, valuable guidance, precious ideas and motivation for science.

I would like to give my special thanks to Dr. Fatma Bilge Emre for sharing her knowledge on biosensors, guidance and motivation during my studies and real friendship.

I would like to thank Prof. Dr. Ruşen Geçit for his valuable support throughout my PhD works, holding my hand and taking me from darkness of others to my brightness inside. I feel deepest appreciations to him for giving me a road with his precious advice.

I owe great thanks to Prof. Dr. Cihangir Tanyeli for his invaluable advices for the experiments and contributions to my organic chemistry knowledge, always believing in me, support and valuable encouragement. I am so grateful to him for being like my friend whenever I need and contributions to my road with his priceless conversations.

I owe my thanks to Assist. Prof. Dr. Emren Nalbant Esentürk for her invaluable collaboration throughout surface modification studies with nano particles, interesting scientific ideas, patience and kind support.

I want to express my sincere thanks to Naime Akbaşoğlu Ünlü and Şerife Özdemir Hacıoğlu for their endless help whenever I need, always believing in me, supports, patience, scientific cooperation besides kind friendship with enjoyable coffee-break memories that I always want to remember and laugh.

I want to give many thanks to Eda Rende and Cihan Efe Kılıç for the great friendship, endless laughs, help, discussions and all columns, work-ups, TLCs throughout working 20 hours a day with Eda Rende.

I owe great thanks to Funda Oğuzkaya, Naime Akbaşoğlu Ünlü, Gözde Öktem for monomer design collaborations, Merve Şendur for electrochemical and spectroelecrochemical studies, Duygu Kozanoğlu for gold nano rods synthesis, Cansel Temiz for contact angle measurements and Fulya Ekiz Kanik for her help at the initial step of biosensor construction and their all kind friendships.

I want to thank Aysel Kızıltay for running HRMS, Tuğba Endoğan for TEM images, Betül Eymür for NMR spectra and their all cheerful friendships. I want to give many thanks to İbrahim Çam for AFM images.

I would like to thank all Toppare Research Group for their collaborations and kind friendships.

I would like to present my appreciation to Yasemin Altun for being my sister. It would not be possible to overcome difficulties without her. We have survived many things that life throws our way during six years.

I owe to my deepest thanks to Ezgi Yavuz for being so cute, our secrets, listening me every time with her endless patience, all breakfasts, lunches, dinners and also coffe-breaks.

I want to thank all my roommates Tuğba Efe, Nazmiye Yapıcı, Aysel Kızıltay, Açalya Alpan, Gonca Tunçbilek, Tuğba Dursun, Hatice Çoban at 205 for their real friendships, supports, laughs, giving to my life more fun and being my big family.

I want to express my great thanks to my father in law, Dr. Abdurrahman Uzun, for financial support and his valuable encouragement during my PhD works.

Words fail to express my eternal gratitude to my dear parents and sister for their insistently support, endless love, always believing in me and motivation during all my life. I am grateful to them for their financial support during my entire career and every single thing makes me stronger.

I want to express my sincere thanks to my husband, Kayahan Uzun, for his patience, great love, always encouraging me and never let me alone despite hundreds of miles away. I also would like to express my great attitude to him for being my best friend besides his everlasting love and always supporting me whoever I am.

Finally, I would like to thank METU Chemistry Department for supporting research.

TABLE OF CONTENTS

ABSTRACT v

ÖZ vii

ACKNOWLEDGMENTS x

LIST OF FIGURES xix

LIST OF TABLES xxiii

ABBREVIATIONS xxiv

CHAPTER 1 1

1. INTRODUCTION 1

1.1 Conducting Polymers 1

1.1.1 Conduction Mechanism in Conjugated Polymers: Doping Process 3

1.1.2 Band Theory 5

1.2 Polymerization Methods 7

1.2.1 Chemical Polymerization 8

1.2.2 Electrochemical Polymerization 11

1.3 Applications of Conducting Polymer 13

1.4 Biosensors 14

1.4.1 Electrochemical Transducers 16

1.4.1.1 Evolution of Amperometric Biosensors 16

1.4.2 Immobilization Techniques 21

1.4.2.1 Physical Adsorption 23

1.4.2.2 Entrapment 24

1.4.2.3 Crosslinking 26

1.4.2.4 Covalent Binding 27

1.5 Biosensor Applications 28

1.5.1 Glucose Biosensors 30

1.6 Conducting Polymers in Biosensing 31

1.7 Surface Modifications for Immobilization Matrices 34

1.8 Aim of the Work 35

CHAPTER 2 37

2. EXPERIMENTAL 37

2.1 Materials 37

2.2 Equipment 38

2.3 Procedures 39

2.3.1 Synthesis of Synthesis of 2-(2,5-di(thiophen-2-yl)-1H-pyrrol-1-yl) acetic acid (3) 39

2.3.2 Synthesis of BIBA Monomer 40

2.3.2.1 Synthesis of 4-(4,7-dibromo-1H-benzo[d]imidazol-2-yl) benzaldehyde (6) 40

2.3.2.2 Synthesis of 4-(4,7-di(thiophen-2-yl)-1H- benzo[d]imidazol-2-yl)benzaldehyde (BIBA) 40

2.3.3 Electrochemical Polymerization of Monomers 42

2.3.3.1 Electropolymerization of SNS Anchored Acetic Acid Monomer 42

2.3.3.2 Electropolymerization of BIBA monomer 42

2.3.4 Spectroelectrochemistry Experiments of PBIBA Polymer 42

2.3.5 Construction of Biosensor 43

2.3.5.1 SNS Anchored Acetic Acid Polymer Based Biosensors Construction 43

2.3.5.1.1 Lysine Modified Biosensor Construction 43

2.3.5.1.2 PAMAM G2 and G4 Modified Biosensors Construction 44

2.3.5.2 PBIBA Polymer Based Biosensors Construction 45

2.3.5.2.1 Non-Modified PBIBA Polymer Biosensor Construction 45

2.3.5.2.2 Gold Nanorods (AuNRs) Modified Biosensor Construction .. 46

2.3.5.2.3 Single-Walled Carbon Nanotubes (SWCNT) Modified Biosensor Construction 46

2.3.6 Amperometric Measurements 48

2.3.7 Optimization Studies for Biosensors 48

2.3.7.1 Effect of Polymer Thickness on the Surface 48

2.3.7.2 Effect of the Modification Materials Amounts 49

2.3.7.3 Effect of Enzyme Amount 49

2.3.7.4 Effect of Crosslinker Amount 49

2.3.7.5 Effect of pH 50

2.3.8 Determination of Analytic Characteristics for Biosensors 50

2.3.8.1 Determination of Kinetic Parameters 50

2.3.8.2 Operational and Storage Stabilities 51

2.3.9 Sample Applications 51

2.3.9.1 Sample Applications Using Lysine, PAMAM G2 and G4 Modified SNS-anchored Acetic Acid Based and PBIBA Based Biosensors 51

2.3.9.2 Sample Applications Using AuNRs and SWCNT Modified PBIBA Based Biosensors 52

CHAPTER 3 53

3. RESULTS AND DISCUSSIONS 53

3.1 Poly-SNS-anchored Acetic Acid Based Glucose Biosensors 53

3.1.1 Electropolymerization of the Monomer 53

3.1.2 Optimization Studies of Poly-SNS-anchored Carboxylic Acid Based Biosensors 55

3.1.2.1 Effect of Polymer Thickness on the Surface 55

3.1.2.2 Effect of Lysine, PAMAM G2 and PAMAM G4 Amounts 57

3.1.2.3 Effect of Biomolecule Amount 58

3.1.2.4 Effect of Glutaraldehyde Amount 60

3.1.2.5 Effect of pH 61

3.1.3 Surface Characterization 62

3.1.3.1 X-Ray Photoelectron Spectroscopy (XPS) 62

3.1.3.2 Atomic Force Microscopy (AFM) 70

3.1.4 Analytical Characterization of Corresponding Biosensors 75

3.1.5 Operational and Storage Stabilities 79

3.1.6 Sample Applications 79

3.2 PBIBA Based Glucose Biosensors 80

3.2.1 Synthesis of BIBA Monomer 80

3.2.2 Electrochemical Polymerization of the Monomer 81

3.2.3 Electrochemical and Spectroelectrochemical Properties 82

3.2.4 Optimization Studies for Biosensors (PBIBA, Au-modified PBIBA and SWCNT-modified PBIBA) 85

3.2.4.1 Effect of Polymer Thickness on the Surface 85

3.2.4.2 Effect of Biomolecule Amount 87

3.2.4.3 Effect of Crosslinker (GA) Amount 88

3.2.4.4 Effect of pH 89

3.2.5 Surface Characterization of Constructed Biosensors 90

3.2.5.1 X-Ray Photoelectron Spectroscopy (XPS) 90

3.2.5.2 Transmission Electron Microscopy (TEM) 93

3.2.5.3 Contact Angle Measurements 97

3.2.6 Analytical Characterization 98

3.2.7 Sample Applications 102

3.2.7.1 Sample Application of Non-Modified PBIBA Based Biosensor .. 102

3.2.7.2 Sample Applications of Modified Biosensors 103

CHAPTER 4 105

4. CONCLUSION 105

REFERENCES 107

APPENDIX A 121

NMR DATA.....121

CURRICULUM VITAE 127

LIST OF FIGURES

FIGURES

Figure 1. 1 Cis- and trans- isomers of polyacetylene 1

Figure 1. 2 Chemical structures of some common conjugated polymers 3

Figure 1. 3 Reversible doping-dedoping process of PTh 4

Figure 1. 4 Band structures of insulator, semiconductor and conductor 5

Figure 1. 5 The charge carries and their related band gaps in PPy 6

Figure 1. 6 Generation of band structures in PAc due to increase in conjugation 7

Figure 1. 7 Chemical oxidative polymerization mechanism of 3-alkyl substituted thiophene 8

Figure 1. 8 Synthesis of PTh *via* a) Yamamoto coupling b) Kumada coupling c) Lin & Dudek coupling 9

Figure 1. 9 Catalytic cycle of Stille reaction 10

Figure 1. 10 Electrochemical polymerization mechanism of thiophene 12

Figure 1. 11 Schematic representation of a biosensor 14

Figure 1. 12 Types of biosensors 15

Figure 1. 13 The oxygen electrode 18

Figure 1. 14 The working principle of second generation biosensors 19

Figure 1. 15 The working principle of third generation biosensors 20

Figure 1. 16 The working principle of adsorbed enzyme 24

Figure 1. 17 The representative illustration of a biosensor constructed *via* entrapment method 26

Figure 1. 18 The representative scheme of enzyme immobilization *via* crosslinking 27

Figure 1. 19 The representative scheme of enzyme immobilization *via* covalent binding..... 28

Figure 1. 20 The reaction mechanism of GOx 31

Figure 2. 1 Synthesis of SNS-anchored acetic acid monomer (3)..... 39

Figure 2. 2 Synthetic pathway of BIBA monomer..... 41

Figure 2. 3 Schematic representation of the surface modifications 45

Figure 2. 4 Preparation of surface modified PBIBA based biosensors 47

Figure 3.1 Repeated potential-scan electropolymerization of SNS-anchored carboxylic acid at 0.1 V s^{-1} in 0.1M ACN/$NaClO_4$/$LiClO_4$ solvent/electrolyte system on graphite electrode (up to 20 cycles). 54

Figure 3. 2 Effect of scan number on biosensor responses (in 50 mM sodium acetate buffer, pH 5.5, 25 ^oC, -0.7 V). The corresponding measurements were performed with 0.75 mM glucose. Error bars show the standard deviation (SD) of three measurements. 56

Figure 3. 3 Effect of biomolecule amount on a) Lys modified b) PAMAM G2 and PAMAM G4 modified biosensors (in 50 mM sodium acetate buffer, pH 5.5, 25 ^oC, -0.7 V). The corresponding measurements were performed with 0.75 mM glucose. Error bars show the standard deviation (SD) of three measurements. 59

Figure 3. 4 Effect of crosslinker (glutaraldehyde) amount on biosensor responses (in 50 mM sodium acetate buffer, pH 5.5, 25 ^oC, -0.7 V). The corresponding

measurements were performed with 0.40 mM glucose. Error bars show the standard deviation (SD) of three measurements. 61

Figure 3. 5 Effect of pH at 25 ^{o}C, -0.7 V. The measurements were performed with 0.40 mM glucose. Error bars show the standard deviation (SD) of three measurements. 62

Figure 3. 6 C1s and N1s XPS spectra of polymer-coated electrode (a,b), Lys, PAMAM G2, PAMAM G4-modified polymer-coated surfaces (c,d; g,h; k,l) and GOx immobilized surfaces on polymer-coated modified surfaces (e,f; i,j; m,n), respectively. 70

Figure 3. 7 3-D topographic AFM height images of Lys-, PAMAM G2-, PAMAM G4-modified polymer-coated electrode surface before (a,c,e) and after (b,d,f) biomolecule (GOx) immobilization at the optimized conditions, respectively. 74

Figure 3. 8 Calibration curve for glucose (in 50 mM sodium acetate buffer, pH 5.5, 25 ^{o}C, -0.7 V). Error bars show standard deviation (SD) of three measurements. ... 75

Figure 3. 9 A characteristic biosensor response of polymer/PAMAM G4-modified biosensor to glucose (in 50 mM sodium acetate buffer, pH 5.5, 25 ^{o}C, -0.7 V, [Glc]; 0.75 mM). 76

Figure 3. 10 Cyclic voltammogram of polymerization in a DCM/ACN (5:95 v:v)/ 0.1 M $LiClO_4$/$NaClO_4$ (1:1 mol) solvent-electrolyte couple. 81

Figure 3. 11 Single scan voltammogram of PBIBA in ACN/$LiClO_4$/$NaClO_4$ solution 82

Figure 3. 12 a) Scan rate dependence of PBIBA b) Linear relationship between scan rate and current density for PBIBA at 50, 100, 200, 300, 400 and 500 mVs^{-1}.. 83

Figure 3. 13 a) Electronic absorption spectra for PBIBA upon p doping between 0.0 V and 1.6 V in a monomer free solution b) Colors of PIBA at its neutral (0.0 V) and different oxidized states. 84

Figure 3. 14 Change of % transmittance and switching time of the polymer at 480 and 710 nm. 85

Figure 3. 15 Effect of scan number during electropolymerization on the biosensor responses (in sodium acetate buffer, 50 mM, pH 5.5, 25 ºC, -0.7 V). Error bars show standard deviations. 87

Figure 3. 16 Effect of loaded GOx amounts on biosensors responses (in sodium acetate buffer, 50 mM, pH 5.5, 25 ºC, -0.7 V). Error bars show standard deviations. 88

Figure 3. 17 Effect of gluteraldehyde (GA) amount on biosensors responses (in sodium acetate buffer, 50 mM, pH 5.5, 25 ºC, -0.7 V). Error bars show standard deviations. 89

Figure 3. 18 Effect of pH on biosensors responses (in sodium acetate buffer, 50 mM, pH 5.5, 25 ºC, -0.7 V). Error bars show standard deviations. 90

Figure 3. 19 (a) C1s and (b) N1s XPS spectra of the polymer surface. 92

Figure 3. 20 (a) C1s and (b) N1s XPS spectra of protein immobilized onto the polymer surface. ..... **Hata! Yer işareti tanımlanmamış.**

Figure 3. 21 TEM images of polymer (a) before and (b) after biomolecule immobilization under optimized conditions. 94

Figure 3. 22 TEM images of AuNRs modified polymer surfaces (a) before and (b) after biomolecule immobilization 95

Figure 3. 23 TEM images of SWCNT modified polymer surfaces (a) before and (b) after biomolecule immobilization. 97

LIST OF TABLES

TABLES

Table 1. 1 Characteristics of conducting polymer based biosensors..... 32

Table 3. 1 Comparison of biosensors examples of GOx (NR: Not Reported, TW: This Work)..... 78

Table 3. 2 Comparison of the constructed biosensors for glucose analysis in the serum samples..... 80

ABBREVIATIONS

ACN	Acetonitrile
AFM	Atomic force microscope
AuNRs	Gold nanorods
BT	Benzo[*c*]thiophene
CB	Conduction band
CNTs	Carbon nanotubes
CP	Conducting Polymer
DCM	Dichloromethane
ECDs	Electrochromic devices
EDC	N-(3-Dimethylaminopropyl)-N'-ethylcarbodiimide hydrochloride
Eg	Band gap
GA	Glutaraldehyde
GOx	Glucose oxidase
HOMO	High Occupied Molecular Orbital
HRMS	High resolution mass spectrometer
ITO	Indium tinoxide
LED	Light emitting diodes
LOD	Limit of detection
LUMO	Low Occupied Molecular Orbital
Lys	Lysine

MWCNT Multiwalled carbon nanotubes

NHS N-hydroxysuccinimide

NR Not reported

PA Polyaniline

PAc Polyacetylene

PAMAM Polyamidoamine

PATh Polyalkylthiophene

PBIBA Poly-4-(4,7-di(thiophen-2-yl)-1H-benzo[d]imidazol-2-yl) benzaldehyde

PCz Polycarbazole

PDTT Polyditihienothiophene

PEDOT Poly(2,3-dihydrothieno[3,4-b][1,4]dioxine)

PF Polyfuran

PFO Polyfluorene

PP Polyphenylene

PPB Poly-1-ynylbenzene

PproDOT Poly(3,4-dihydro-2*H*-thieno[3,4-*b*][1,4]dioxepine

PPV Polyphenylenevinylene

PPy Polypyrrole

PSe Polyselenophene

PTh Polythiophene

SAMs Self assembled monolayers

SN	Sulphur Nitride
SWCNT	Singlewalled carbon nanotubes
TEM	Transmission electron microscope
TW	This work
VB	Valence band
XPS	X-Ray photoelectron spectroscopy

CHAPTER 1

1. INTRODUCTION

1.1 Conducting Polymers

Conducting polymers (CPs) are intelligent macromolecular systems having conjugated π electrons in their backbone. Their first report in the literature was back in 1862 when Letheby was achieved the electrochemically oxidation of aniline in sulphuric acid solution [1]. This new macromolecule, probably polyaniline, was a partially conductive material. In 1973, the inorganic polymer of sulphur nitride $(SN)_x$ was discovered as a highly conducting molecule with 10^3 S cm^{-1} conductivity at room temperature [2]. However, this material had very limited application due to its highly explosive property. Polyacetylene (PAc), well-known conducting polymer, was developed as black powder, insoluble and air-sensitive material using $Et_3Al/Ti(OPr)_4$ (Et=ethyl, Pr=propyl) by Natta and co-workers in 1958 [3]. In the early 1970s, Shirakawa *et al*. investigated the effects of concentrated catalyst solution on this coordination polymerization. During these experiments, a silvery well-defined PAc film was successfully synthesized using nearly thousand times of catalyst by mistake. Both copper colored film of *cis*-PAc and silvery colored film of *trans*-PAc were synthesized and their conductivities were measured as 10^{-8} -10^{-7} Scm^{-1} for *cis*-PAc and 10^{-3}-10^{-2} Scm^{-1} for *trans*-PAc by Shirakawa and co-workers [4] (Fig. 1.1).

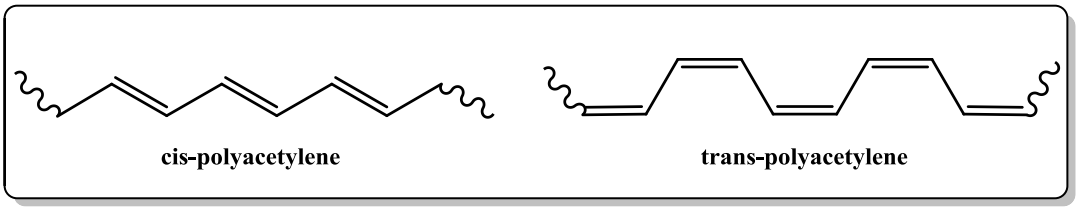

Figure 1. 1 Cis- and trans- isomers of polyacetylene

Alan Heeger and Alan MacDiarmid were in a collaboration on identifying $(SN)_x$ type polymers' conductivity when Shirakawa visited them at University of Pennsylvania. Then, they exposed the polyacetylene film to halogens and reported the enhancement in conductivity. Iodine exposured trans-polyacetylene showed the conductivity of 3000 Scm^{-1} that was eleven orders of magnitude increase over undoped polyacetylene [5,6]. Thus, the major contribution to the conductivity research of plastics belongs to Hideki Shirakawa, Alan J. Heeger and Alan G. MacDiarmid who were awarded with Nobel Prize in Chemistry in 2000. This magnificent breakthrough allowed developing new stable and processable materials that have high conductivity upon doping process. For example, the electrochemical synthesis of conductive polypyrrole was carried out by Diaz *et al.* in 1979 [7]. The synthesis of aromatic and heterocyclic macromolecules triggered a new challenging research area studied by material scientist over three decades [8-11] (Fig. 1.2).

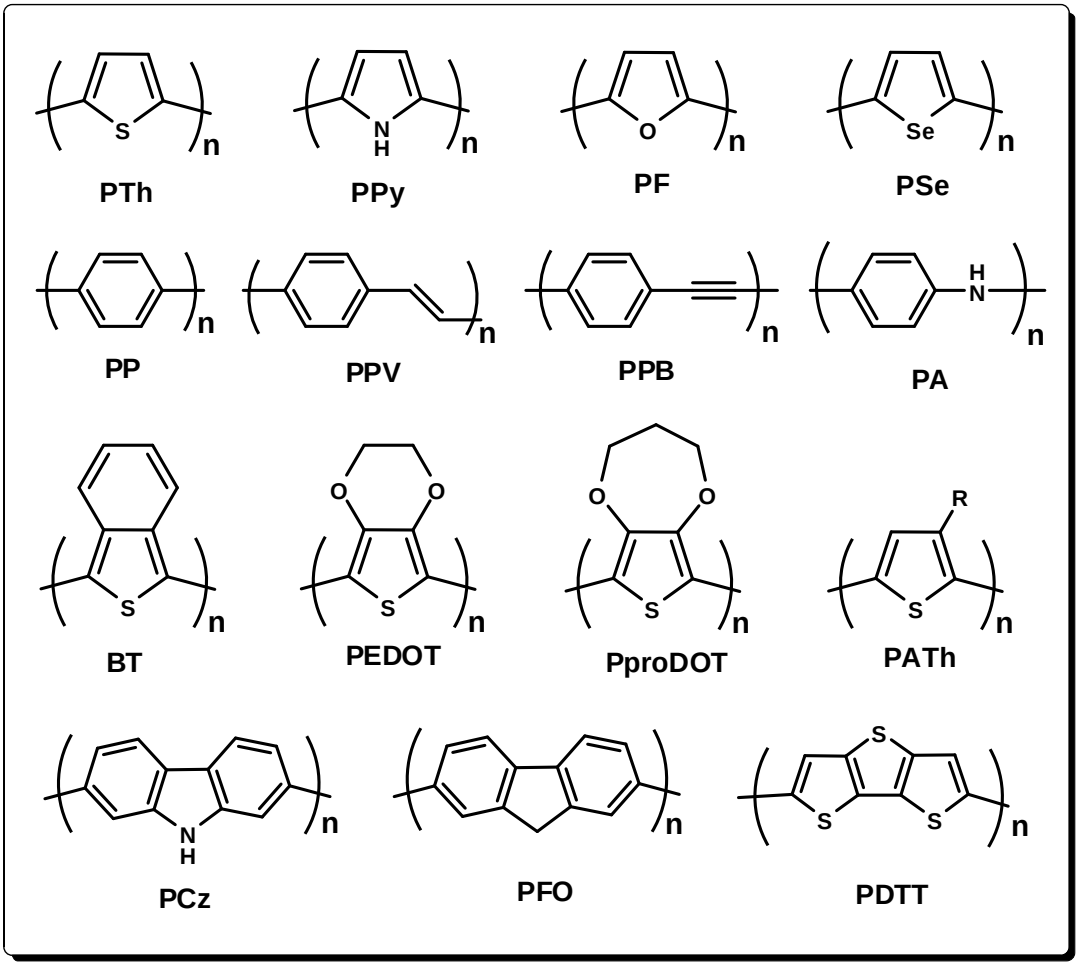

Figure 1. 2 Chemical structures of some common conjugated polymers

1.1.1 Conduction Mechanism in Conjugated Polymers: Doping Process

Conductivity in conjugated polymers can be accomplished by a unique process named *doping which is the charge injection (ejection) method to (from) the polymer chain* [12]. However, those polymers are insulators or poor conducting materials in their neutral states. Doping on the polymer chain is reversible process which includes both oxidation and its reversible couple reduction reactions in order to progress doping-dedoping (Fig.1.3).

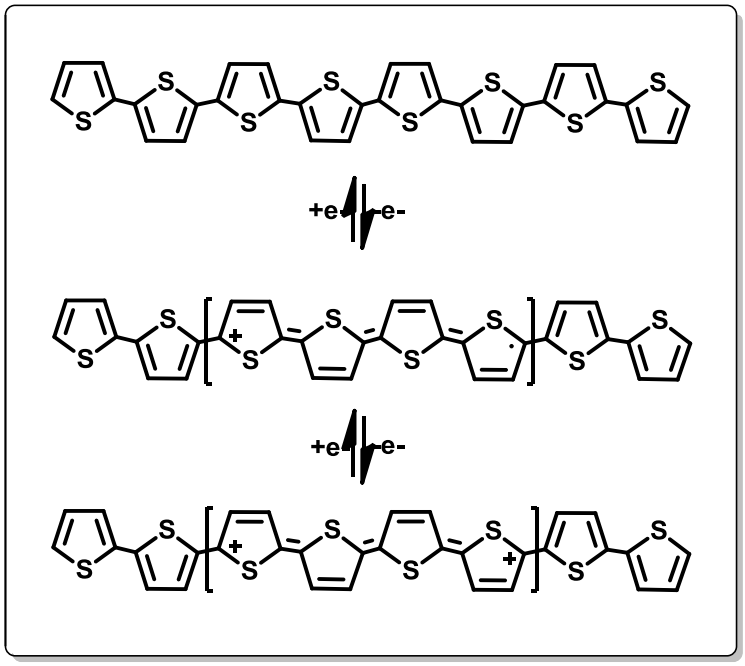

Figure 1. 3 Reversible doping-dedoping process of PTh

A polymer chain can be doped *via* chemical, photochemical, interfacial or electrochemical doping techniques. In general, electrochemical doping process is favorable since, homogeneous doping of the polymer chain is easily achieved *via* this technique contrary to other ones [13].

Electrochemical doping which affects electronic structure of the polymer chain as well as mechanical and optical properties is achieved via mainly two ways; p- and n-doping. During the oxidation process of a polymer, an electron in valence band is abstracted and positively charged carriers occur (p-type doping), conversely, addition of an electron to the conduction band leads the formation of negatively charged carriers during reduction (n-type doping). The organic anions can be easily oxidized by oxygen and moisture resulting in unstable chains. Hence, p-dopable polymers are much more stable than n-dopable ones [14-15]. Conductivity can be altered with different doping levels on the polymer chain [16].

1.1.2 Band Theory

The conductivity characteristic of materials can be elucidated by their band gap (Eg). In accordance with the well-known definition, *the band gap is the energy difference between the highest occupied electronic level in valence band (VB) and the lowest unoccupied electronic level in conduction band (CB)* [17]. According to this concept, materials are classified as conductors, semiconductors and insulators. In metallic conduction, there is no band gap since the conduction and valence bands overlap to form a partially filled band which provides the conduction *via* free movement of charge carriers. On the other hand, it's not possible any transition of charge carriers from the VB to the CB due to the high energy gap in insulators.

Semiconductors have a bang gap between those of metals and insulators. Although most of the conventional polymers show the insulating property, conducting polymers have the semiconducting behavior with their filled VB and empty CB (Fig.1.4). Besides the narrow energy gap of conducting polymers, electrons can be populated between VB and CB *via* doping process.

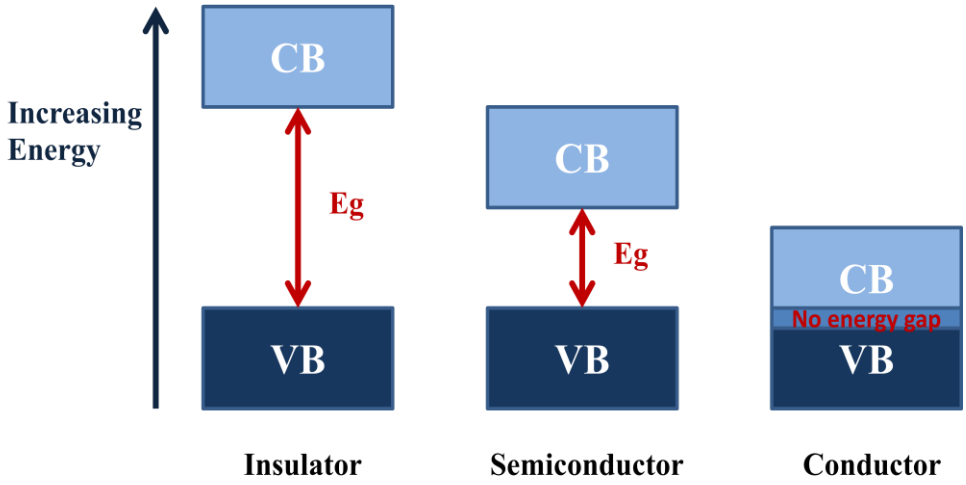

Figure 1. 4 Band structures of insulator, semiconductor and conductor

During the oxidation of a polymer, an electron is abstracted from the valence band and a radical cation occurs on the polymer chain. This generated positive charge provides delocalization of the electrons on the conjugated backbone. Meanwhile, the lone pair electrons of heteroatom participate in the electron mobility through the polymer and lead to the formation of a quinoid structure. [18] (Fig. 1.5).

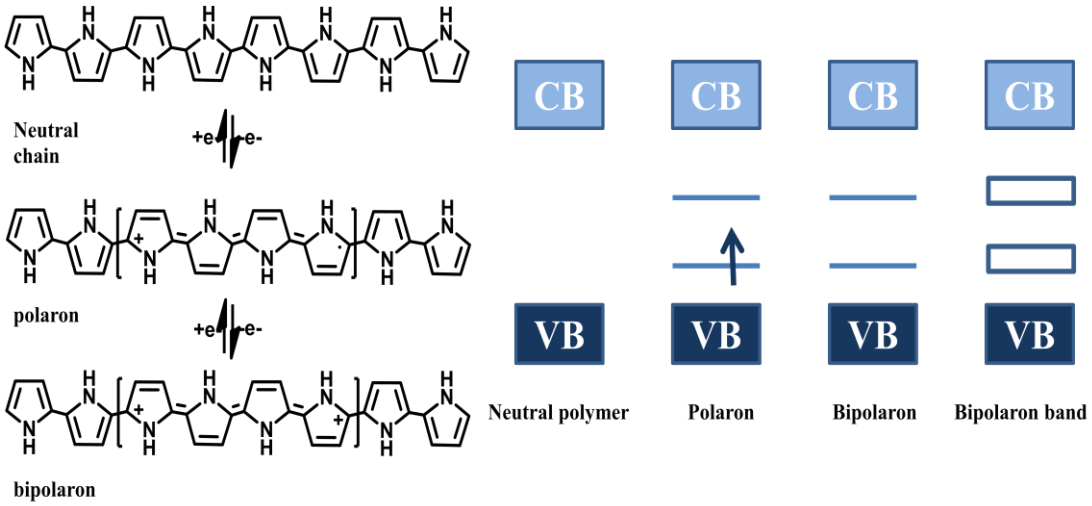

Figure 1. 5 The charge carries and their related band gaps in PPy

Subsequently, removal of the new electron from the polaron chain creates a dication and bipolaron energy bands lie between HOMO and LUMO levels. The formation of polaron and bipolaron structures allows holes causing extension of delocalization on the polymer chain. Thus, the absorbance of polarons is red shifted compare to neutral polymer chain.

A conducting polymer chain consists of alternating single and double bonds which lead to overlapping of π orbitals. Delocalization is provided by this overlapped π orbitals enhancing the conjugation throughout the repeating units. Addition of new HOMO and LUMO levels to the electronic structure generate continuum energy bands since the electronic levels do not position as discrete levels [19]. Although PAc is the basic macromolecule, it serves for the clear understanding of the band theory due to its simplicity (Fig. 1.6.).

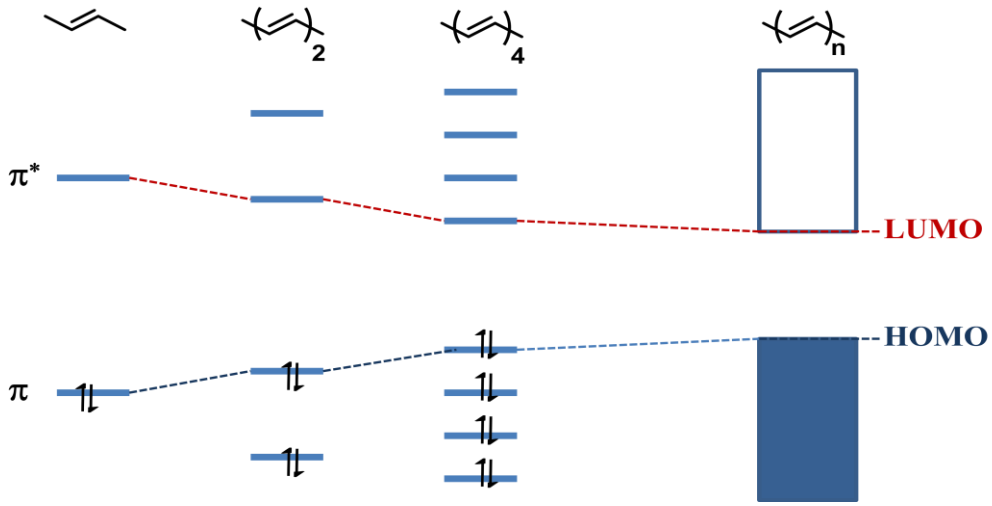

Figure 1. 6 Generation of band structures in PAc due to increase in conjugation

1.2 Polymerization Methods

Conducting polymer synthesis has become a foremost research area interested in discovering new macromolecules and their exciting properties in the last four decades. Chemical and electrochemical methods are commonly used procedures along with many different techniques such as photochemical polymerization, ring-opening metathesis polymerization, Grignard reaction and transition metal-catalyzed polymerization [20].

Chemical synthesis techniques are applicable for large amount of polymer fabrication which needs extra purification techniques such as work-up, crystallization and chromatography. Yet, electrochemical polymerization does not require any extra purification and prevents time consumption. In addition to easy control of film thickness on the thin surfaces, electrochemical polymerization provides already doped polymer at the end of the process contrary to chemical polymerization.

1.2.1 Chemical Polymerization

Chemical polymerization is usually carried out *via* mainly two techniques which are chemical oxidative polymerization and metal-catalyzed cross-coupling reactions [21]. The chemical oxidative polymerization mechanism using ferric chloride is suggested in the literature. In 1986, Sugimoto *et al.* reported that oxidative polymerization of unsubstituted thiophene in the presence of $FeCl_3$ was achieved on the catalyst surface which was not soluble in chloroform and was not polymerized with radical or radical cation. Since chloride ions quench the thiophene radicals or radical cations, dimer formation is blocked [22]. Niemi *et al.* worked on this mechanism using 3-alkyl substituted thiophene and $FeCl_3$ in 1980 [23]. The radicalic mechanism of chemical oxidative coupling was clearly identified for thiophene by Olinga and François. In this study, acetonitrile was used as the solvent where $FeCl_3$ is soluble [24]. According to proposed mechanism of oxidative thiophene polymerization, the reaction is performed in a bulk solution of monomer, $FeCl_3$ (or another Lewis acid) and solvent. The electro active radical cation of thiophene ring which is formed in response to reduction of ferric chloride react with the monomer to yield the dimer, oligomer and polymer (Fig. 1.7.) [25].

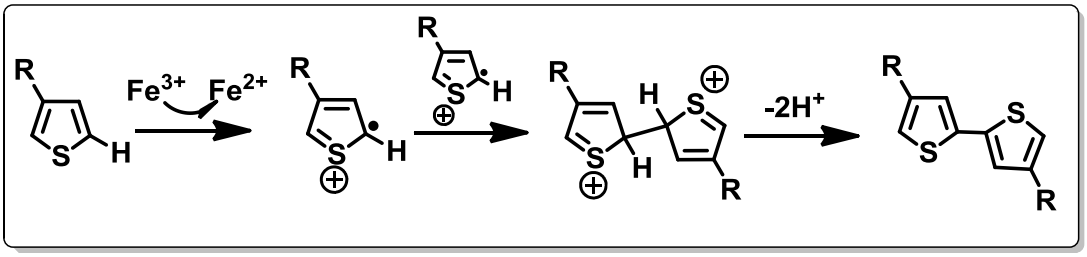

Figure 1. 7 Chemical oxidative polymerization mechanism of 3-alkyl substituted thiophene

Even though there are many types of metal catalyzed polymerization reaction in literature, Yamamoto's method is the first chemical pathway related to the

polythiophene synthesis using magnesium (Mg) in tetrahydrofuran (THF) with nickel(bipyridine)dichloride (Ni(bipy)Cl_2) as catalyst. In 1980, simultaneously with Yamamoto *et al.*, Kumada and co-workers improved a new procedure which includes the cross coupling between heteroaryl halide and Grignard reagent (Mg in THF) (Fig. 1.8.) [26]. Lin and Dudek integrated acetylacetonate type catalysts ($Ni(acac)_2$, $Pd(acac)_2$, $Fe(acac)_2$, $Co(acac)_2$) to Yamamoto coupling reaction in THF [27].

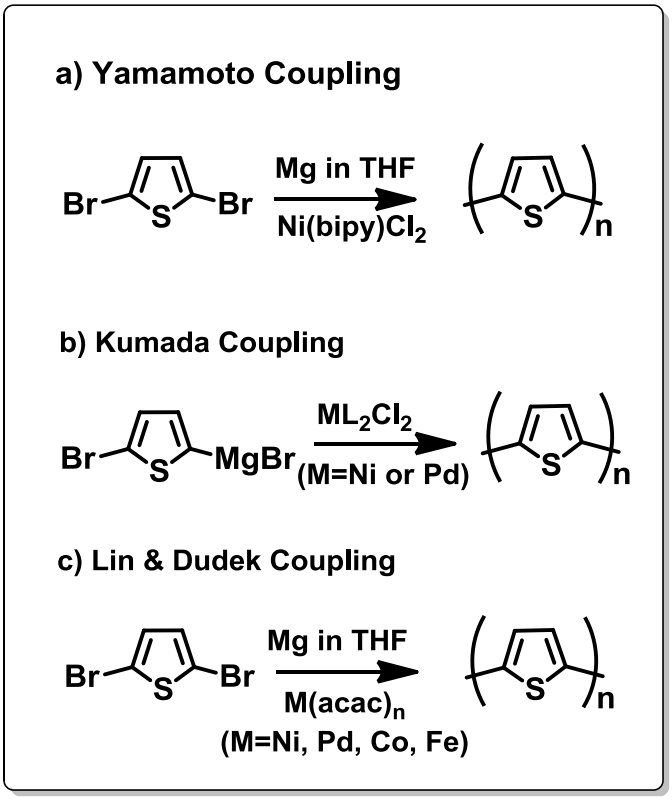

Figure 1. 8 Synthesis of PTh *via* a) Yamamoto coupling b) Kumada coupling c) Lin & Dudek coupling

Palladium catalyzed cross coupling reactions were firstly reported by Kosugi, Shimizu, and Migita at the end of 1970s [28-30]. On the other hand, the mechanistic studies of this reaction were investigated by Stille for the first time in 1978 [31]. According to detail mechanism, palladium mediated cross-coupling reaction starts

with in situ reduction of Pd (II) to Pd (0) as precursor of catalytic cycle and continues with three steps in a catalytic cycle [32]. In oxidative addition step, a halide constituent coordinates with the Pd (0) to yield the Pd (II). The second step is transmetalation where an organostannane derivative participates in the cycle and generates the organopalladium intermediate. Subsequently, the complex undergoes reductive elimination to give the desired product and Pd (0) which initiates a new cycle of coupling (Fig. 1.9). Stille reaction is more popular than the other transition metal cross coupling reaction due to the stability to air, easy preparation of reaction conditions and simple purification technique. The toxicity of tin groups hinders the industrial applications of this coupling in a large scale.

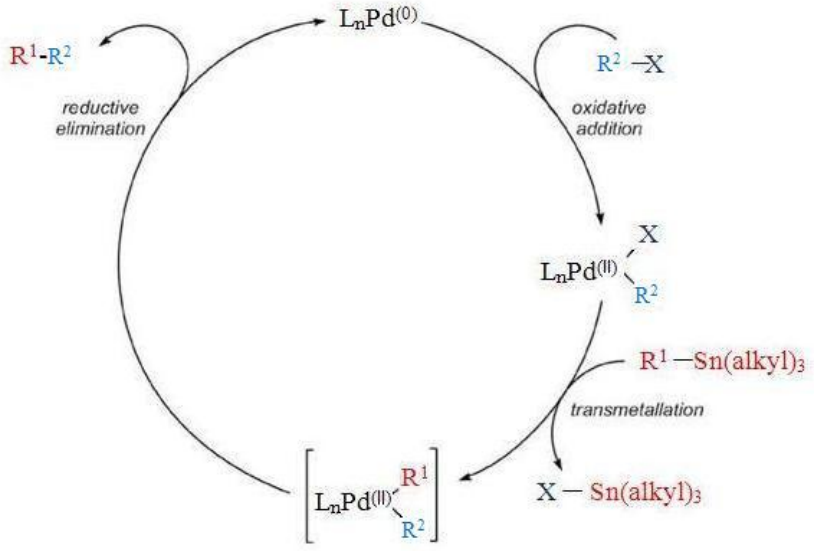

Figure 1. 9 Catalytic cycle of Stille reaction

1.2.2 Electrochemical Polymerization

Electrochemical synthesis of conducting polymer is a highly widespread polymerization technique owing to its simplicity, reproducibility and selectivity. In this method, rather small amounts of monomer are dissolved in a convenient inert solvent or solvent system containing supporting electrolyte. Electronic and optical characterization of a conjugated polymer can be easily achieved with a polymer film coated on the electrode. During the electropolymerization, the polymer is obtained in doped state. Hence, any subsequently doping process is not required contrary to conventional polymerization process. Furthermore, it is possible to control polymer thickness and morphology as superior to chemical polymerization.

Electropolymerization contains mainly electrogenerated radical cations and their coupling reactions followed by a reoxidation. The electrochemical polymerization mechanism can be explained electrochemical-chemical-electrochemical reaction series which is shorten $E(CE)_n$ and represented schematically in Fig. 1.10 [33].

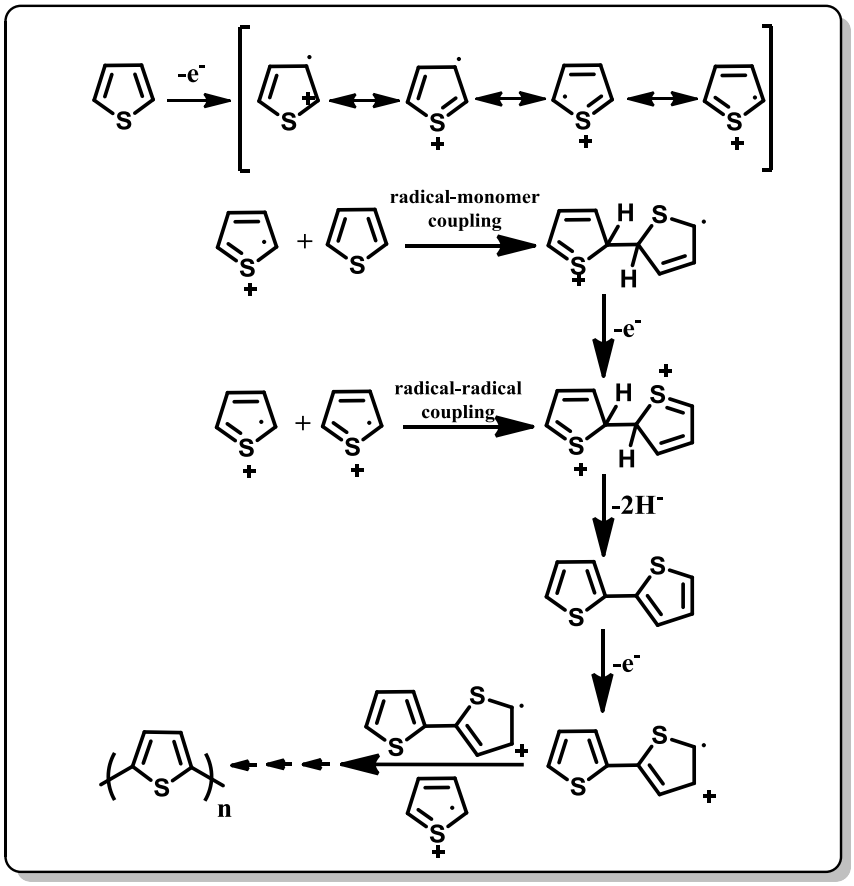

Figure 1. 10 Electrochemical polymerization mechanism of thiophene

According to this mechanism, firstly, monomer is oxidized via electron releasing upon applied potential and a resonance stabilized radical cation occurs. In this step, the radical cation concentration in the vicinity of working electrode should be much higher than the monomer concentration diffused from the bulk solution since polymerization easily undergoes. The second step represents the chemical reactions that include the coupling mechanism of radical cations with each other or radical cation with the monomer. At the end of these coupling reactions, a neutral dimer is obtained via loss of two protons. Due to applied potential, the neutral dimer is oxidized to yield new radical cations. The coupling reactions follow the cation formation to yield the trimer. In this manner, electrochemical polymerization continues with chemical and electrochemical reactions following to each other to prolong the polymer chain. Oligomers become insoluble in the electrolytic solution and on the electrode surface.

1.3 Applications of Conducting Polymer

Conducting polymers with their fascinating electronic and optical properties inspire many researchers to investigate on developing new materials and their properties. In that manner, these excellent materials are very popular in a variety of application areas. Π– Conjugated polymers have low energy optical transition, low ionization potential and high electron affinity which make them convenient materials for technological research [34].

Furthermore, mechanical, electronic and optoelectronic properties of conducting polymers can be generated for the desired purpose. Molecular architecture has a crucial role in design and synthesis of these intelligent macromolecules. Many surface coating materials with corrosion resistance can be easily developed due to controlling mechanical and surface properties of conducting polymers [35-37]. In recent years, usage of conducting polymers in electrochromic devices (ECDs) becomes interesting research area for the scientists [38-41]. Thin layer electrochromic conducting polymers show color change upon applied potential. Electrochromic property leads to several applications such as smart windows, rear-view mirrors and visors. Another interesting application of conducting polymers is their use in light emitting diodes (LED). Owing to their light emitting property, conducting polymers are applied in televisions, cellular telephones, clock radios, audio equipments, automotive dashboard displays, aircraft cockpit displays and some other electroluminescent displays [42]. Other promising applications of conducting polymers are energy storage equipments and organic solar cells which have great importance for clean and low-cost energy. In recent years, one of the most striking applications concerning the conducting polymers is biomedical applications including bioimaging, sensors, artificial muscles and drug releasing systems. The multifunctionality of these polymers allows integrating them to many interesting organizations. Due to biocompability of the materials, internal (implant) or external to the body studies can be achieved in biomedical and bioengineering applications [43-46].

1.4 Biosensors

A biosensor can be defined as a sensing device incorporating a biological recognition element intimately connected to a transducer which transforms the signal resulting from reaction between biomaterial and analyte into a meaningful signal [47]. The main objective is to obtain selective, sensitive, reproducible and meaningful signal from a biosensor in a short time. Hence, the stable, selective and low cost biosensor construction becomes a great challenge for many researchers and marketing.

Biosensors consist of mainly two parts as biological recognition elements and transducers. The working principle of a biosensor is illustrated in Figure 1.11. Recognition elements which are the key part of a biosensor provide the sensitive interaction with the specific analytes refraining interferences. The biomaterials used in biosensors are classified as catalytic ones (enzymes, microorganisms, tissues) and non-catalytic ones (nucleic acids, antibodies, receptors). According to desired purpose, these biologic elements maintain the reliable recognition of relevant substrate. Transducer as another crucial part of biosensor converts the chemical signal which is generated by the reaction between biomolecule and the substrate into an observable signal. Transducers are adapted in the biosensing systems up to the nature of biochemical reactions.

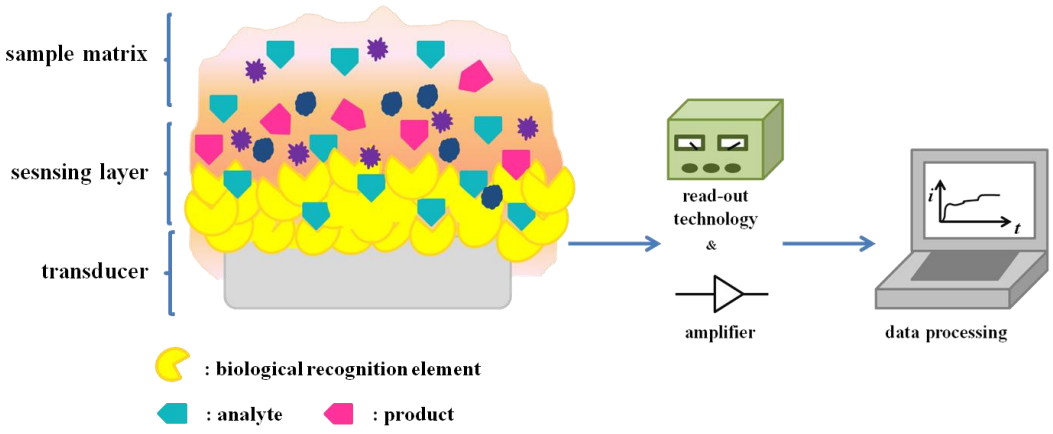

Figure 1. 11 Schematic representation of a biosensor

Biosensors can also be classified depending on the transduction types (Fig. 1.12). Transduction mechanism can be mainly sorted three categories as optical detection, electrochemical detection and mass detection methods [48]. Electrochemical transducers are commonly used ones thanks to their cost and easy to fabrication.

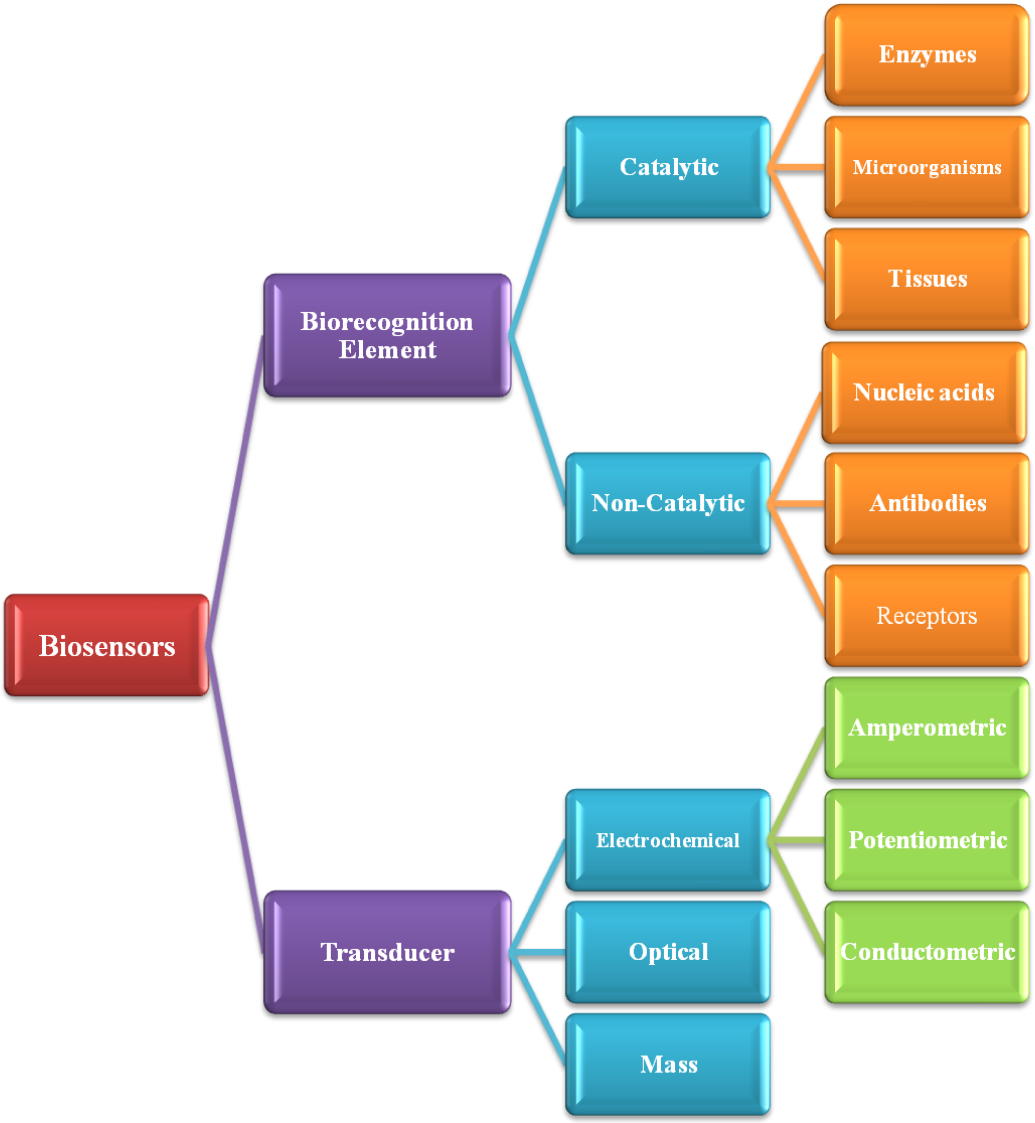

Figure 1. 12 Types of biosensors

1.4.1 Electrochemical Transducers

Electrochemical transducers serve the sensitive electrochemical signals. Furthermore, these signals should be obtained as a result of selective interaction among biorecognition element and analyte. The detection limits of these signals which are electrochemically obtained are compatible with optical ones [49-51]. Transducers are electrodes which can be easily modified depending on desired purpose in electrochemical biosensors. Owing to different electrochemical changes in biorecognition reactions, there are several types of transduction mechanism can be categorized as amperometric, potentiometric and conductometric.

1.4.1.1 Evolution of Amperometric Biosensors

Amperometric biosensors measure the current change resulting from the redox reactions produced upon constant applied potential. In other words, the constant potential which is needed for the oxidation or reduction of the substance to be analyzed is applied to the electronic cell and a sharp rise or fall occurs in the current. The height of this peak is proportion to the concentration of electroactive species. In addition, current change is followed as a function of time in amperometric measurements.

Defining the electron transfer mechanism between the biomaterials and the electrode surface has the key role to design and fabricate an amperometric biosensor. Oxidases and dehydrogenases are commonly used as catalytic molecules in measurements. Those enzymes endorse the oxidation-reduction reactions with their cofactors or metal species in their active sides. Thus, the electrons which are generated as a result of these redox reactions are transferred to the electrode surface. Besides the many complex detection mechanisms in biosensor design; the direct monitoring of either the decrease in the analyte or increase in the redox generated product are the most

straightforward methods. Furthermore, a mediator can be participated to enhance the electron transfer in enzymatic reactions [47].

The first biosensor fabrication was carried out in 1962 by Clark and Lyons who constructed an oxygen electrode where glucose oxidase (GOx) enzyme was used as the biorecognition element [52]. In "first-generation" biosensor construction, molecular oxygen is used as the oxidizing agent. Hence, the consumption of the oxygen as co-substrate or the increasing of the H_2O_2 as product is monitored in order to detect glucose concentration [53-55].

This pioneer system has great importance in the medical applications besides being an enormous model for the improvement of many other biosensors. Even though, the working performance of these bioelectrochemical devices is well, some operational problems affect the progress. One of the major drawbacks is the ambient oxygen level control. During this type of electrochemical reactions, oxygen level has to be controlled and kept constant. Otherwise, the monitoring analyte concentration cannot be proportional to the decrease in oxygen level. Another difficulty is to determine the potential applied to the working electrode. The potential should not be too high to oxidize all of the electroactive species and the interferences such as ascorbic acid, urea and oxalic acid in the medium [56]. Therefore, the oxygen depletion can be determined at -0.7 V (vs. Ag / AgCl reference electrode) with these type biosensors. The ambient oxygen is reduced when -0.7 V potential is applied to the working electrode. Therefore, oxygen is depleted during the catalytic reactions of oxidase enzyme. In consequence of this deficiency, the oxygen dissolved in bulk solution diffuses through the working electrode [57]. The diffused oxygen concentration can be measured as the current change in amperometric studies [58] (Fig. 1.13). The oxygen consumption is proportional to the substrate concentration upon catalytic reactions. Hence, the current difference is directly correlated with substrate concentration.

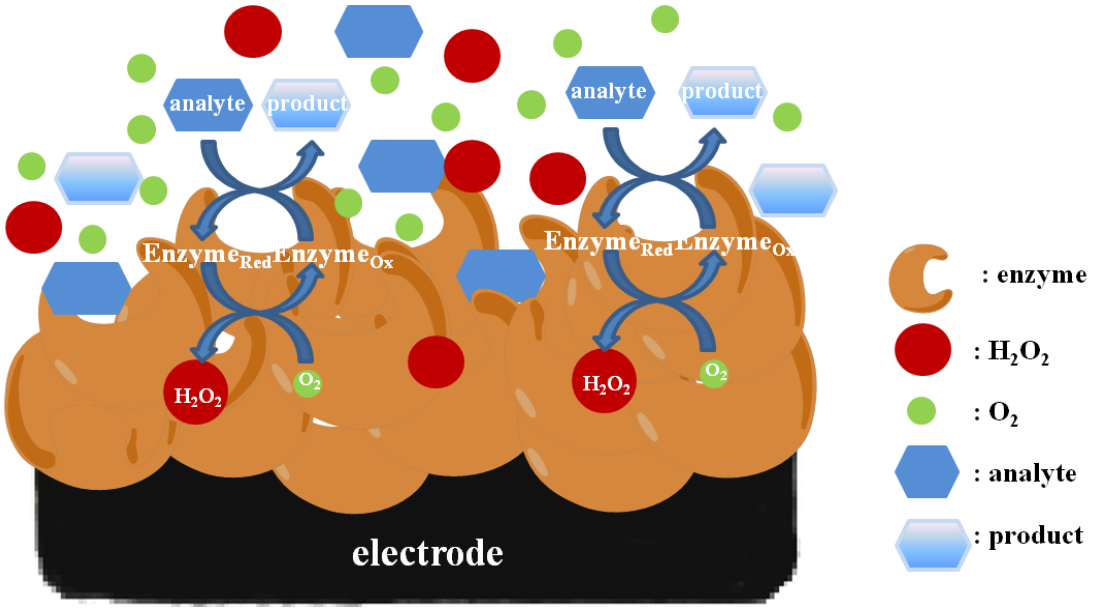

Figure 1. 13 The oxygen electrode

The transition metal cations and their complexes as oxidizing agents can be incorporated with enzymatic biosensing system instead of oxygen. These moieties called as "mediators" are utilized to develop the efficient electron transfer and provide low applied potential; hence the interference effect can be prevented using appropriate potential. Owing to application of iron cations to the bioelectronic systems for sensing, "second-generation" biosensors were introduced to the literature [59-64].

Mediators have an efficient and specific role in electron transfer between biological recognition elements and the transducers (Fig. 1.14). Therefore, mediators should have no side reaction with electroactive species in the medium and their electrochemically redox reactions should be reversible. The redox potential should be compatible with the cofactor(s) of enzyme and the oxidized or reduced forms of mediators should be stable at this potential. Mediators can allow the chemical functionalization yielding efficient immobilization for biomolecule to the transducer. Through the surface modification, mediators can be easily attached for instance, polymers having functional side chains, redox enzymes or electrode surfaces *via*

covalent binding. The cost, experimental processibility and toxicity of mediators should be noted in choosing the effective one. In this respect, ferrocene derivatives, organic dyes, ferricyanide, ruthenium complexes and osmium complexes can be used as mediators in specific reactions [65]. However, the accuracy and long term stability of biosensing detection can decrease with the usage of diffusing redox mediators. Due to either the leaching of the non-binding mediators from the electrode surface or the coverage active sides of enzyme by mediators, the current signals and biosensing performance show variations [66]. In addition, all of the commercial mediators are not biocompatible but these drawbacks cannot be obstacles in using the mediators in biosensing research [67-70].

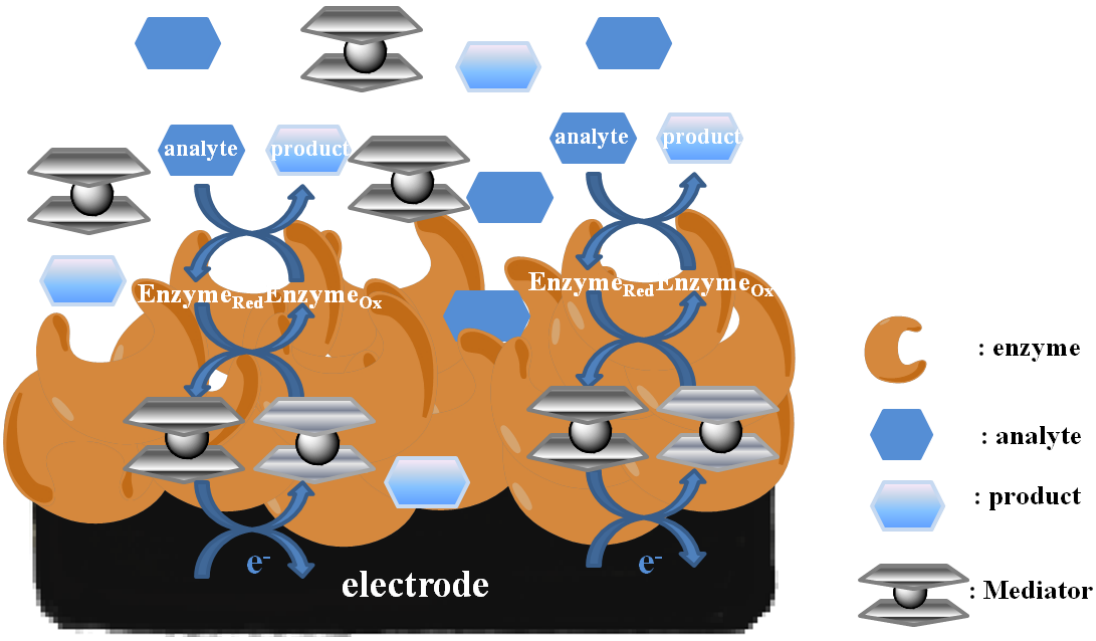

Figure 1. 14 The working principle of second generation biosensors

The "third-generation" approach in biosensing exhibits the direct electron transfer between active sides of biomolecule and the transducer [71-72] (Fig. 1.15). For this purpose, the redox enzyme is directly immobilized on the electrode surface and interacts with the electrode materials by hydrogen bond, electrostatic, dipole-dipole or hydrophobic interplays [73]. The adsorption which has main contributions among

all of the interactions helps to understand electron transfer mechanism on more complex systems. However, protein structures incline to denature during the adsorption process on the metal or carbon electrode surfaces. Furthermore the stability of this type of biosensors depends on pH, temperature, electrode surface material and the ionic strength of the solution as well as the other type biosensors [74].

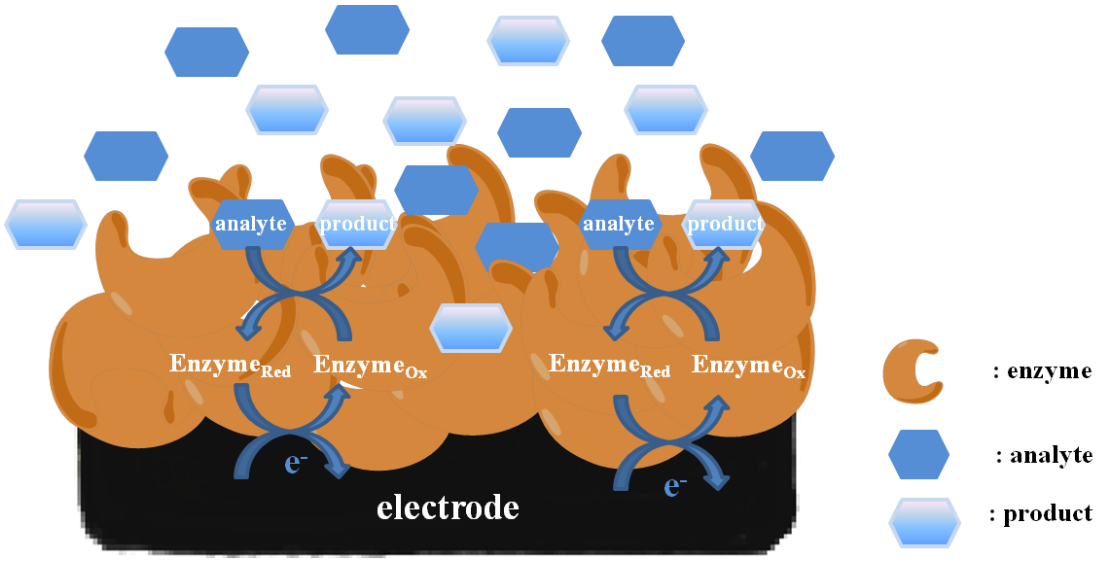

Figure 1. 15 The working principle of third generation biosensors

The electrode surface can be modified with self-assembled monolayers (SAMs) to overcome the denaturation problem of proteins and enhance the biosensor stability. Since the beginning of the 1980s till today this technique attracted great attention in the biosensors design and has been successfully deployed in construction of many biosensors [75-77]. The milestone technology is easily applicable due to the relatively straightforward formation of SAMs [77]. Through the surface modification of SAMs, biomolecules or mediators can be conveniently attached *via* covalent binding on the surface [78-80]. Moreover, the modification with SAMs on the electrode surface provides the stability towards pH, temperature and variety of applied potential [81-83].

The distance between the redox center in enzyme, generally cofactor, and the electrode surface is a critical parameter in terms of efficient electron transfer. Therefore, two redox sites having shorter distances or small redox shuttle enzymes should be chosen instead of one cofactor. The efficient electron transfer can be provided by controlling the distance and modifying the surface [84]. Introducing the conducting materials or nanostructures allow the active sites of enzymes to positioning closer to the electrode surfaces [85]. However, the electron transfer efficiency also depends on the immobilization matrix properties, electrode surface materials, the nature of the enzyme and the redox mediator.

Amperometric measurements proceed with a three electrode system consists of a working electrode as Pt, Au or C-based ones, a counter electrode and a reference electrode. During measurements, a convenient constant potential is applied to the working electrode with respect to reference electrode in a buffer medium. After the addition of the substrate to the solution, current change is recorded depending on the substrate concentration. Current change represents either oxygen consumption or the H_2O_2 formation upon applied potential in enzyme catalyzed amperometric biosensors.

1.4.2 Immobilization Techniques

The main step of the enzyme-based biosensor construction is the enzyme immobilization stage. Enzymes catalyze many complex chemical processes with their excellent properties such as selectivity and specificity [86]. These delicate protein structures should be applied under mild conditions to maintain high stability. The main drawbacks of using an enzyme are low stability, low ratio in reusability, low reliability, inhibition by products or high concentration substrates in the medium, susceptibility of pH, temperature and so on [87]. Since the beginning of 21st century, many interdisciplinary research areas have worked on eliminating such problems under the perspective of biotechnology. The main goal of the immobilization is

reducing the inconvenient parameters *via* improvement of basic procedures. Since the enzymes as well as other biomolecules have very low stability in solution, immobilization process enhances the enzyme stability and prolongs the shelf life with easy fabrication. A biomolecule constructed with immobilization can be easily removed from the solution and purified from the contaminations and products in the solution. The aliquot enzyme can be repeatedly operated, hence the cost, material amount and time of operation are reduced.

Selected biorecognition molecule needs to be fastened on the electrode surface to provide rigidification of three-dimensional (3D) structure. Moreover, it needs to maintain the activity at a required level with convenient microenvironment. It is important not only affording efficient electron transfer between analyte and the transducer but also providing the high operational stability and long shelf life. Besides, the charges on the surface, hydrophilic/hydrophobic interactions are helpful as well as hydrogen bonding, covalent binding and complexation for a robust attachment of biomolecule on the transducer.

The immobilization matrix properties have superior importance in terms of determining the appropriate immobilization technique. The model matrix should be biocompatible, inert for the microbial attacks, hydrophilic, easy to synthesize and available at low cost [88-89]. The ability of matrix modification introduces many advantages to ensure durable biosensors. For instance, the functionalization of the surface allows to adapting the chemical structure, tuning chemical and physical properties which aim to obtain robust interaction between enzymes and the electrode surface in the course of immobilization. Another noticeable advantage for surface modification is tunability of the distance between transducer and the redox enzyme. For an example case, the surface modification of the transducer with a redox polymer creates 3D network which allows decreasing in the distance among two redox centers and also creates the fastened immobilization of enzyme molecules. Thus, the diffusion of analytes, products, counter ions and electron transfers can be easily assured between the solution media and electrode. Moreover, an appropriate surface matrix allows to applying low potential at which the interference effects can be

eliminated. Among the different types of matrices, porous ones are more preferable than the smooth ones, since the porosity provides higher enzyme loading due to high surface area.

Determination of appropriate immobilization method is the crucial step in order to prevent the loss of enzyme activity ie. by protecting the chemical nature and binding sites of enzyme. The chosen immobilization technique should be convenient in terms of the matrix type, nature of the biomolecule, determination method and the chemical microenvironment of analyte. Since the immobilization method affects the stability, selectivity, sensitivity, operational performance and response time, the protection of enzyme activity and increasing the biosensor performance are possible by choosing the most appropriate immobilization method [90]. Consequently, the chemical and physical interactions between the enzymes and the transducer exactly affect the biosensor performance. Choice of the immobilization technique has the key role providing to obtain durable, sensitive and selective biosensors architecture. In recently, physical adsorption, entrapment, covalent attachment and crosslinking are the commonly used immobilization techniques for a variety of biomolecules [91-95].

1.4.2.1 Physical Adsorption

The adsorption technique which depends on the enzyme adsorption on the suitable surface with non-covalent interactions is the simplest approach for straightforward preparation. In this technique, the water insoluble support is needed as the immobilization matrix. Cellulose, silica gel, clays, conducting polymers, carbon nanotubes (CNTs) and/or nanoparticles containing matrices can spontaneously adsorb enzymes or other biomolecules [96-99]. The enzyme is attached to the surface *via* Van der Waals forces, hydrogen bonds, hydrophobic interactions and salt linkages [100-101]. Since these interactions depend on relatively weaker forces, the

immobilization process can be reversed by changing the environmental conditions such as pH, temperature, ionic strength and polarity of the solvent. Thus, the biosensing performance, stability and shelf life of the biosensors are easily affected by these conditions. The adsorption is cheap and easy to apply; a short time processable method generally protects the enzyme activity. According to these properties, the corresponding method is attractive economically and enhances processability. However, the biorecognition element can easily leach from the surface due to weak interactions. This problem can be handled using a dialysis membrane which utterly covers the biomaterial and prevents the leakage of the enzyme. The representative scheme of the enzyme adsorption is shown in Figure 1.16.

Figure 1. 16 The working principle of adsorbed enzyme

1.4.2.2 Entrapment

Enzyme entrapment is one of the simplest methods used as the enzyme immobilization. This technique can be achieved in different types changing according to polymer types. One of them includes the gel formation in which the biomolecule containing polymeric gel is prepared and the biocomponent is trapped in a polymeric network on the transducer surface. Starch, polyacrylamides, nylon are

commonly used as gels. In this method, the main drawback is the enzyme leaking through the pores in the gel [102]. Crosslinking can be helpful to solve this problem. The reaction can be slow since the enzyme trapping in a network causes a diffusion barrier for the substrate.

Another easy fabrication method is the electrochemical polymerization where a biocomponent is dissolved together with the monomer in an aqueous medium. The electrochemical oxidation of the monomer proceeds to obtain a polymer network entrapping the enzyme molecules. During the electropolymerization process, the most enzymes with their negative charges behave as dopants and can be homogeneously incorporated into conjugated polymers at a physiological pH. Hence, the biomolecules become trapped within the polymer network. This method allows to entrapping mediators, co-enzymes, another enzymes and additives adding the monomer solution. Since the electropolymerization technique yields a homogeneous distribution of enzymes in the polymer matrix, the substrate and product can be easily diffused whereas the enzymes molecules are not be allowed to migrate through the solution. Thus, the constructed biosensors are reproducible, stable and the easy to fabricate [103].

In this one-step technique, polymeric dialysis membrane, sol-gel capsules and polymeric structures can be used as the matrices for the entrapment of a biomolecule [104-106]. Since there is no need to modify the enzyme, biological activity is not altered. Furthermore, the commonly used conducting polymers as matrices led to controlling thickness, surface morphology and the pore size of the matrix [107]. The main disadvantage of this technique is poor solubility or insolubility of the monomers in water. Therefore, the incorporation of the biomolecule within the polymer matrix can be difficult during the electropolymerization of the monomer. Thanks to partial solubility of pyrrole in water, the entrapment of different enzymes in polypyrrole can be easily achieved by one-step fabrication [108-110]. In the literature, different types of enzymes, especially glucose oxidase, were studied by entrapping with conducting polymers thanks to their stability and the conductivity properties [111-115]. The representative scheme of the entrapment technique is illustrated in Figure 1.17.

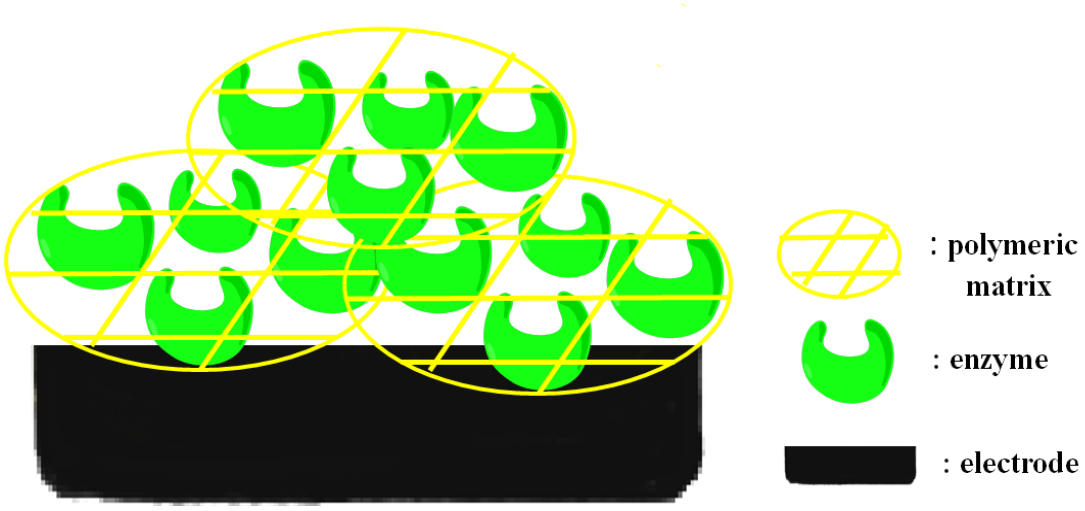

Figure 1. 17 The representative illustration of a biosensor constructed *via* entrapment method

1.4.2.3 Crosslinking

Crosslinking is one of the commonly used immobilization techniques where attachment of a biomolecule is achieved with intermolecular crosslinking of protein molecule or covalent binding to the functional groups of the supporting material such as gel or polymer matrix on the surface. This straightforward technique is also used to stabilize the adsorbed protein on the surface and prevent the enzyme leakage [116-117]. Bifunctional and low molecular weight reagents, such as glutaraldehyde, hexamethylenediisocyanate, 1,5-difluoro-2,4-dinitrobenzene are popular crosslinkers used in this method. However, this kind of crosslinking agents may cause the bioactivity loss, since the intermolecular or intramolecular crosslinking of the proteins are performed in harsh conditions leading to changing active center of the enzyme. This method provides the short response time; however there is low mechanical strength and some diffusion limitations. Nevertheless, it is convenient method for adsorbed biomaterials and surface modifications [118-120]. Figure 1.18 summarizes the construction of enzyme immobilization *via* crosslinking.

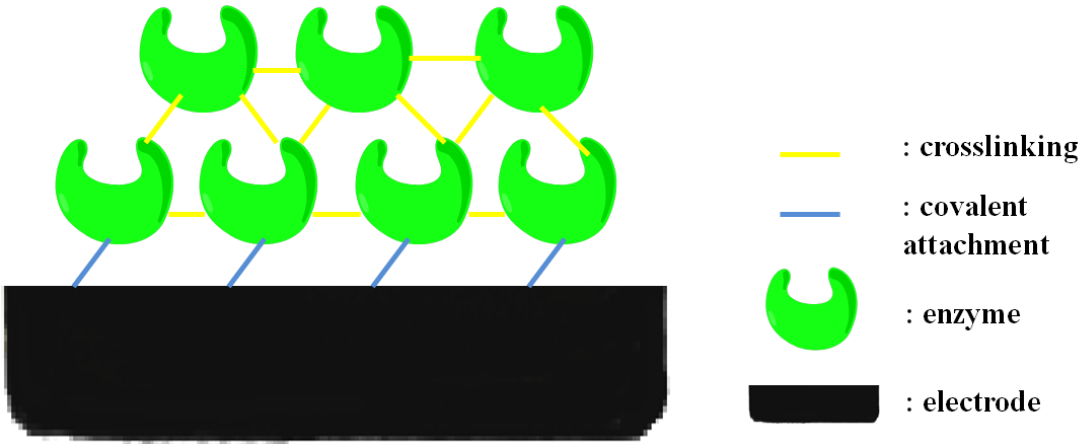

Figure 1. 18 The representative scheme of enzyme immobilization *via* crosslinking

1.4.2.4 Covalent Binding

The protein immobilization based on covalent attachments is the most profoundly method allowing robust covalent bonds between the functional groups of proteins and the matrix (Fig. 1.19). Since functional groups in the amino acids are not essential for the catalytic activity of the enzyme, these reactive groups such as amines, carboxylic acids, imidazoles, thiols and hydroxyls are appropriate for the covalent attachments. The corresponding method is maintained fundamentally by three steps comprising enzyme or/and the surface activation, enzyme coupling and discarding the unreacted enzymes or reagents [121]. In the first step, functional groups of the enzymes or the pendant groups of the supporting material is activated by the help of the multifunctional reagents such as glutaraldehyde, carbodiimide, *N*-hydroxysuccinimidyl, epichlorohydrin etc. [122-124]. Subsequently, the enzyme reacts with the previously functionalized immobilization matrix or vice versa in order to perform the covalent linkage. According to the functional groups of the matrix, a

variety of coupling reactions have been promoted in the literature [125]. Conducting polymer matrices, SAMs, nanoparticles and porous sol-gel composites enable the prominent supports to yield the covalent bonds [126-129]. Throughout all the

process, aqueous solutions should be preferred to protect the enzyme activity. Such kind of reactions should also be carried out under the mild conditions involving low temperature, appropriate pH levels and low ionic strength.

The immobilization of enzymes *via* covalent bonds to the transducer enables amide, ether or thio-ether bonds formation. Thus, enzyme is strongly bounded to the surface providing the stability in many cases. During the covalent integration of the enzymes, the redox centers of the matrix closes to the active sides of enzyme resulted with the efficient electron transfer.

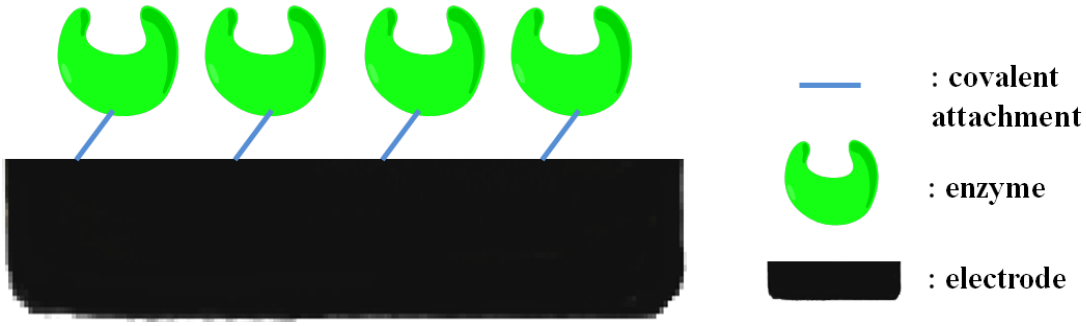

Figure 1. 19 The representative scheme of enzyme immobilization *via* covalent binding

1.5 Biosensor Applications

Biosensors opening to many developments day to day are widely used in a variety of application areas. The qualitative and quantitative analysis of the prominent substrates has essential importance in terms of not only the academic researches but also the foremost industrial applications such as food, health care, environmental science and agriculture.

Health care is the main operation area of biosensors in terms of both industry and

research. Immobilized enzyme sensors offer some simple techniques for the diagnosis and treatment of many diseases. Biosensors also provide the opportunity of use of drugs and some metabolites monitoring a noteworthy part of the treatment. Measurements of blood are required to periodically control the patient's metabolic state. The disposable biosensors giving the analysis results in a minute are enhanced so that the time consumption can be minimized with these homemade devices. However, the classical instruments generally used in the hospitals enable the multiple analysis and the continuous measurements. Another promising application of biosensors is implantation in the skin for continuous monitoring of a metabolite. In such systems, deficiency of the corresponding metabolite is sensed by an implanted biosensor and results from this signal give an order to a microprocessor for directly releasing the metabolite or the enzyme to the blood stream.

Biosensors undertake a crucial role in monitoring the potential analytes in air, water, solids or other environmentally conditions. These measurements cover the organophosphates, pesticides and heavy metal ions as river water contaminants, airborne bacteria determination. Disposable biosensors should be preferred to study with the harmful samples such as contaminated waste water. Besides the pollution monitoring, the farming, mining and veterinary science are the environmentally application areas of biosensors.

Food industrial process requires a continuously observation aspiring to control whole production. The measurements of sugars, yeasts, malts, alcohols, phenolics, other products, reactants and side-products enhance the quality and yield of the products. Fermentation process which especially determines the quality of drinks can also be determined by specific biosensors. To sum up, the biosensors have the wide range of application area in food and beverage industry as well.

1.5.1 Glucose Biosensors

Glucose monitoring is one of the most elaborated subjects in biosensing by researchers and industry. Recently, the commercially available, portable and disposable glucose biosensors have been developed by many researchers and presented at the market [130]. This type of glucose biosensors provides convenience to diabetes patients for monitoring their blood glucose level in a short time with high accuracy. Regularly detection of the glucose concentration in blood has an important role in the diagnosis and treatment of diabetes. Since the healthcare professionals recommend the diabetes patients to have a regime for taking limited sugar, the determination of glucose concentrations in productions of food industry has a vital importance.

Glucose monitoring generally depends on amperometric measurements with the help of glucose oxidase (GOx) in the presence of the molecular oxygen. Upon applied potential, firstly, β-D-glucose is oxidized to glucono-δ-lactone which is subsequently hydrolyzed into gluconic acid. Afterwards, molecular oxygen is reduced to hydrogen peroxide [131] (Figure 1.20).

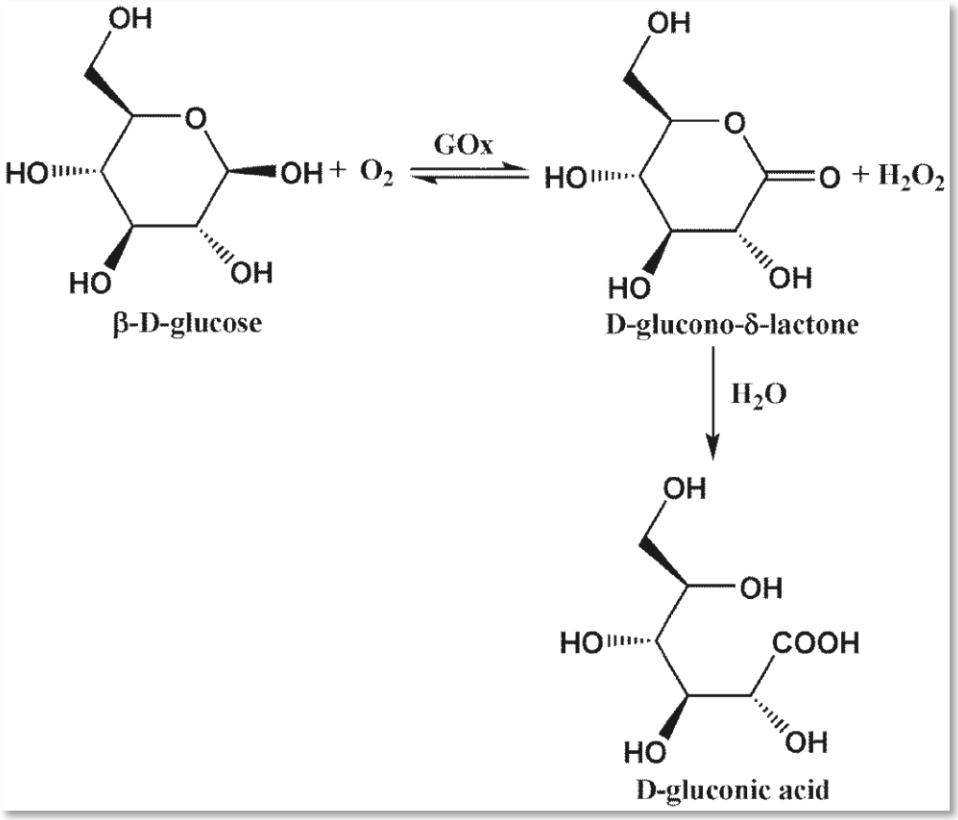

Figure 1. 20 The reaction mechanism of GOx

1.6 Conducting Polymers in Biosensing

The combination of electronic and chemical properties of conducting polymers contributes the improvement of biosensors. The integration of biomolecules such as amino acids, antibodies, enzymes into the conducting polymers with different techniques leads to construct new generation biosensors [132-138] (Table 1.1). Thus, the use of conducting polymers as immobilization matrices permits the revolution of biosensors as faster and more economical devices in diagnosis and treatment.

Table 1. 1 Characteristics of conducting polymer based biosensors

Matrix	Biosensing molecule	Immobilization method	Ditection limit	Linearity	Stability	Ref.
Poly(o-aminophenol/ CNT)	Glucose Oxidase	Electropolymerization	0.01 mM	Up to 5 mM	30 days	[132]
Polyaniline/ MWCNT	Choline Oxidase	Crosslinking	0.3 μM	$1x10^{-6}$ - $2x10^{-3}$ M	30 days	[133]
Poly-3,4-ethylenedioxythiophene	Tyrosinase	Entrapment	NR	5-500 nm	12 days	[134]
1,2-Diaminobenzene	Glucose Oxidase	Covalent	0.05 mM	0.05-5 mM	90 days	[135]
Polypyrrole/ MWCNT/ COOH	DNA	Entrapment	NR	$1x10^{-5}$-$3x10^{-8}$ M	NR	[136]
Polyaniline	Cholesterol Oxidase, Cholesterol Esterase and Peroxidase	Covalent	25 mg dL^{-1}	25-500 mgdL^{-1}	6 weeks	[137]
Polypyrrole	HRP	Entrapment	0.01 mM	0.01-0.1 mM	6 months	[138]

NR: Not Reported

In most of the biosensing designs, conductive surfaces are used as the transducers that can be operated to shuttle electrons between redox center of biomolecule and the electrode surface [139-141]. Since these mediated biosensors allow the biomolecule to get closer to the electrode surface, the overall current signal increases depending on the efficient electron transfer.

Besides several techniques for synthesis of the conducting polymers, electropolymerization provides a direct deposition on the electrode surface. Furthermore, electrochemical synthesis of the conjugated polymers is preferred in biosensor construction due to its high reproducibility, simplicity in fabrication, and control over the physical properties such as film thickness and morphology on the surface under mild conditions. Therefore, the homogeneous and stable conducting polymer film can be obtained in each run.

Controlling the polymer morphology is a remarkable parameter for immobilization in order to promote three dimensional architecture of biomolecule [142]. These biocompatible macromolecules can be chemically modified to upgrade their physical and chemical properties upon demand. Thus, the interaction between enzymes and the immobilization matrix can be successfully achieved in order to construct more stable and sensitive biosensors. Owing to their biocompability of conjugated polymers, immobilized enzyme activity is protected and biochemical reactions are carried out in a convenient microenvironment.

The electronic and chemical properties of conjugated polymers lead to access robust interactions for immobilization platform and biorecognition element by different techniques such as adsorption and covalent attachments. The increase in functional groups which can bind with the biomolecule on the surface influences the enzyme loading. Since the transferred electrons resulting from the biochemical reactions between enzymes and substrate molecules increased due to high enzyme loading, the overall current is increased as expected.

1.7 Surface Modifications for Immobilization Matrices

For rapid response with high reproducibility in clinical, food, environmental and health care monitoring, biosensor architecture has charming innovation for four decades. Considering the biosensor operation, an appropriate immobilization matrix selection and attachment of desired enzyme to the surface by a convenient technique play crucial roles on enzyme-substrate interactions. Thus, the improvement of ideal biosensor strategies focuses on promoting the desired immobilization platform and defining the most efficient biomolecule attachment technique besides the optimization of microenvironmental conditions.

Surface modification is essential for upgrading the biosensor performance. The electrode surface should be well organized to provide an increase in immobilized enzyme molecules and protect the bioactivity. Thus, the aim is fabrication of an immobilization matrix compatible with three dimensional structure of enzyme [143]. Since matching between two surfaces makes the redox centers of these macromolecules come closer, electron transfer is performed faster with an increase in overall current. Moreover, functional groups having potential to attach biomolecule on the surface can be supplied depending on the choice of modification material. Thus, these robust interactions hinder the enzyme leaching from the surface causing more selective and stable biosensor construction.

Immobilization of a biomolecule on an organic polymeric film is the most straightforward technique among the several alternative surface modification methods [144-146]. Controlling the surface characteristics such as morphology and the thickness makes the electropolymerization a feasible method for getting promising polymer films open to surface modifications. Furthermore, appropriate functionalizations of monomer by chemical methods allow obtaining impressive immobilization platforms having desired characteristics. Amino acids and dendrimers can be also used in surface modification to enhance the specific functional groups on the surface [147]. Nanomaterials especially carbon nanotubes

(CNTs) and metallic nanoparticles can be preferred as surface modification materials to enhance the biosensor performance [148-150]. Among the many different surface modification approaches, the optimal one should be defined by comparing and evaluation different approaches.

1.8 Aim of the Work

This study is mainly focused on the generation of new immobilization matrices for glucose detection. Thanks to their managing ability over the surface morphology and also conductivity, conjugated polymers present researchers the creation skills of many supporting materials. In this context, the biocompatible conducting polymer based immobilization matrices are designed and established to provide covalent attachments of GOx as a model enzyme in this study. It is planned to enhance the stability of designed biosensors with a low limit of detection (LOD), high linear range and efficient electron transfer via surface modifications. Thus, poly-2-(2,5-di(thiophen-2-yl)-1H-pyrrol-1-yl) acetic acid (SNS-anchored acetic acid polymer) surfaces are covalently modified with Lysine amino acid, PAMAM G2 and G4 dendrimers to determine the increasing functional groups effect on the biosensor performance [151]. A novel functional polymer poly-4-(4,7-di(thiophen-2-yl)-1H-benzo[d]imidazol-2- yl)benzaldehyde (PBIBA) is designed and synthesized as a new immobilization matrix. The electronic and optoelectronic properties of this promising polymer are studied as well [152]. The PBIBA based biosensor was also modified with gold nanorods (AuNRs) and single-walled carbon nanotubes (SWCNTs) to increase the electron transfer ability and enlarge the surface area for connections large amount of GOx. All the designed biosensors are tested on real samples to determine their reliabilities.

CHAPTER 2

2. EXPERIMENTAL

2.1 Materials

Glucose oxidase (GOx, β-D-glucose:oxygen 1-oxidoreductase; EC 1.1.3.4, 21 200 units per g) from Aspergillus niger, D-glucose, N-(3-Dimethylaminopropyl)-N'-ethylcarbodiimide hydrochloride (EDC), glycine methyl ester hydrochloride, succinyl dichloride, sodium borohydride, dichloromethane (DCM), bromine, hydrobromic acid were purchased from Sigma (St. Louis, USA). PAMAM G4 (25% C12 dendrimer, 10 wt% solution in methanol), PAMAM G2 (25% C12 dendrimer, 20 wt% solution in methanol) and glutaraldehyde (GA; 50 wt% solution in water), 2,1,3-benzothiadiazole, ethyl acetate, chloroform, bis(triphenylphosphine)palladium(II)dichloride, n-butyllithium solution (2.5 M in hexane), tributyltin chloride, single-walled carbon nanotube (carbon>90 %, ≥80.0% (carbon as SWNT), 0.7-1.4 nm diameter), zirconium(IV)chloride, terephtalaldehyde, $NaClO_4$ and $LiClO_4$ were purchased from Sigma-Aldrich. N-hydroxysuccinimide (NHS) was purchased from Fluka (Buchs, Switzerland). Acetonitrile (ACN), hydrochloric acid, sodium hydroxide were purchased from Merck (Darmstadt, Germany). Thiophene was purchased from Acros Organics (Geel, Belgium). 4-(4,7-Dibromo-1H-benzo[d]imidazol-2-yl)benzaldehyde, 4-(4,7-di(thiophen-2-yl)-1H-benzo[d]imidazol-2-yl) benzaldehyde, tributyl (thiophene-2-yl) stannane, 1,4-di(thiophen-2-yl)butane-1,4-dione, methyl-2-(2,5-di(thiophen-2-yl)-1*H*-pyrrol-1-yl) acetate were synthesized. All chemicals used in monomer synthesis were commercially available and used without any purification. THF was distilled over sodium and benzophenone. All other chemicals were analytical grade. Real human serum samples were obtained from the Middle East Technical University (METU) Medical Center from patients volunteered for that matter.

2.2 Equipment

^{1}H NMR and ^{13}C NMR spectra were recorded in DMSO-d6 on Bruker Spectrospin Avance DPX-400 spectrometer and the chemical shifts were expressed in ppm relative to DMSO-d6 (δ: 2.50 and 39.50 ppm for ^{1}H and ^{13}C NMR, respectively) and $CDCl_3$ (δ: 7.24 and 77.00 ppm for ^{1}H and ^{13}C NMR, respectively) as the internal standard.

A Waters Synapt MS System HRMS (High Resolution Mass Spectrometer) was used to confirm the synthesized materials.

Amperometric and cyclic voltammetry measurements were done on Palm Instrument (PalmSens, Houten, Netherlands) and Ivium CompactStat (Ivium Technologies, The Netherlands) with a traditional three-electrode configuration. A graphite electrode (Ringsdorff Werke GmbH, Bonn, Germany, type RW001, 3.05 mm diameter and 13 % porosity) as the working, Ag/AgCl (3 M KCl saturated with AgCl) and Pt electrode (Metrohm, Switzerland, www.metrohm.com) were used as the reference and counter electrodes, respectively. During all electrochemical measurements, the electrodes were placed in an electrochemical cell with an internal volume of 10 mL. All amperometric measurements were carried out at room temperature.

Veeco MultiMode V AS-12 (‘‘E’’) model AFM (Atomic Force Microscope) was used for surface characterization of all layers in biosensors construction.

XPS (X-ray Photoelectron Spectroscopy) was carried out on a PHI 5000 Versa Probe (F ULVAC-PHI, Inc., Japan/USA) model X-ray photoelectron spectrometer instrument with monochromatized Al Ka radiation (1486.6 eV) as an X-ray anode at 24.9 W. The pressure inside the analyzer was maintained at 10^{-7} Pa. The binding energy scale was referenced by setting the C–H peak maximum in the C1s spectrum to 285.0 eV and the atomic composition estimated using Multipak software.

Transmission electron microscope (CTEM) images were recorded using FEI Tecnai G2 Spirit BioTwinCTEM Microscope.

Contact angle measurements were performed for each polymer and biosensors surfaces using the sessile drop method with a KSV CAM 200 contact angle meter (KSV Instruments, Finland). During the experiments, a drop of distilled water was dripped into each surface. The drop profile was recorded with a CCD camera allowed monitoring the changes in contact angle for each surface. All reported data were given as the average of fifteen measurements ± SD.

2.3 Procedures

2.3.1 Synthesis of Synthesis of 2-(2,5-di(thiophen-2-yl)-1H-pyrrol-1-yl) acetic acid (3)

2-(2,5-Di(thiophen-2-yl)-1H-pyrrol-1-yl) acetic acid was synthesized according to previously described procedure [153] (Fig. 2.1). Methyl 2-(2,5- di(thiophen-2-yl)-1H-pyrrol-1-yl)acetate (0.7 mmol, 212.38 mg) was dissolved in 15 mL methanol at room temperature. After KOH (1.9 mmol, 106.6 mg) addition to the mixture, the reaction was allowed to proceed under reflux conditions until all esters were consumed. The crude product was concentrated and extracted with water and diethyl ether. To maintain the pH at 1.0, 6.0 N HCl was added to the aqueous phase and then extracted with diethyl ether. The organic phase was dried over $MgSO_4$ and evaporated under reduced pressure (0.171 g, 85 %).

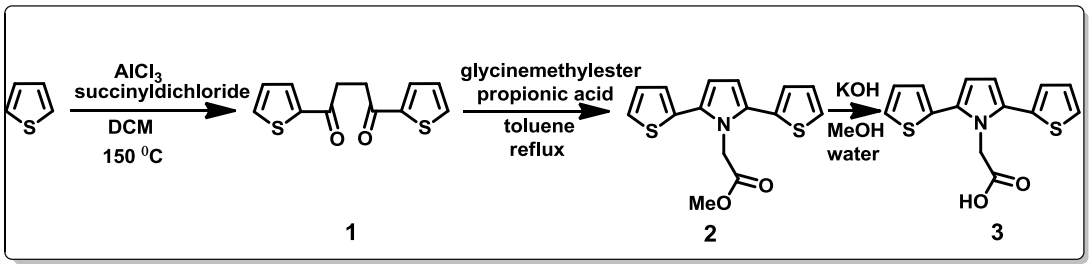

Figure 2. 1 Synthesis of SNS-anchored acetic acid monomer **(3)**

2.3.2 Synthesis of BIBA Monomer

2.3.2.1 Synthesis of 4-(4,7-dibromo-1H-benzo[d]imidazol-2-yl) benzaldehyde (6)

3,6-Dibromobenzene-1,2-diamine **(5)** was synthesized in accordance with previously reported method in literature [154]. After the bromination of 2,1,3- benzothiadiazole in the presence of HBr/Br_2, reduction of 4,7-dibromobenzo[c][1,2,5]thiadiazole **(4)** was performed with $NaBH_4$ in ethanol. 3,6-Dibromobenzene-1,2-diamine (8.50mmol,2.30g), terephthalaldehyde (34 mmol, 4.56 g) and $ZrCl_4$ (0.43 mmol, 97.75 mg) were dissolved in acetonitrile (ACN) (150 mL) and the mixture was stirred at room temperature for 24 h. After the solid product was filtered, 150 mL ACN was added and the mixture was heated overnight under reflux conditions [155]. Afterwards the purified product was filtered as a pale yellow solid (5.1 mmol, 1.53 g, 60 %). ^{1}H NMR (d-DMSO): δ 10.11 (s, 1H), 8.56 (d, 2H, J = 8.26 Hz), 8.10 (d, 2H, J = 8.36 Hz), 7.44 (s, 2H). ^{13}C NMR (d-DMSO): 192.5, 151.5, 136.9, 133.9, 129.7, 129.5, 127.8, 127.6, 127.6.

2.3.2.2 Synthesis of 4-(4,7-di(thiophen-2-yl)-1H- benzo[d]imidazol-2-yl)benzaldehyde (BIBA)

Tributyl(thiophene-2-yl)stannane was synthesized according to a previously described method [156]. 4-(4,7-Dibromo-1H-benzo[d]imidazol-2-yl)benzaldehyde **(6)** (0.70 g, 1.70 mmol) and tri-butyl(thiophen-2-yl)stannane (3.18 g, 8.50 mmol) were dissolved in anhydrous THF (50 mL) and dichlorobis(triphenylphosphine)-palladium(II) (50 mg, 0.05 mmol) was added at room temperature. The mixture was refluxed for 12 h under argon atmosphere. Solvent was evaporated under vacuum and the crude product was purified by silica gel column chromatography as a yellow

solid (Fig. 2.2). (eluent: DCM) (0.60 g, 45 %). ^{1}H NMR (d-DMSO): δ 12.89 (s, 1H), 10.12 (s, 1H), 8.62 (d, 2H, J = 8.23 Hz), 8.26 (d, 1H, J = 3.56 Hz), 8.11 (d, 2H, J = 8.22 Hz), 7.72–7.65 (m, 4H), 7.40 (d, 1H, J = 7.85 Hz), 7.28 (dt, 1H, J = 4.74 and 3.91 Hz), 7.25 (dt, 1H, J = 4.76 and 3.91 Hz). ^{13}C NMR (d-DMSO): δ 192.2, 150.8, 140.2, 139.1, 138.4, 136.2, 134.3, 132.3, 129.2, 127.8, 127.5, 127.1, 126.1, 125.8, 125.5, 123.5, 122.8, 118.9, 117.6. HRMS: Calculated $[M]^{+}$ 387.0626, Measured $[M]^{+}$ 387.0631.

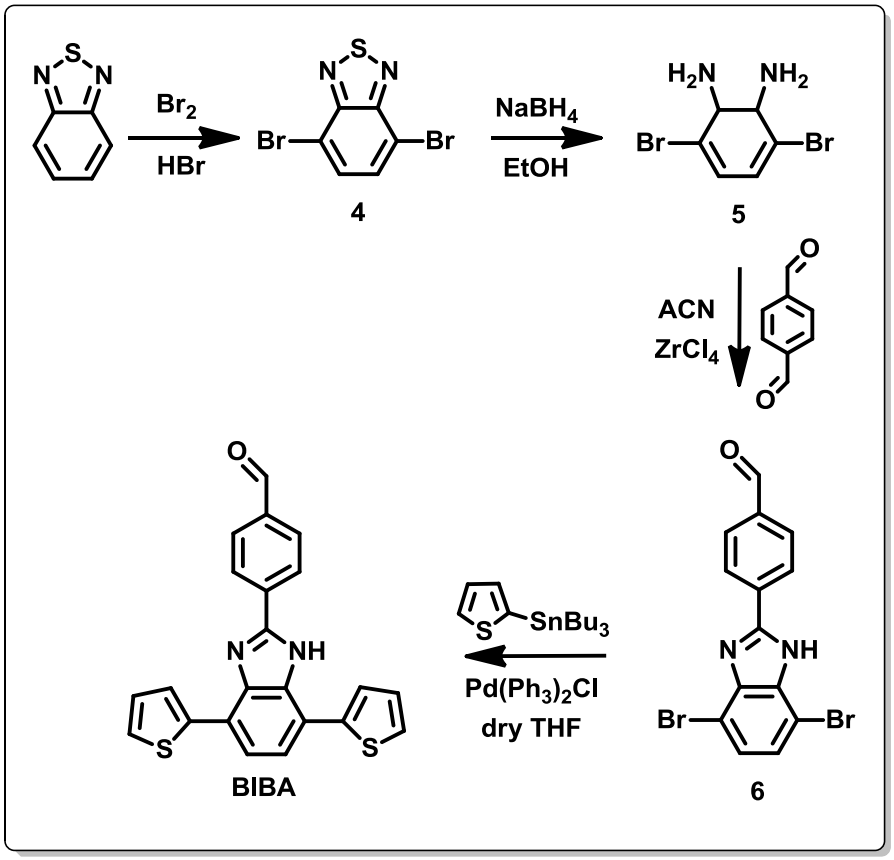

Figure 2. 2 Synthetic pathway of BIBA monomer

2.3.3 Electrochemical Polymerization of Monomers

2.3.3.1 Electropolymerization of SNS Anchored Acetic Acid Monomer

Prior to electrochemical polymerization, spectroscopic grade graphite rods were polished on emery paper and washed thoroughly with distilled water. Cyclic voltammograms were obtained with a standard three electrode configuration. Electrochemical polymerization of monomer was potentiodynamically carried out between the potential range 0.0 V and 1.1 V (versus Ag/AgCl reference electrode) in 0.1M ACN/ $NaClO_4$/$LiClO_4$ (as the supporting electrolyte) medium at a scan rate of 0.1 V s^{-1} on the graphite electrode.

2.3.3.2 Electropolymerization of BIBA monomer

For electropolymerization, corresponding monomer was dissolved in dichloromethane (DCM), due to poor solubility and mixed with ACN containing 0.1 M $LiClO_4$/$NaClO_4$ (1:1 mol) (DCM:ACN 5:95, v:v). Electrochemical polymerization of monomer was potentiodynamically carried out between the potential range 0.5 V and 1.8 V (versus Ag/AgCl reference electrode) at a scan rate of 0.1 V s^{-1} on the graphite electrode.

2.3.4 Spectroelectrochemistry Experiments of PBIBA Polymer

For spectroelectrochemistry studies, indium tinoxide (ITO) coated glass slide, platinum and silver wires were used as the working, counter and pseudo reference

electrodes, respectively. Electrochemical polymerization of corresponding monomer was potentiodynamically carried out between the potential range 0.5 V and 1.8 V (versus Ag wire as reference electrode) in the presence of 0.1M $NaClO_4/LiClO_4$ (1:1 mol) in (DCM:ACN 5:95, v:v) medium at a scan rate of 0.1 V s^{-1} on the graphite electrode. After the polymerization process, polymer coated ITO was washed with fresh ACN to remove unreacted monomer on the surface. Cyclic voltammogram of the polymer in a monomer free 0.1M $LiClO_4/NaClO_4$ (1:1 mol) acetonitrile solution was performed at a scan rate of 0.1 Vs^{-1}. During spectroelectrochemical investigation of the polymer, stepwise oxidation was applied while the UV-vis–NIR spectra were recorded.

2.3.5 Construction of Biosensor

2.3.5.1 SNS Anchored Acetic Acid Polymer Based Biosensors Construction

2.3.5.1.1 Lysine Modified Biosensor Construction

To prepare the Lys-modified biosensor, the SNS anchored acetic acid polymer-coated graphite electrode was immersed in 1.5 mL EDC:NHS (4:1) in 50 mM sodium phosphate buffer (pH 7.0) for 3 h. After washing with distilled water, the electrode was put into 1.5 mL Lys solution (4.5 mg in 50 mM sodium phosphate buffer, pH 7.0) for 3 h. During this procedure, amide bond formation was achieved between the carboxylic acid groups of the polymer and the amine groups of Lys. For the immobilization of enzyme, a proper amount of GOx solution (2.5 mg in 5.0 mL, 50 mM sodium phosphate buffer, pH 7.0) and glutaraldehyde (5.0 mL, 1.0 % in 50 mM sodium phosphate buffer, pH 7.0) were spread over the modified electrodes and treated for 2 h at ambient conditions prior to use.

2.3.5.1.2 PAMAM G2 and G4 Modified Biosensors Construction

The PAMAM dendrimer-modified electrodes were prepared as follows: The SNS anchored acetic acid polymer-coated graphite electrode was immersed in EDC:NHS (4:1) solution (5.0 mL) in 50 mM sodium phosphate buffer, pH 7.0 for 30 min. Then, the electrode was left in PAMAM solution (1.0 % PAMAM in 50 mM sodium phosphate buffer, pH 7.0) for 1 h. Afterwards the electrode was placed in $NaBH_4$ solution (5.0 mM) to reduce the Schiff base formation. GOx (1.0 mg in 2.5 mL 50 mM sodium phosphate buffer, pH 7.0) and GA (2.5 mL, 1.0 % in 50 mM sodium phosphate buffer, pH 7.0) solutions were spread over the modified electrode and it was allowed to stand at room temperature for 2 h. After immobilization, the unbound enzyme molecules were removed by rinsing the electrode surface with phosphate buffer solution and distilled water. All illustrations of Lysine, PAMAM G2 and G4 modified biosensors are summarized in Figure 2.3.

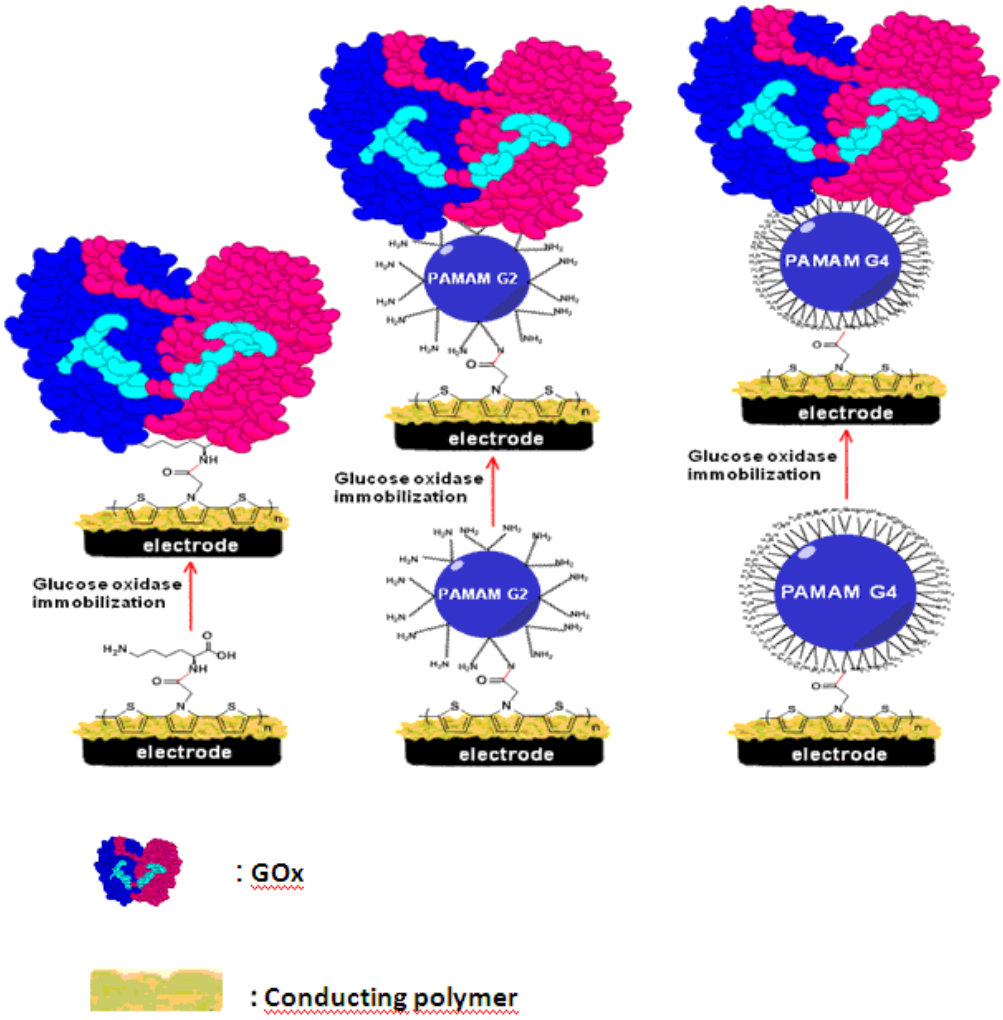

Figure 2. 3 Schematic representation of the surface modifications

2.3.5.2 PBIBA Polymer Based Biosensors Construction

2.3.5.2.1 Non-Modified PBIBA Polymer Biosensor Construction

After the graphite rod was cleaned with emery paper and dried thoroughly, corresponding BIBA monomer was electropolymerized on graphite electrode in the presence of 0.1M $LiClO_4/NaClO_4$ (1:1) in ACN/DCM (5:95,v:v) between the potential range 0.5 V and 1.8 V at a scan rate of 0.1 Vs^{-1}. In the biomolecule

conjugation step, GOx (50 U in 5 μL 50 mM phosphate buffer, pH=7.0) was immobilized with the help of GA (0.1 % in 5 μL distilled water) on the polymer coated graphite electrode.

2.3.5.2.2 Gold Nanorods (AuNRs) Modified Biosensor Construction

To fabricate the biosensor, BIBA monomer was coated on the purified graphite electrode by electropolymerization. After the polymerization, 4 μL AuNRs solution in distilled water which was mixed in a minute in an ultrasonic bath at room temperature was dropped into polymer surface and was allowed to dry for an hour. The AuNRds solution was synthesized by Emren Nalbant Esentürk Research Group according to a previously reported method [157]. GOx (1.25 mg in 5 μL 50 mM sodium phosphate buffer, pH 7.0) and GA (5 μL, 0.1 % in 50 mM sodium phosphate buffer, pH 7.0) solutions were spread over the modified electrode and it was allowed to stand at room temperature for 2 h. After immobilization, the unbound enzyme molecules were purified by rinsing the electrode surface with distilled water.

2.3.5.2.3 Single-Walled Carbon Nanotubes (SWCNT) Modified Biosensor Construction

The solution of 4 μL SWCNT in distilled water (1 mg SWCNT/ 1 mL distilled water left for 30 minutes in an ultrasonic bath at room temperature) was added on the graphite electrode surface which was purified with an emery paper before. After the electron surface was dried in an hour, corresponding monomer BIBA was electrochemically polymerized on the surface in the presence of 0.1M

$LiClO_4/NaClO_4$ (1:1) in ACN/DCM (5:95,v:v) between the potential range 0.5 V and 1.8 V at a scan rate of 0.1 Vs^{-1}. The surface was washed with water and phosphate buffer (50 mM, pH= 7.0) for removal of the organic residues. GOx (1.25 mg in 5 µL 50 mM sodium phosphate buffer, pH 7.0) and GA (5 µL, 0.1 % in 50 mM sodium phosphate buffer, pH 7.0) solutions were spread over the modified electrode and it was allowed to stand at room temperature for 2 h. After immobilization, the unbound enzyme molecules were purified by rinsing the electrode surface with distilled water. The polymer based biosensor and modified surfaces were illustrated in Fig. 2.4.

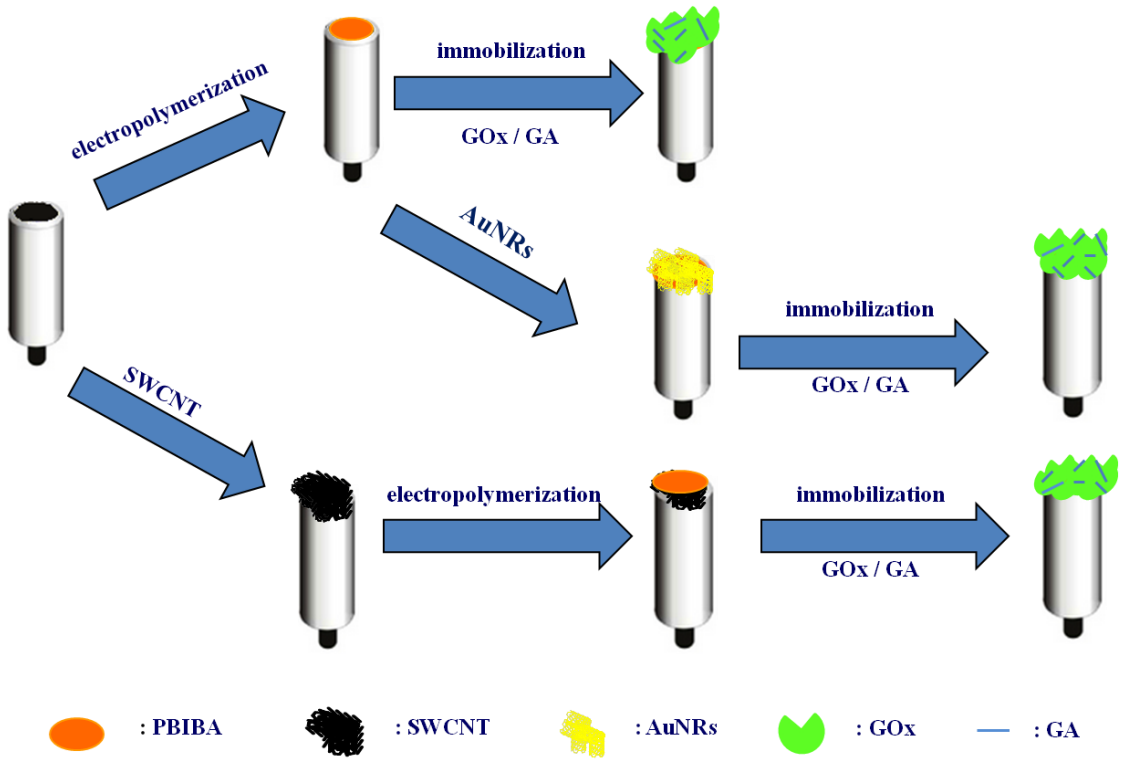

Figure 2. 4 Preparation of surface modified PBIBA based biosensors

2.3.6 Amperometric Measurements

All amperometric studies were carried out in sodium acetate buffer via application of -0.7 V versus Ag/AgCl electrode while mildly stirring at room temperature. In all experiments, current change due to the consumption of the molecular oxygen was detected; therefore, the difference between the baseline current and the steady state current after the addition of substrate was monitored. All measurements were performed by addition of glucose to the buffer solution (10 mL) in an electrochemical cell at steady state. After each measurement, the buffer solution in the cell was refreshed and the electrodes were washed with distilled water. The kinetic parameters were determined by testing the biosensors on various glucose concentrations; on the other hand, the same amounts of substrate were used for each biosensor. In all experiments, the average of three repetitive results was recorded for each glucose concentration to obtain calibration curves and standard deviations of these measurements were calculated.

2.3.7 Optimization Studies for Biosensors

2.3.7.1 Effect of Polymer Thickness on the Surface

Determination of the optimum polymer thickness is a very crucial parameter to obtain a stable biosensor. This parameter was optimized for each biosensor by changing the scan number during the electropolymerization. The same amount of surface modification materials, enzyme and cross linker were added to the polymer surface for immobilization. The amperometric measurements were carried out for each different scan number and results were recorded together with the standard deviations. The highest value was defined the optimum scan number and this value was used during other optimizations.

2.3.7.2 Effect of the Modification Materials Amounts

The optimization of the modification materials amounts assists to getting optimum morphology for a biosensor. The different amounts of modification materials were spread over the surface before or after the electropolymerization step. The amperometric studies were performed for the biosensors having the same scan number, same enzyme and same cross linker amounts. The highest result was recorded as the optimum modification material amount.

2.3.7.3 Effect of Enzyme Amount

The electrodes having optimum polymer thickness and surface modifiers were prepared. Afterwards; different amounts of GOx enzyme were immobilized on the surface with the help of the same amount of GA as cross linker. Amperometric measurements were achieved with the same concentration of substrate and the results were recorded. The biosensor with the highest response value was determined for the optimum enzyme loading. For the further studies, the biosensors were prepared according to this optimum value.

2.3.7.4 Effect of Crosslinker Amount

Glutaraldehyde was used as a crosslinker in all the biosensor preparations. For defining the optimum cross linker amount, the biosensors having the same parameters except cross linker were fabricated and the different amounts of cross linker were spread over the biosensors. According to highest response value against the same substrate concentration, the optimum amount of crosslinker was determined

and this amount was used the further measurements.

2.3.7.5 Effect of pH

Different buffer solutions with the same concentration and different pH values were prepared. The amperometric measurements were operated with the optimum biosensor responses to the same substrate concentration at different pH values. The results were recorded with the standard deviation values of three repetitive responses. The all further studies were performed with the optimum electrode at the optimum pH.

2.3.8 Determination of Analytic Characteristics for Biosensors

The optimum biosensors were prepared and tested for different substrate concentrations at optimum pH values at room temperature. The calibration curves were plotted for substrate concentrations (mM) versus current response (μA) with standard deviation values. The linearity equations, linear range and limit of detection (LOD) value were calculated at the optimum parameters.

2.3.8.1 Determination of Kinetic Parameters

Kinetic parameters (K_m^{app} and I_{max}) of the optimized enzyme biosensors were calculated from the Lineweaver–Burk plot at constant temperature and optimum pH. K_m is an important parameter which shows the affinity of enzyme through the substrates and represents the concentration value at V_{max} [158].

2.3.8.2 Operational and Storage Stabilities

The operational stability of each optimized enzyme electrode was determined by repetitive measurements of the substrate concentrations at constant temperature under the optimum conditions in the same day.

The storage stability of each biosensor was examined by measuring the amperometric responses every day for the same substrate concentrations under the optimized conditions. Between each subsequent measurement the biosensors were stored in contact with the working buffer at 4 ^{o}C.

2.3.9 Sample Applications

The corresponding biosensors were tested for real samples such as human blood serum samples and beverages. The results were given with relative errors (%).

2.3.9.1 Sample Applications Using Lysine, PAMAM G2 and G4 Modified SNS-anchored Acetic Acid Based and PBIBA Based Biosensors

The biosensors were tested for real human serum samples to determine the concentration of glucose in order to test biosensors' accuracy. All experiments were performed in compliance with relevant laws and approval of ethical committee. These samples were first analyzed in a local hospital and the actual glucose levels were determined with a reference method. During the measurements, the certain amounts of blood serum samples were injected as the substrate in the buffer solution

instead of the glucose solution. The experiments were performed at the optimized conditions and a constant temperature of 25 ^{o}C. The results were compared with the ones obtained in the hospital results.

2.3.9.2 Sample Applications Using AuNRs and SWCNT Modified PBIBA Based Biosensors

The glucose concentrations in various beverages with different brands were analyzed by the designed biosensors. During the measurements, each sample injected through the buffer solution instead of standard glucose solution at steady state. The same samples were tested by spectroscopic techniques and the results were compared each other.

CHAPTER 3

3. RESULTS AND DISCUSSIONS

3.1 Poly-SNS-anchored Acetic Acid Based Glucose Biosensors

Poly-SNS-anchored carboxylic acid moiety was reported as a promising immobilization matrix for GOx in a previous work [153]. In this study, it is aimed to enhance the spots which provide the covalent attachment with GOx *via* surface modification techniques. Amine group, one of the mostly used functional groups for immobilization, was preferred to yielding covalent binding between modified polymer matrix and GOx. In order to achieve an efficient covalently bound GOx immobilization and define the increasing junction point effect of surface modification material over biosensor performance, Lysine amino acid, PAMAM G2 and PAMAM G4 dendrimers were utilized on the polymer matrix with their amine functional groups. Before that, as a first step electropolymerization of SNS-anchored carboxylic acid monomer was performed at convenient ambient conditions.

3.1.1 Electropolymerization of the Monomer

Electrochemical synthesis of poly-SNS-anchored carboxylic acid polymer was achieved by multiple scan voltammetry technique in a 0.1M $NaClO_4/LiClO_4$ (1:1 mol) in (DCM: ACN 5:95, v:v) medium at a scan rate of 0.1 V s^{-1} on the graphite electrode. In order to determine the electroactivity and oxidation reduction potentials of polymer, all electrochemical studies were performed in three electrode cells using graphite electrode as the working, Pt wire as the counter and Ag/AgCl as the pseudo reference electrodes. The potentials were swept between 0.0 V and 1.1 V versus Ag/AgCl electrode (Fig. 3.1).

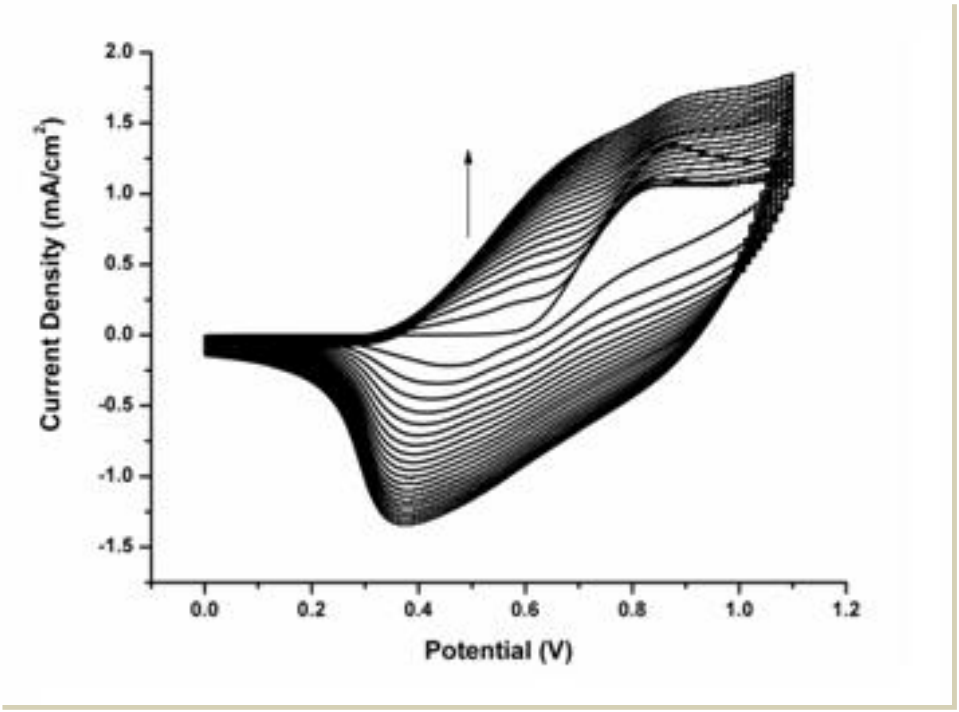

Figure 3.1 Repeated potential-scan electropolymerization of SNS-anchored carboxylic acid at 0.1 V s^{-1} in 0.1M ACN/$NaClO_4$/$LiClO_4$ solvent/electrolyte system on graphite electrode (up to 20 cycles).

The electropolymerization of monomer is accomplished with $E(CE)_n$ mechanism reactions which involve electrogeneration of radical cations and their regular chemical couplings [159-160]. According to cyclic voltammogram of polymerization, irreversible oxidation peak of monomer was observed at 0.85 V and reversible redox peaks of polymers were appeared at 0.4 V and 0.65 V. The increasing in current values with the increasing number of cycle proves the polymerization and the electroactivity of the polymer on the surface.

3.1.2 Optimization Studies of Poly-SNS-anchored Carboxylic Acid Based Biosensors

3.1.2.1 Effect of Polymer Thickness on the Surface

The thickness of the polymer layer on the surface can be easily arranged by controlling of the scan number during electropolymerization process. In order to determine polymer thickness effect on the biosensor performance, the biosensors having different scan numbers of polymers were prepared by keeping all other parameters constant and corresponding responses related to the same glucose concentrations were recorded (Fig. 3.2).

As illustrated in Figure 3.2 the thickness of conducting polymer layers affect the biosensor performance due to changing morphology of the surface. Decreasing the polymer thickness in correlation with scan number eliminates the steric hindrance effect on the surface and allows the efficient electron transfer between the electrode surface and the biomolecule. Furthermore, modifying agents such as amino acid and PAMAM G2, PAMAM G4 dendrimers can easily get closer to the surface to form covalent attachment with the polymer. Since the thin polymer layer includes less functional group leading to produce covalent attachments between surface modifiers and polymer, fewer modifiers can interact with the surface. Thus, the surface volume cannot be enhanced to immobilize desired amount of GOx enzyme. In contrary to that handicap, increasing in the polymer thickness can allow positioning more functional groups of modifiers providing an interaction with more amount of GOx enzyme on the surface. On the other hand, due to robust covalent and electronic interactions between biomolecule and the modified electrode surface, huge enzyme molecules can be stabilized on the surface to give wide range of reactions with corresponding substrate. In a thick polymer layer, the electron transfer rate decreases relying on an increase in the diffusion layer distance between polymer coating and the electrode surface. To provide both efficient charge transfer and stabilization of desired enzyme amount on the surface, the optimum polymer layer thickness should

be determined for each modifier agent. According to optimization studies, 20 cycles of polymer production was determined as to satisfy the optimum thickness for the Lys- and PAMAM G2-modified electrodes. On the other hand a 10 scan polymerization was found to be the optimum for the PAMAM G2-modified biosensor (Fig. 3.2). The charge and film thickness in the optimum conditions were also calculated as 60 mC (1.33 mm) and 120 mC (2.67 mm) for 10 and 20 cycles of polymer, respectively.

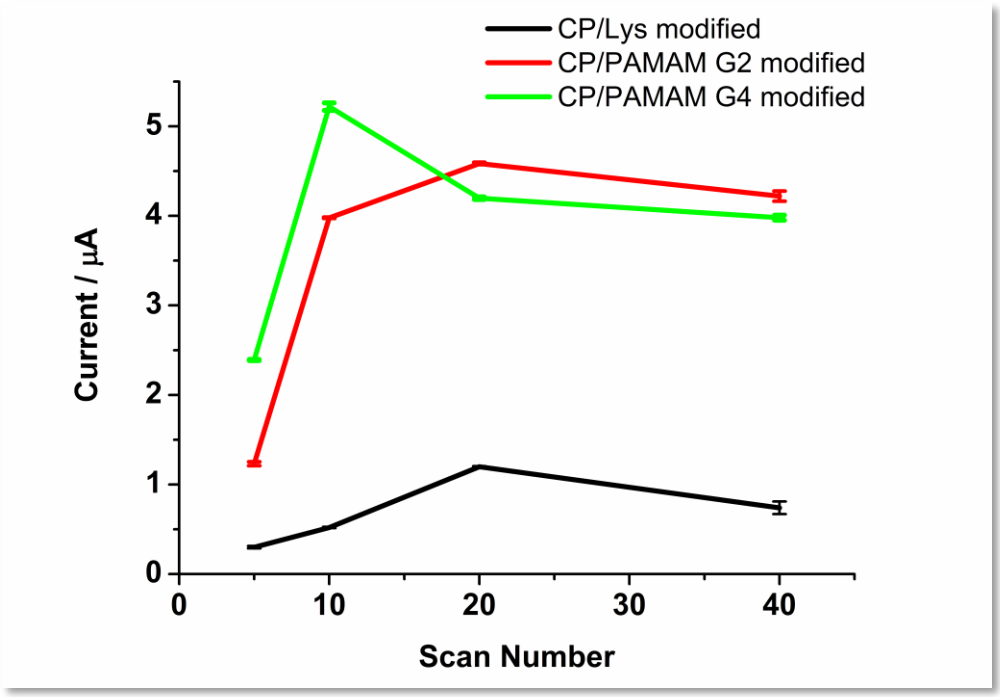

Figure 3. 2 Effect of scan number on biosensor responses (in 50 mM sodium acetate buffer, pH 5.5, 25 ^{o}C, -0.7 V). The corresponding measurements were performed with 0.75 mM glucose. Error bars show the standard deviation (SD) of three measurements.

3.1.2.2 Effect of Lysine, PAMAM G2 and PAMAM G4 Amounts

The drawback of the enzyme leaching from the biosensor surface throughout the measurements can be prevented by providing the stabilization of biomolecule on the electrode surface. In this regard, creation of new immobilization matrices is a noteworthy quest subject for development of sensitive and long-term stable biosensors. Ideally, a biosensor matrix should be a well orginized surface and include high ligand density having stable attachments of biomolecule during the immobilization step. Thus, surface modification of immobilization matrix has a significant role to enhance the overall performance of a biosensor. In order to produce two-dimensional matrices or three dimensional supramolecular architectures, the conducting polymer coated surfaces were modified with Lys amino acid, PAMAM G2 and PAMAM G4 dendrimers, respectively. The common feature of these modifiers is amine functional group content which leads to covalent attachment with enzyme molecules using convenient chemicals. On the other hand, it is possible to compare the effect of structural differences on overall biosensor performance.

The enhancement of the diffusion layer distance from the surface makes the charge transfer decrease and causes the responses to decline. On the contrary, deficiency of functional groups on the immobilization matrix triggers enzyme leaching from the surface through chemical interactions between matrix and the enzyme molecules. Considering the structural differences of surface modifiers, the effect of Lys, PAMAM G2 and PAMAM G4 amounts over biosensor responses were investigated by amperometric techniques. For this purpose, different amounts of surface modifiers were covalently attached on the conducting polymer coated surface using EDC and NHS reagents. After the same amount of GOx enzyme was immobilized on the modified surfaces with the help of the GA, the current responses against the same glucose concentration were recorded. The results of amperometric measurements exhibits that 2.5 mg Lys (in 5.0 mL 50 mM phosphate buffer, pH 7.0), 2.5 mL 0.5 % PAMAM G2 and 2.5 mL 0.5 % PAMAM G4 amounts are the optimum values for

surface modification of SNS-anchored carboxylic acid polymer.

3.1.2.3 Effect of Biomolecule Amount

Sensitivity of the biosensors can be correlated with the amount of immobilized enzyme. To determine the effect of enzyme loading on the responses, different amounts of enzyme varied from 0.5 mg (10.40 Units) to 6.0 mg (125 Units) were immobilized on the modified electrode surfaces coated with the optimum thickness of polymer, amino acid and the dendrimer. The enzyme was stabilized using equal amount of GA (1.0 %) for each biosensors. As illustrated in Figure 3.3, the highest signals were obtained with the biosensors prepared with 4.5 mg (93.75 Units) GOx for Lys-modified and 1.0 mg (20.80 Units) GOx for PAMAM G2 and G4-modified biosensors.

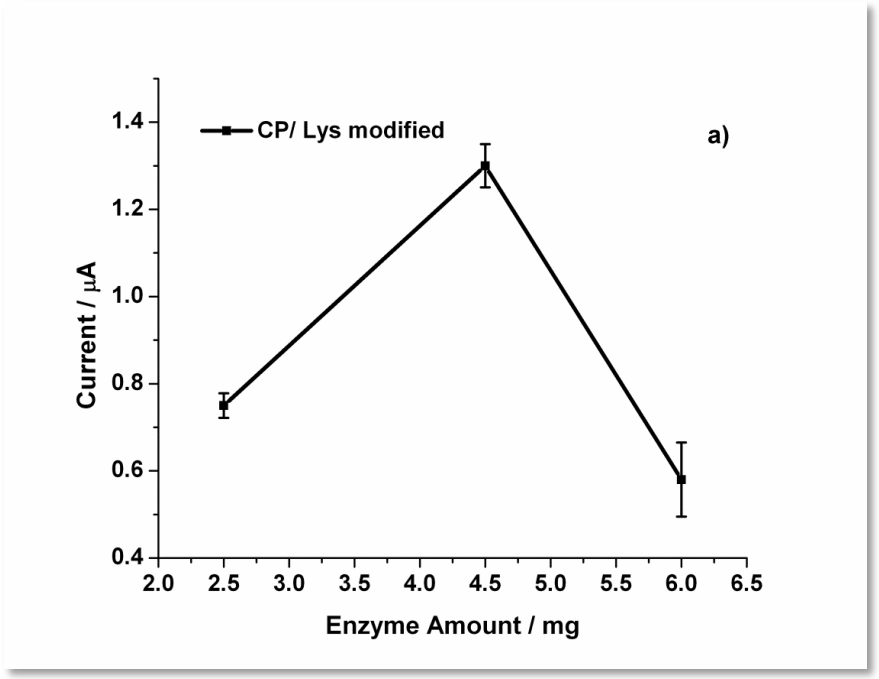

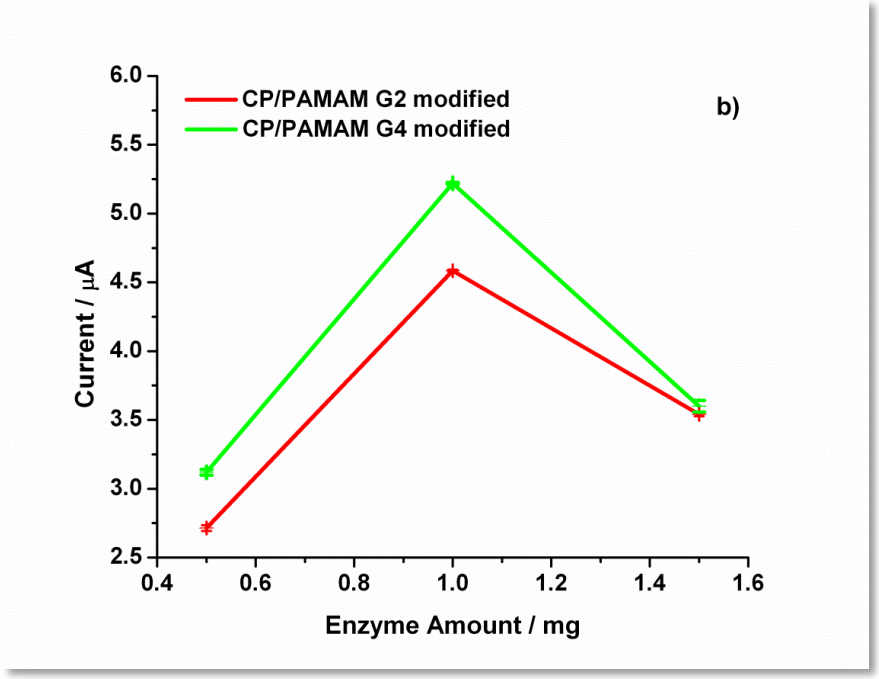

Figure 3. 3 Effect of biomolecule amount on a) Lys modified b) PAMAM G2 and PAMAM G4 modified biosensors (in 50 mM sodium acetate buffer, pH 5.5, 25 ^{o}C, -0.7 V). The corresponding measurements were performed with 0.75 mM glucose. Error bars show the standard deviation (SD) of three measurements.

3.1.2.4 Effect of Glutaraldehyde Amount

Glutaraldehyde (GA) is a specific reagent mostly used as a crosslinker for enzyme stabilization on electrode surface [161-162]. The excess amount of GA causes the highly crosslinked network preventing charge transfer. Furthermore, the excess crosslinkages occur between the internal amine groups of enzymes, thus current responses decrease depending on the activity loss of biomolecules [163]. The low amount of GA leads to decrease in current responses hence, the covalent attachments between modified electrode surface and the biomolecule can not be efficiently satsfied, and due to the deficiency of crosslinker, the biomolecule can leak from the surface to the solution media. GA enables cross-linking between the amine groups of Lys, dendrimers and the amine groups of enzyme molecules. In this study, different amounts (0.01 %, 0.05 %, 1.0 %, 2.5 %) of GA were used in the preparation of each electrode. A 1.0 % GA amount was determined as the optimum GA for each biosensor (Fig. 3.4).

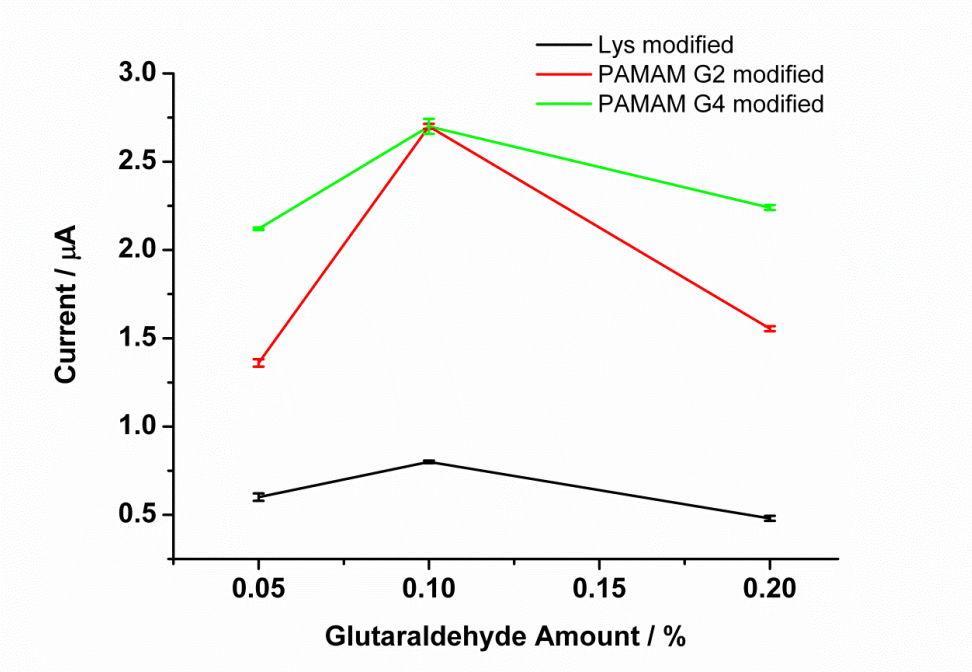

Figure 3. 4 Effect of crosslinker (glutaraldehyde) amount on biosensor responses (in 50 mM sodium acetate buffer, pH 5.5, 25 ^{o}C, -0.7 V). The corresponding measurements were performed with 0.40 mM glucose. Error bars show the standard deviation (SD) of three measurements.

3.1.2.5 Effect of pH

Since the bioactivity of the enzyme depends on the pH of the solution, and extreme pH conditions cause enzyme denaturation, the optimum pH values should be determined. The optimization experiments were carried out by preparing an optimum enzyme electrode and the biosensor was tested with 0.40 mM glucose as the substrate in different pH values. Thus, the responses were recorded and effect of pH versus responses is summarized in Figure 3.5. The biosensors showed the maximum responses at 50 mM pH 5.5 sodium acetate buffer and this optimum pH value was used in further amperometric measurements.

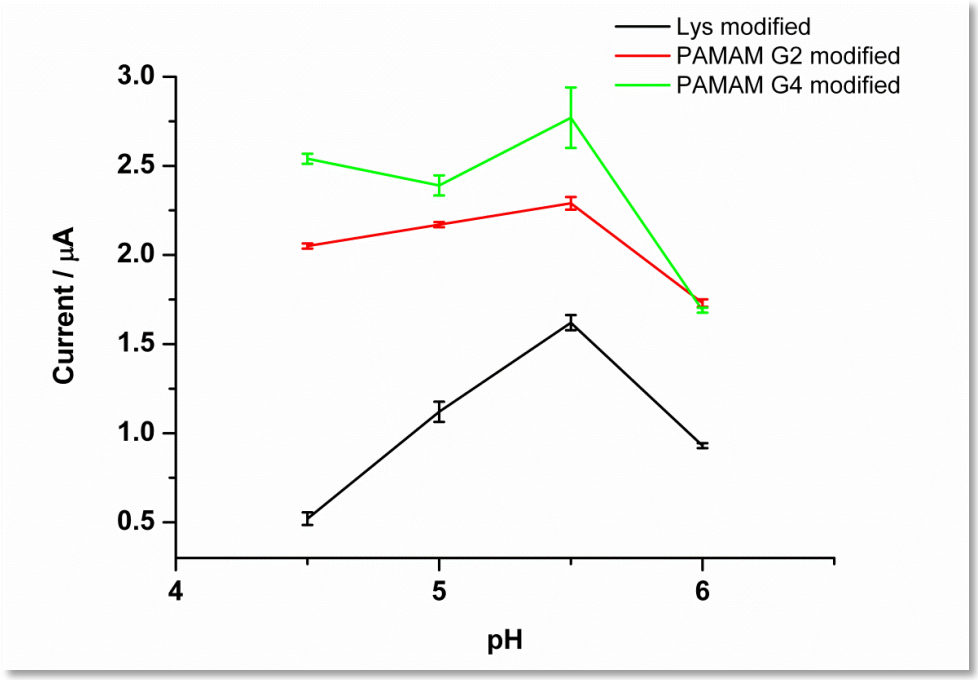

Figure 3. 5 Effect of pH at 25 ^{o}C, -0.7 V. The measurements were performed with 0.40 mM glucose. Error bars show the standard deviation (SD) of three measurements.

3.1.3 Surface Characterization

3.1.3.1 X-Ray Photoelectron Spectroscopy (XPS)

The characterization of the modified layers was performed *via* X-ray photoelectron spectroscopy (XPS). It is possible to determine the amide bond formation between carboxylic acid groups of the polymer and amine groups of Lys, PAMAM G2 and G4 molecules. X-Ray photoelectron spectra of the polymer, Lys, PAMAM G2 and PAMAMG4-modified electrodes and enzyme coated surfaces are indicated in Figure 3.6. The C1s and N1s spectra were well fitted by a fitting program.

In addition to C–N, C=N (286.1 eV) groups and characteristic carboxyl group (290.6 eV) in figure 10 a, the specific signals representing aromatic C_{α}, C_{β} of pyrrole ring

and C–S were indicated at 283.8 eV and 284.9 eV, respectively. According to protein immobilization, the new expected chemical bonds between protein and the polymer were formed and readily detected through XPS analysis (Figures 3.6c-d). The protein-immobilized surface (Fig. 3.6c) exhibited two signals at 287.0 eV and 288.1 eV (C=O and (C=O)–N respectively), indicating the presence of an amide bond as expected. No such signal for an amide bond was detected for the untreated polymer coated electrode (Fig. 3.6a) confirming the successful deposition of GOx molecules on the surface of the SNS-anchored carboxylic acid polymer. The similar information regarding the immobilization of biomolecule can also be obtained from the N1s spectra (Fig. 3.6b-d). In Figure 3.6d, two new peaks can be fitted regarding to nitrogen envelope of free $–NH_2$ and amide bond nitrogens at 398.2 eV and 396.7 eV in addition to the previously obtained spectrum representing only the polymer (Fig. 3.6b).

The Lys immobilized surface (Fig. 3.6e) exhibited a signal at 287.841 eV (–N–(C=O)) which was assigned to the presence of an amide bond between the polymer and Lys molecules, as expected. In addition to the C1s data, there are two new signals representing $–NH_2$ (398.433 eV) and –N–(C=O)– (400.499 eV) in the N1s spectrum of the Lys-modified surface (Fig. 3.6f) [164]. The increase in the intensity of –C=N–, –C=O (284.167 eV), and (C=O)–N (285.675 eV) peaks in the C1s spectrum (Fig. 3.6e) and the –N–(C=O)– (398.35 eV) peak in the N1s spectrum (Fig. 3.6f) were observed due to protein immobilization on the surface. Figures 3.6g–h represent the C1s and N1s spectra of the PAMAM G2-modified polymer-coated electrode and the protein immobilized surfaces on these layers, respectively. As illustrated in these spectra, the signals of $–NH_2$ (398.67 eV) and –N–(C=O) (397.67 eV) in N1s (Fig. 3.6h) show the increase in their intensity depending on the increasing terminal amine groups of PAMAM G2 dendrimers on the surface [165]. These expected results prove that the attachment of PAMAM G2 dendrimer was successfully carried out. The protein immobilized surface exhibited a characteristic signal at 291.36 eV representing the (C=O)– OH group of GOx enzymes on the modified surface (Fig. 3.6i). Similar results for the modification of the polymer-coated electrode with PAMAM G4 and the immobilization of the biomolecules were reported in Figure 3.6k–n.

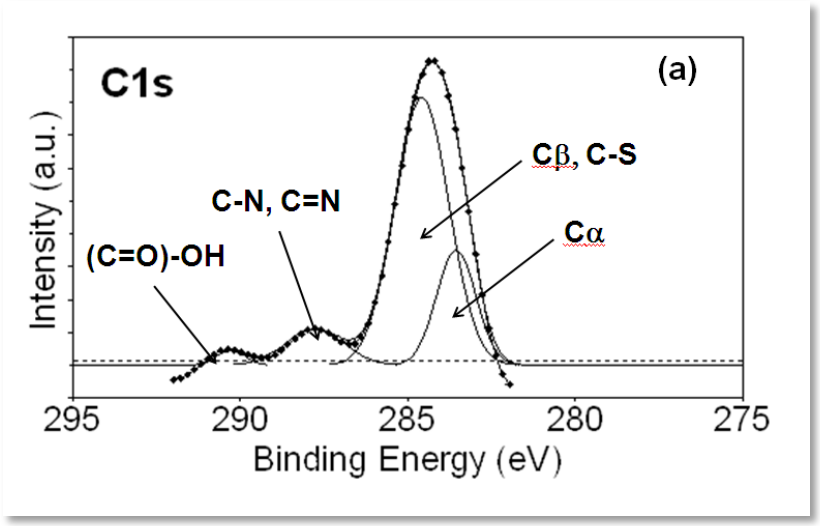

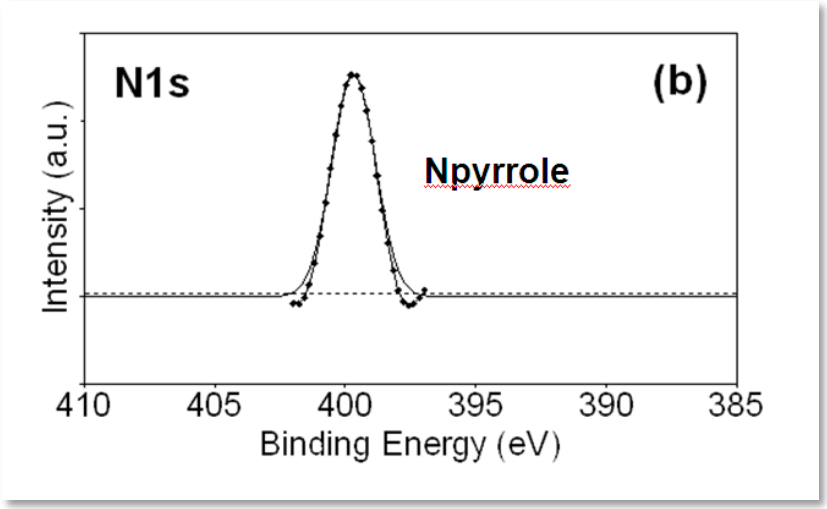

Figure 3. 6 C1s and N1s XPS spectra of polymer-coated electrode (a,b), Lys, PAMAM G2, PAMAM G4-modified polymer-coated surfaces (c,d; g,h; k,l) and GOx immobilized surfaces on polymer-coated modified surfaces (e,f; i,j; m,n), respectively.

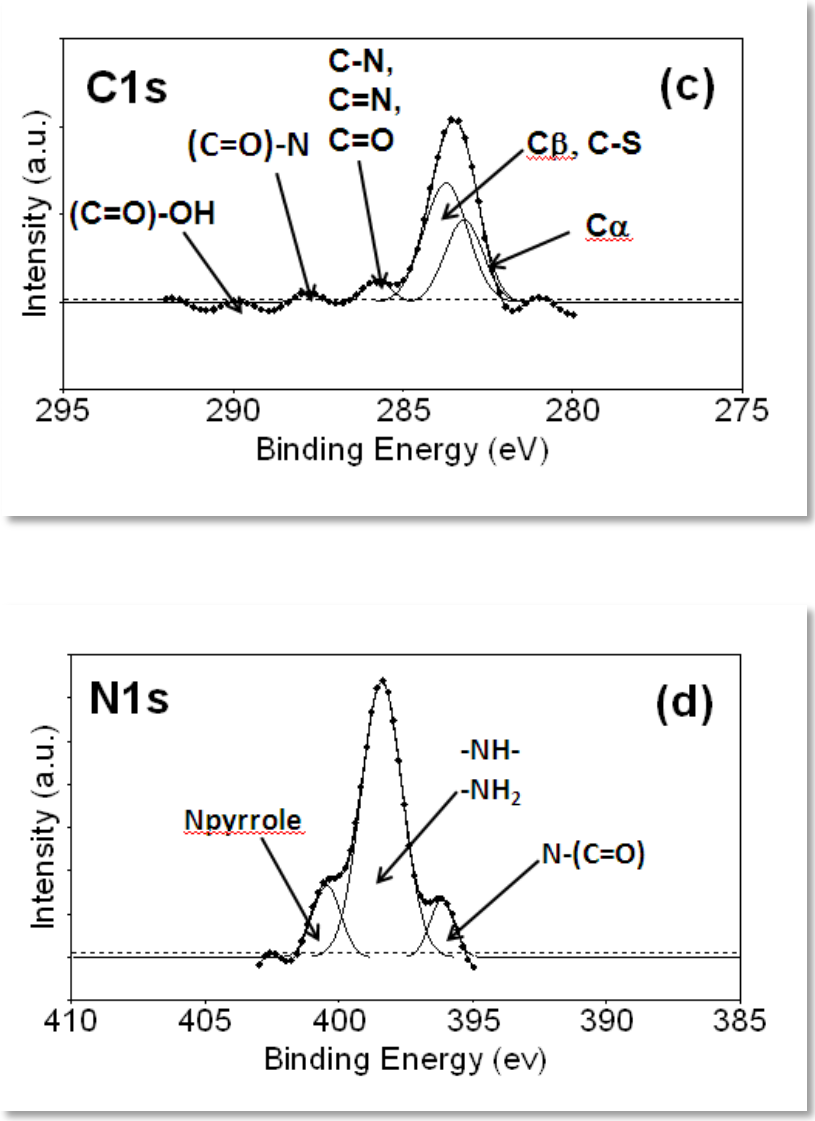

Figure 3. 7 (continued) C1s and N1s XPS spectra of polymer-coated electrode (a,b), Lys, PAMAM G2, PAMAM G4-modified polymer-coated surfaces (c,d; g,h; k,l) and GOx immobilized surfaces on polymer-coated modified surfaces (e,f; i,j; m,n), respectively.

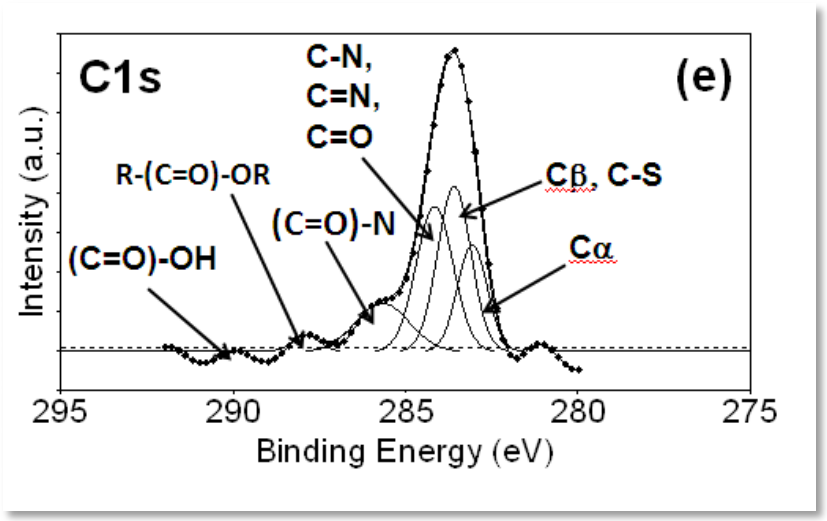

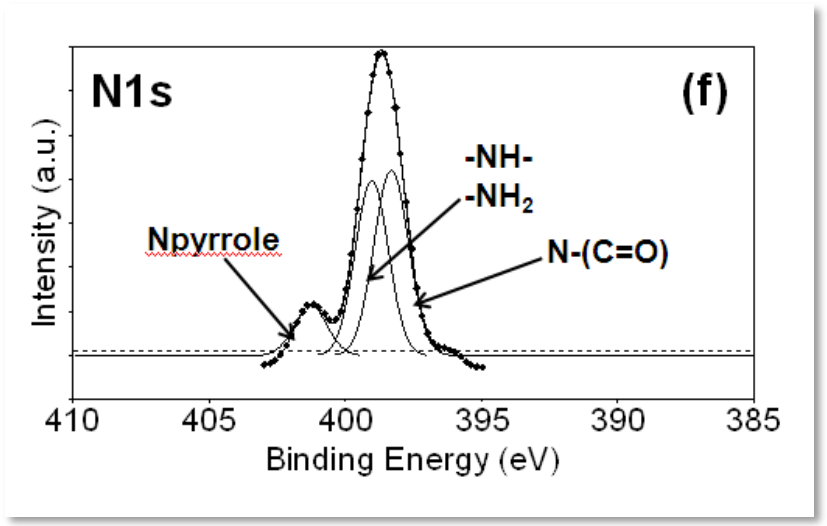

Figure 3. 8 (continued) C1s and N1s XPS spectra of polymer-coated electrode (a,b), Lys, PAMAM G2, PAMAM G4-modified polymer-coated surfaces (c,d; g,h; k,l) and GOx immobilized surfaces on polymer-coated modified surfaces (e,f; i,j; m,n), respectively.

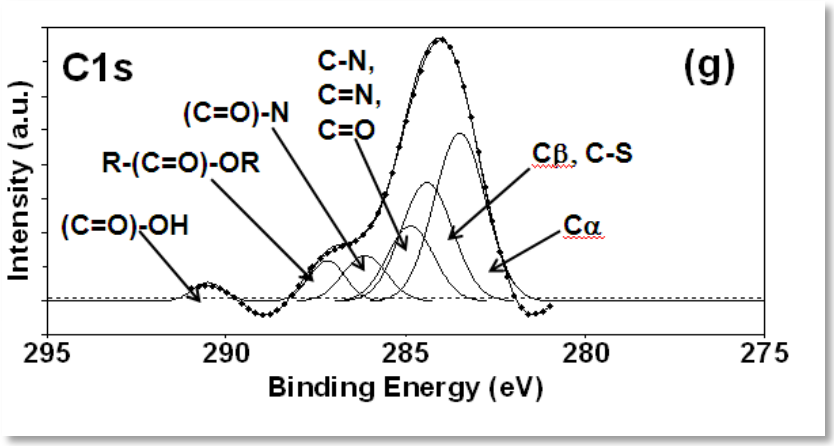

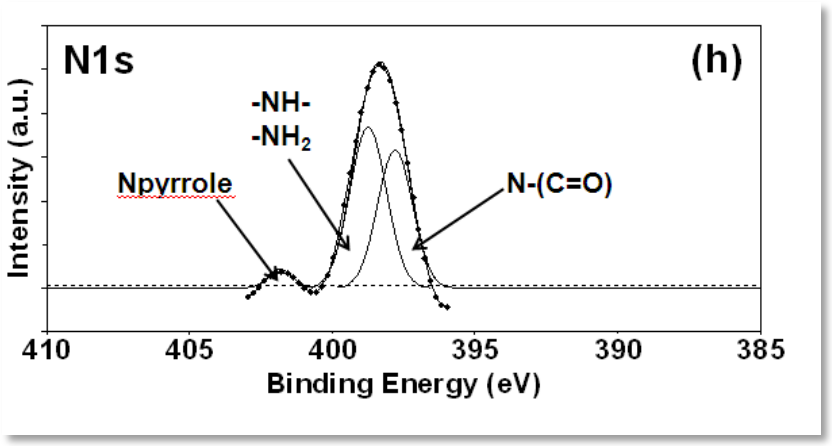

Figure 3. 9 (continued) C1s and N1s XPS spectra of polymer-coated electrode (a,b), Lys, PAMAM G2, PAMAM G4-modified polymer-coated surfaces (c,d; g,h; k,l) and GOx immobilized surfaces on polymer-coated modified surfaces (e,f; i,j; m,n), respectively.

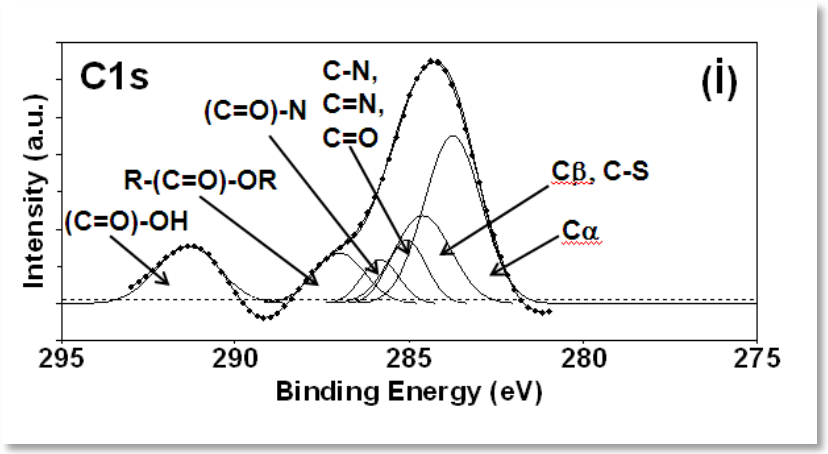

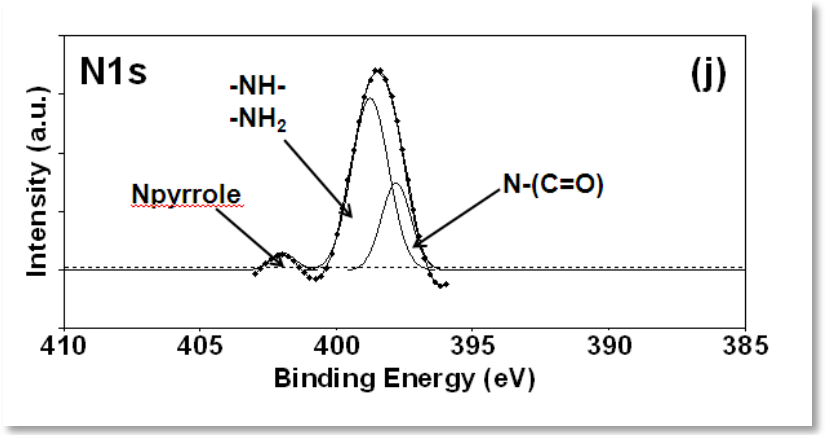

Figure 3. 10 (continued) C1s and N1s XPS spectra of polymer-coated electrode (a,b), Lys, PAMAM G2, PAMAM G4-modified polymer-coated surfaces (c,d; g,h; k,l) and GOx immobilized surfaces on polymer-coated modified surfaces (e,f; i,j; m,n), respectively.

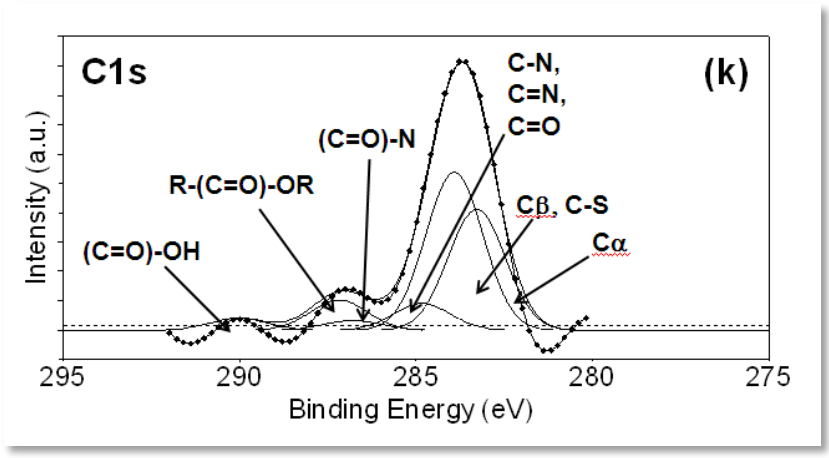

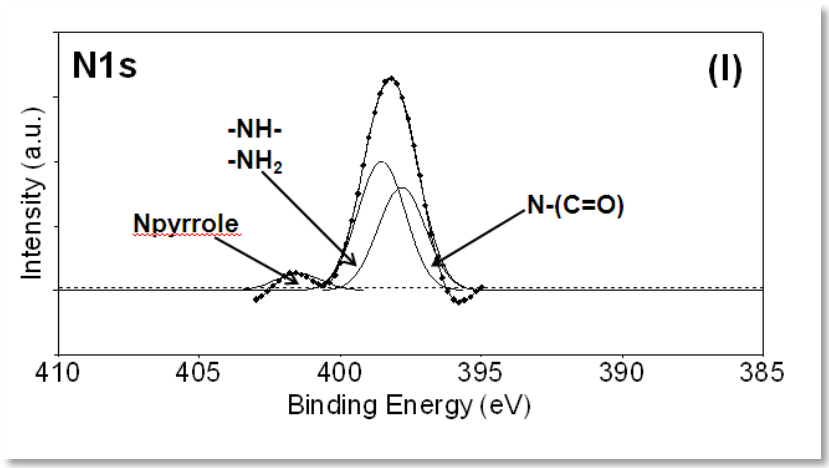

Figure 3. 11 (continued) C1s and N1s XPS spectra of polymer-coated electrode (a,b), Lys, PAMAM G2, PAMAM G4-modified polymer-coated surfaces (c,d; g,h; k,l) and GOx immobilized surfaces on polymer-coated modified surfaces (e,f; i,j; m,n), respectively.

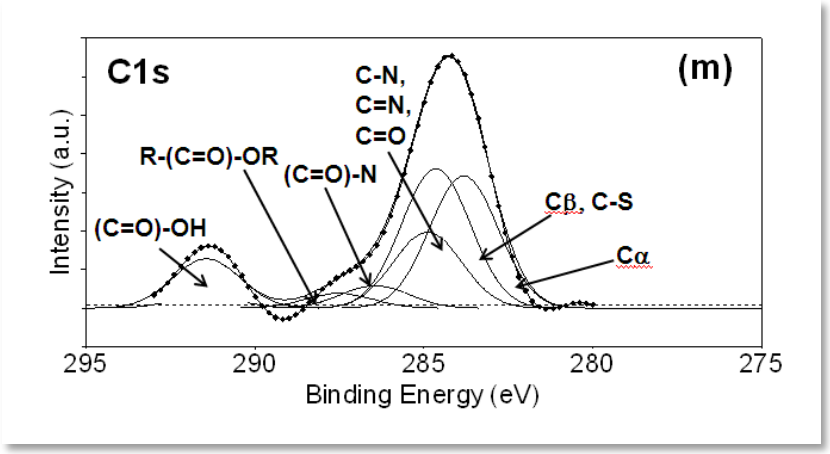

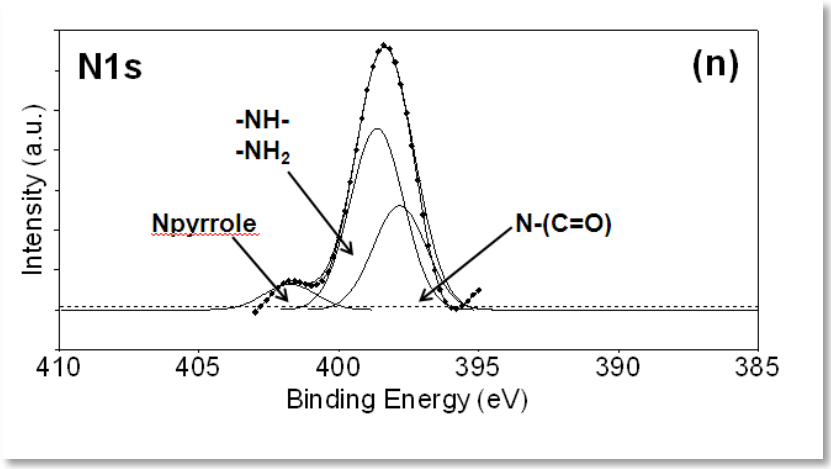

Figure 3. 12 (continued) C1s and N1s XPS spectra of polymer-coated electrode (a,b), Lys, PAMAM G2, PAMAM G4-modified polymer-coated surfaces (c,d; g,h; k,l) and GOx immobilized surfaces on polymer-coated modified surfaces (e,f; i,j; m,n), respectively.

3.1.3.2 Atomic Force Microscopy (AFM)

The surface morphology was investigated for each coated electrode *via* AFM in intermittent mode. Figure 3.7 shows the characteristic AFM images of the surface

topography of the modified electrodes at various deposition steps of Lys, PAMAM G2 and G4, respectively. In the vertical direction, darker areas represent the deeper side, contrary to lighter ones. The Lys-modified surface is fairly smooth (Fig. 3.7a). On the other hand, the GOx immobilized surface is rough and non-uniform (Fig. 3.7b). Depending on the smaller molecular dimension of Lys, the size of the surface features is relatively smaller on the Lys-modified one compared to PAMAM dendrimer surfaces. Surface roughness reached the maximum value when the GOx was immobilized on the PAMAM G4 layer (Fig. 3.7e); this is because the PAMAM G4 matrix is more indented than those of the PAMAM G2 and Lys matrices (Fig. 3.7a-c). Surface roughness (RMS) values were obtained as 0.8 nm and 0.5 nm for the Lys-modified surface. For PAMAM G2-modified one, they were 1.9 nm and 0.8 nm. As for the PAMAM G4-modified surface the values were 2.0 nm and 1.0 nm before and after biomolecule immobilization, respectively. Similar observations were also found a previous work in which the enzyme was immobilized on the gold surface after layer by layer modification with PAMAM G4 structure [166]. It is obvious that the immobilization of the enzyme molecules brings the homogeneity of the formed structure on the surface.

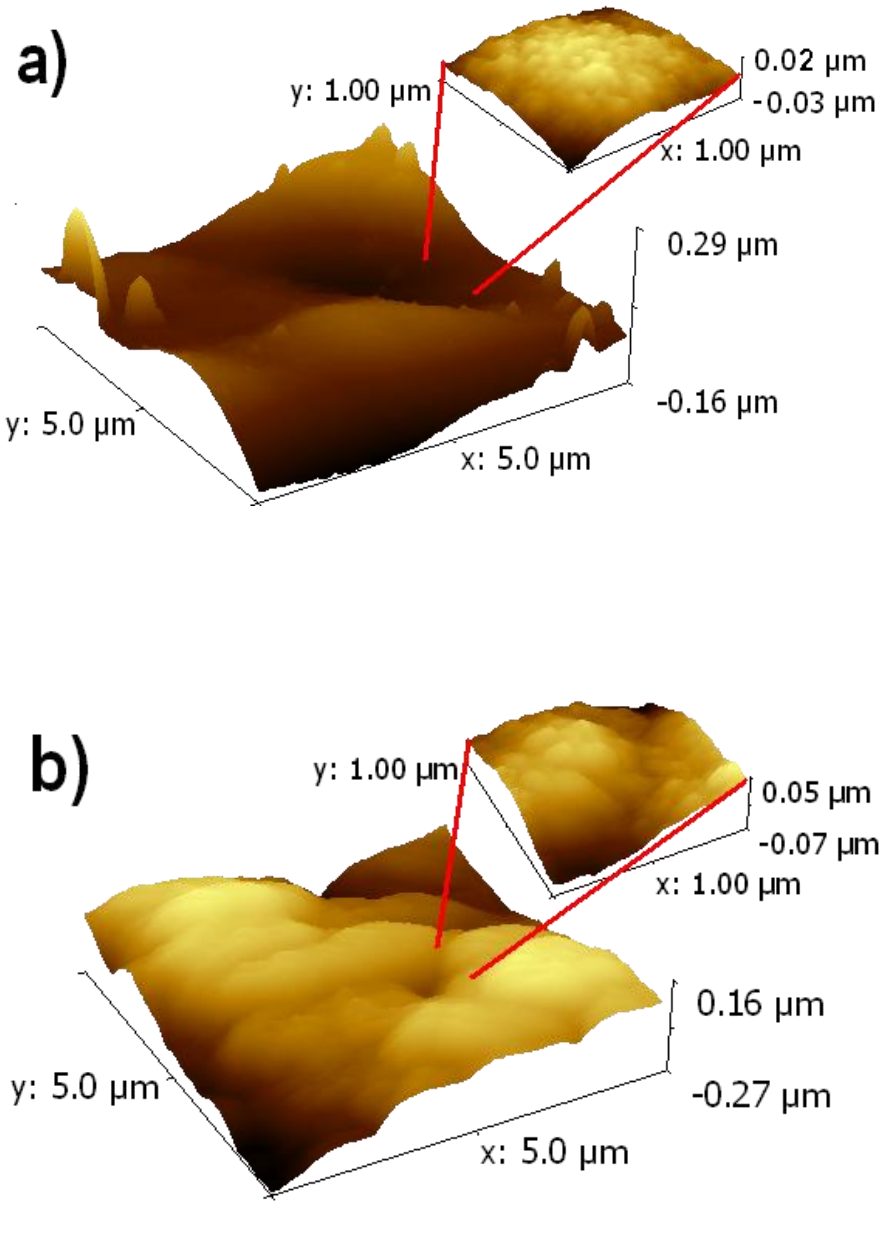

Figure 3. 13 3-D topographic AFM height images of Lys-, PAMAM G2-, PAMAM G4-modified polymer-coated electrode surface before (a,c,e) and after (b,d,f) biomolecule (GOx) immobilization at the optimized conditions, respectively.

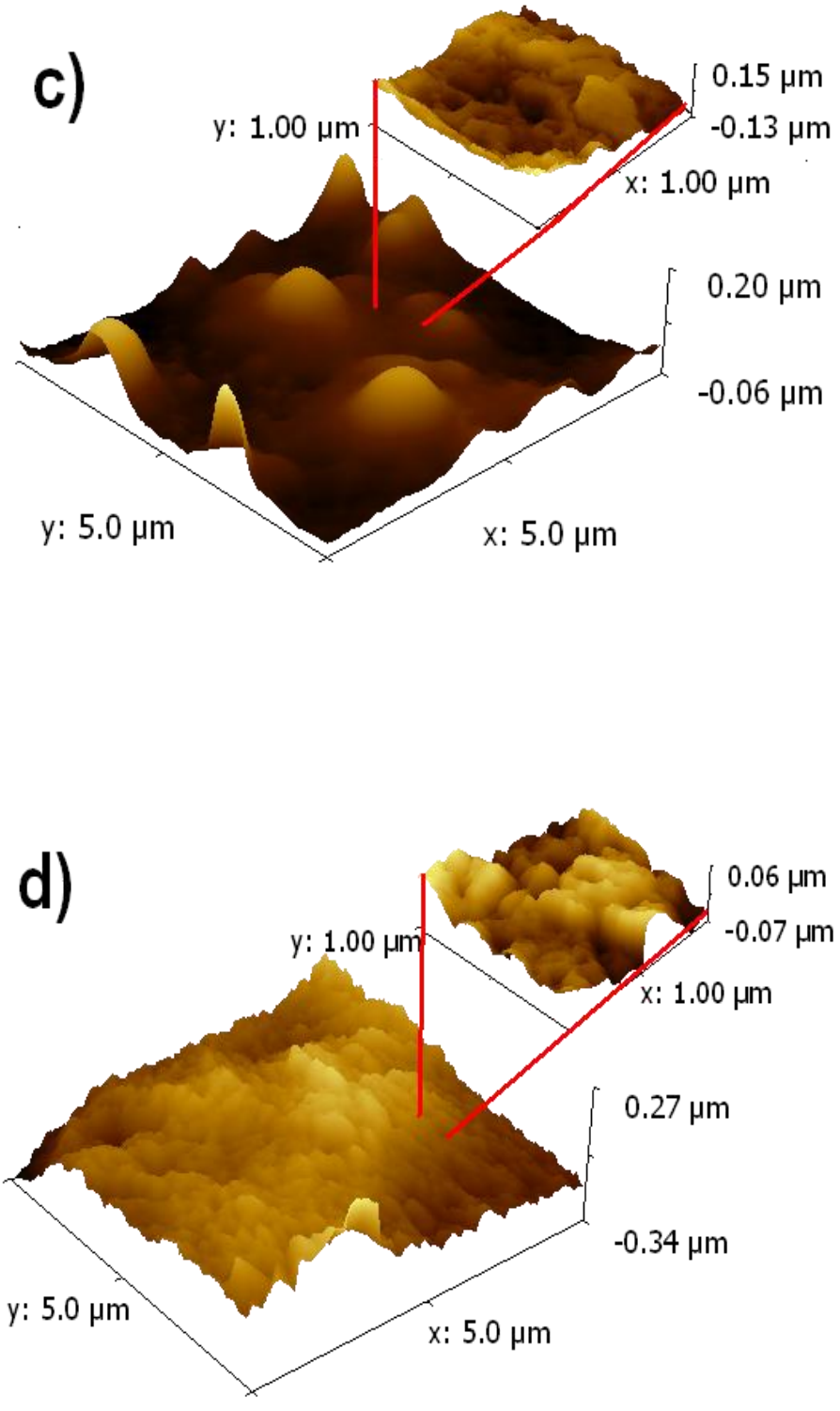

Figure 3. 14 (continued) 3-D topographic AFM height images of Lys-, PAMAM G2, PAMAM G4-modified polymer-coated electrode surface before (a,c,e) and after (b,d,f) biomolecule (GOx) immobilization at the optimized conditions, respectively.

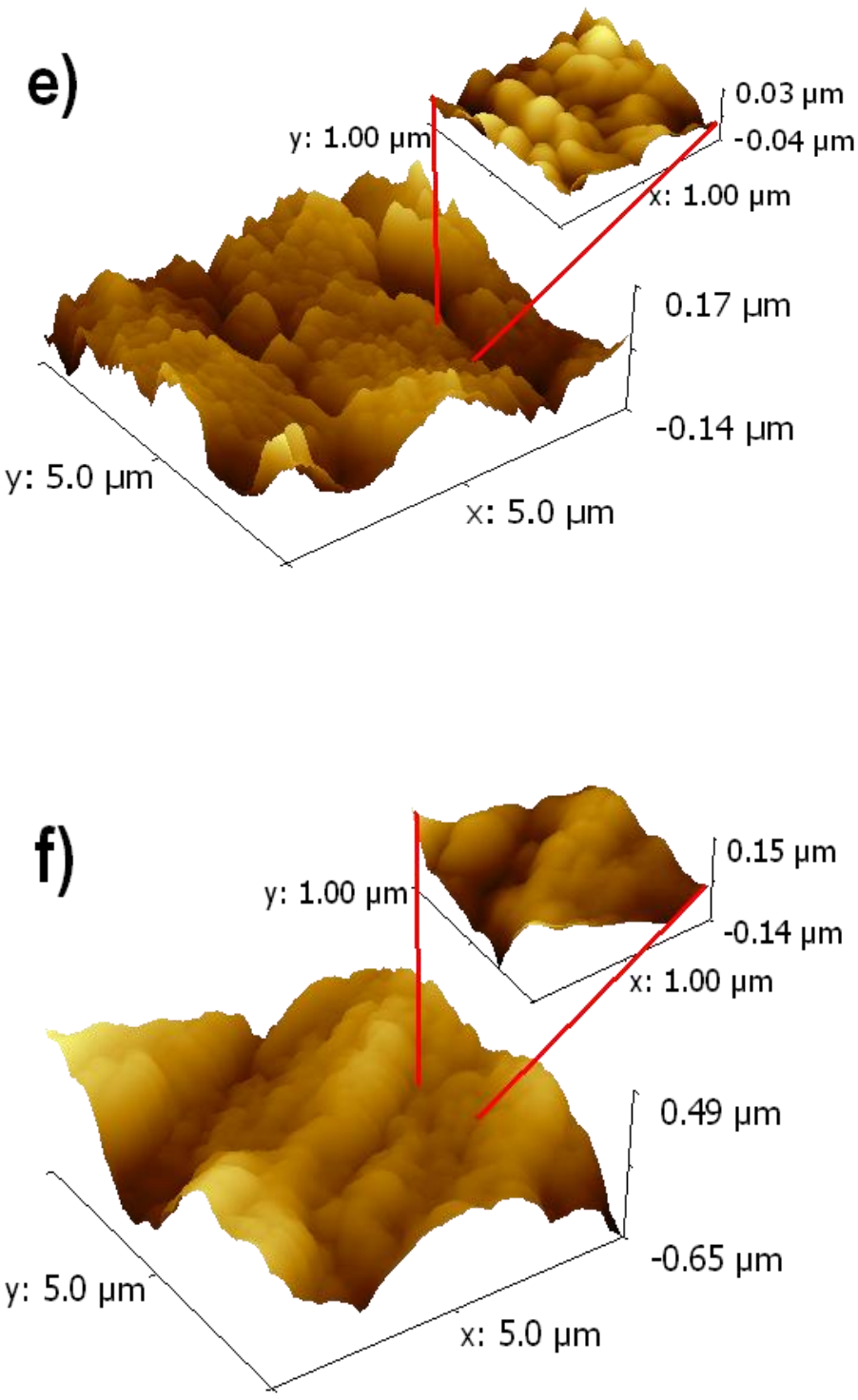

Figure 3. 15 (continued) 3-D topographic AFM height images of Lys-, PAMAM G2, PAMAM G4-modified polymer-coated electrode surface before (a,c,e) and after (b,d,f) biomolecule (GOx) immobilization at the optimized conditions, respectively.

3.1.4 Analytical Characterization of Corresponding Biosensors

The amperometric responses of optimized biosensors to glucose were recorded by adding varying concentrations of substrate into sodium acetate buffer solution. The variation of current versus different glucose concentrations profile is shown in Figure 3.8. Linearity ranges of each biosensor were determined as 0.01–2.40 mM for the Lys-containing electrode and 0.02–1.2 mM for the PAMAM G2 and G4 ones with the correlation coefficients of 0.999, 0.997, and 0.997, respectively.

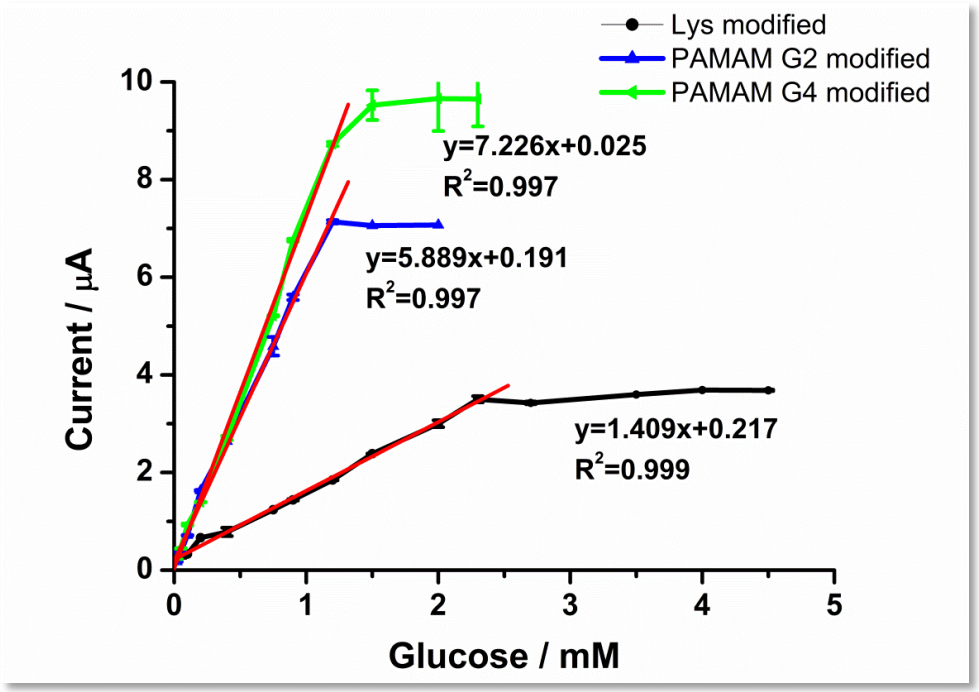

Figure 3. 16 Calibration curve for glucose (in 50 mM sodium acetate buffer, pH 5.5, 25 ^{o}C, -0.7 V). Error bars show standard deviation (SD) of three measurements.

A characteristic glucose biosensor response was depicted in Figure 3.9. As a representative example of PAMAM G4-modified biosensor response, Figure 3.9 illustrates that the biosensor has a rapid and sensitive response to glucose and reaches

a steady-state equilibrium current in 5 s. All three biosensors have such a quick response to substrate.

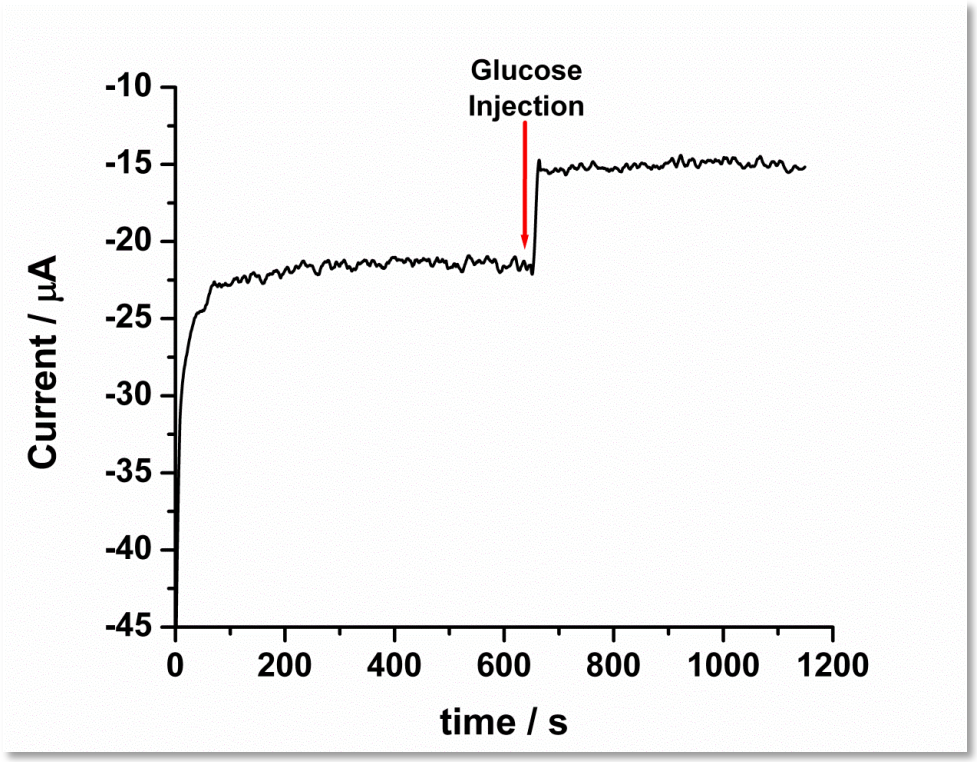

Figure 3. 17 A characteristic biosensor response of polymer/PAMAM G4-modified biosensor to glucose (in 50 mM sodium acetate buffer, pH 5.5, 25 ^{o}C, -0.7 V, [Glc]; 0.75 mM).

Kinetic parameters of the optimized enzyme biosensors were found from the Lineweaver–Burk plot at constant temperature and pH 5.5 and are listed in Table 3.1 comparatively with literature results. Limit of detection (LOD) values for Lys-, PAMAM G2- and G4-containing biosensors were calculated as 19.0, 3.47 and 2.92 μM, respectively when the signal-to-noise characteristics of these data (S/N ratio) are 3. When the immobilization of GOx was achieved with the modifications using carbon nanotubes and gold nanoparticles, much higher K_m^{app} values were recorded

[167-169]. This may well be not only due to the conducting polymer layer but also increasing in diffusing limitations due to surface modifications. Polymer/Lys or PAMAM matrices exhibit higher affinity toward the glucose substrate; hence, the modifications served our purposes perfectly. Moreover, the response time was also shortened by the help of surface orientation of the enzyme molecules [153]. When the results were compared with a PAMAM-modified glucose biosensor, better analytical parameters and LOD value were recorded [170]. Moreover; the modifications are easier than that of the PAMAM G4-containing biosensor which requires multistep modification processes. On the other hand, results showed that the hyperbranched structure of PAMAM generation yields more enhanced stability and affinity towards the substrate than to that of the Lys modification. Furthermore, in the modifications with dendrimers, much smaller enzyme amounts were used in the preparations. This displays that the enzyme molecules were locked more precisely and well-oriented, and hence, the analytical parameters turned out to be better. The polymer/PAMAM G4-modified biosensor showed the best results among the three biosensors. Although it has a higher K_m value than the PAMAM G2-modified biosensor, with the higher number of primary amine groups, the enzyme can be attached more efficiently. Accordingly, the stability and electron transfer and thus the rate of formation of product were improved. Since K_m is the concentration of substrate which allows the enzyme to achieve half I_{max}, it is natural that with the crowded microenvironment around the enzyme molecules, the PAMAM G4-modified biosensor has a higher K_m than that of the G2-modified one to achieve higher I_{max}.

Some electroactive species such as ascorbic acid, urea, oxalic acid, paracetamol etc. may affect the biosensor response while working with real samples, especially in physiological fluids. The interference effects of these molecules were investigated between 0.001 M and 0.010 M. No interference effect was observed in all concentrations of ascorbic acid, urea, oxalic acid and paracetamol at the working potential.

Table 3. 1 Comparison of biosensors examples of GOx (**NR:** Not Reported, **TW:** This Work)

Surface modification	**Immobilization Tech.**	**K_m/I_{max}**	**Limit of Detection**	**Shelf Life**	**Ref.**
Au/Poly(*o*-aminophenol/carbon nanotubes)	Electropolymerization	22.8 mM	0.01 mM	30 days	[132]
Polypyrrole	Self-encapsulation	25.25 mM/ 625 nA	9.00 µM	NR	[168]
Poly[3-(3-*N*,*N*-diethylaminopropoxy)thiophene]-SWCNT	Adsorption	3.80 mM	5.00 µM	NR	[169]
GOx/CNT/Teflon	Adsorption	30 mM	33.00 µM	1 day	[170]
PANI nanofibers and nanocomposite of Au NPs	Covalent binding	NR	0.500 µM	14 days	[171]
PAMAM G4	Covalent binding	1.67 mM/ 4.49 µA	11.84 µM	30 days	[172]
Poly-SNS-anchored carboxylic acid	Covalent binding	1.17 mM/ 11.28 µA	4.00 µM	30 days	[153]
Poly-SNS-anchored carboxylic acid /Lysine	Covalent binding	2.25 mM/ 5.93 µA	19.00 µM	28 days	TW
Poly-SNS-anchored carboxylic acid /PAMAM G2	Covalent binding	1.19 mM/ 12.37 µA	3.47 µM	35 days	TW
Poly-SNS-anchored carboxylic acid /PAMAM G4	Covalent binding	1.59 mM/ 17.75 µA	2.92 µM	42 days	TW

3.1.5 Operational and Storage Stabilities

The operational stability of each optimized enzyme electrode was obtained by repetitive measurements of 0.4 mM glucose at constant temperature. After 35, 77, and 50 measurements with Lys, PAMAM G2 and G4-modified electrodes, respectively, no activity loss was observed during a 22 h operation time.

The shelf life of each biosensor was examined by measuring the amperometric responses every day for 0.4 mM glucose under the optimized conditions. Between each subsequent measurement the biosensors were stored in contact with the working buffer at 4 ^{o}C. The shelf lives of the biosensors were determined for 4, 5 and 6 weeks (no activity loss). The aqueous compatibility of the improved immobilization matrices protects the enzyme from the environmental effects.

3.1.6 Sample Applications

The biosensors were tested for real human serum samples to determine the concentration of glucose in order to test biosensors' accuracy. All experiments were performed in compliance with relevant laws and ethical committee approved the experiments. These samples were first analyzed in a local hospital and the actual glucose levels were determined with a reference method. During the measurements, the certain amounts of blood serum samples were injected as the substrate in the buffer solution instead of the glucose solution. The experiments were performed at the optimized conditions and a constant temperature of 25 ^{o}C. The results were compared with the ones obtained in the hospital results in Table 3.2. The results confirm that the designed biosensors are suitable for use with real human blood samples.

Table 3. 2 Comparison of the constructed biosensors for glucose analysis in the serum samples.

Sample	Hospital data (mM)	Lys-modified biosensor (mM)	Relative error (%)	PAMAM G2 modified biosensor (mM)	Relative error (%)	PAMAM G4 modified biosensor (mM)	Relative error (%)
1	0.200	0.195	2.500	0.205	0.500	0.201	0.500
2	0.189	0.184	2.600	0.187	1.050	0.192	1.587
3	0.185	0.186	0.540	0.184	0.540	0.186	0.540
4	0.183	0.181	1.092	0.182	0.546	0.185	1.092
5	0.179	0.180	0.558	0.180	0.558	0.177	1.117
6	0.170	0.166	2.352	0.172	10.176	0.169	0.588

3.2 PBIBA Based Glucose Biosensors

3.2.1 Synthesis of BIBA Monomer

Among the immobilization techniques of the biomolecules, covalent attachment plays a crucial role due to providing robust interaction between transducer and the biomolecule. Thus, the transducer surface can be modified or functionalized to allow covalent bond formation of biorecognition elements for enhancing the stability and sensitivity of biosensors. 4-(4,7-Di(thiophen-2-yl)-1*H*-benzo[d]imidazol-2-yl)benzaldehyde (BIBA) monomer was designed and synthesized to utilize the polymer of this monomer as the immobilization matrix for GOx. The aim is to create covalent attachments between the aldehyde groups of the polymer and the amine groups of the enzyme. For this purpose, bromination and subsequently reduction of 2,1,3- benzothiadiazole unit were performed to obtain 3,6-dibromobenzene-1,2-

diamine moiety which allows the formation of acceptor unit through a reaction with terephtaldehyde. The corresponding monomer (BIBA) was successfully synthesized *via* Stille Coupling reaction of stannylated thiophene unit and the acceptor unit.

3.2.2 Electrochemical Polymerization of the Monomer

Electropolymerization of the monomer was accomplished in dichloromethane (DCM) and acetonitrile (ACN) (5:95, v:v) containing 0.1 M LiClO4/NaClO4 (1:1 mol). Indium tinoxide coated glass slide, platinum and silver wires were used as the working, counter and pseudo reference electrodes, respectively. Silver wire pseudo reference electrode was calibrated against Fc/Fc^{+} (0.3 V). In the first cycle monomer oxidation was revealed at 1.57 V (Fig. 3.10).

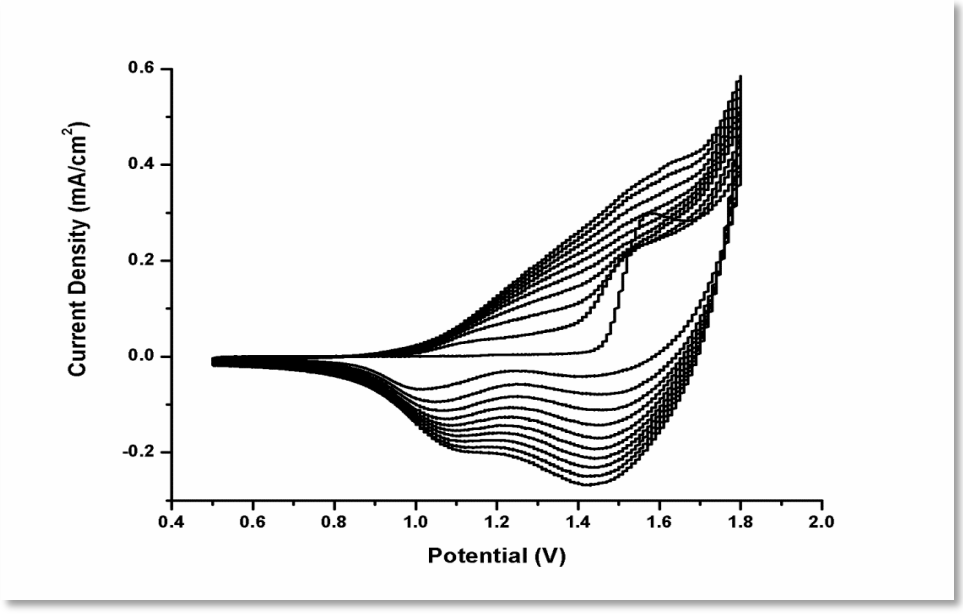

Figure 3. 18 Cyclic voltammogram of polymerization in a DCM/ACN (5:95 v:v)/ 0.1 M $LiClO_4/NaClO_4$ (1:1 mol) solvent-electrolyte couple.

3.2.3 Electrochemical and Spectroelectrochemical Properties

Polymer coated ITO was washed with fresh ACN to remove unreacted monomer. Cyclic voltammogram of the polymer in a monomer free 0.1M $LiClO_4/NaClO_4$ (1:1 mol) acetonitrile solution, revealed a polymer redox couple at 1.43/1.18 V (Fig. 3.11). HOMO level of the polymer was calculated as −6.1 eV. There are rare examples of n-doping for benzimidazole containing polymers, similarly for this derivative n-doping property could not been observed [152,173]. Using the optical band gap of the polymer, LUMO level was calculated as −4.18 eV (LUMO=Eg+HOMO).

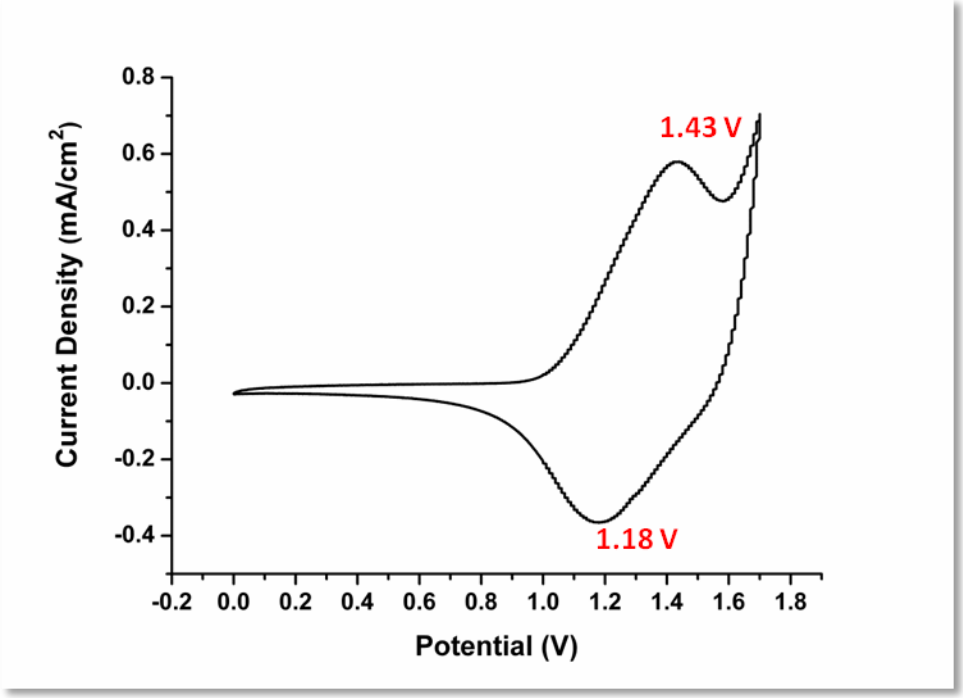

Figure 3. 19 Single scan voltammogram of PBIBA in ACN/$LiClO_4/NaClO_4$ solution

In Figure 3.12 relation between the scan rate and current density of the polymer was

investigated and it was observed that the anodic and cathodic peaks were proportional to each other even at different scan rates. In addition current versus scan rate graph showed the linear relationship between scan rates and current (Fig. 3.12b). This reveals that the electrochemical processes are not diffusion-controlled according to modified Sevcik equation for non-diffusion controlled electrochemical processes (doping-dedoping) [174]. The polymer is well-adhered on the electrode and can efficiently promote the electron transfer improving the electrochemical performance of electrode.

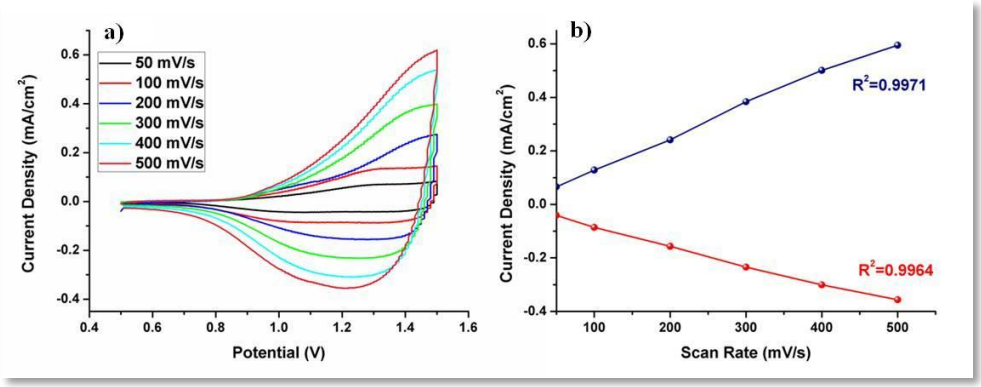

Figure 3. 20 a) Scan rate dependence of PBIBA **b)** Linear relationship between scan rate and current density for PBIBA at 50, 100, 200, 300, 400 and 500 mVs^{-1}.

During spectroelectrochemical investigation of the polymer, stepwise oxidation was applied while the UV-vis–NIR spectra were recorded. By this method optical changes for the polymer in different applied potentials could be observed. Since HOMO level of donor unit in donor–acceptor–donor type polymers is high enough to make an energy transition to LUMO of the polymer, consecutively two π–π* transitions were observed for these types of polymers in their neutral state. The polymer as a donor–acceptor–donor type revealed two π–π* transitions at 347 nm and 478 nm, hence the polymer revealed yellowish-orange color in its neutral state and the optical band gap of the polymer was calculated as 1.92 eV from the onset of

the longer wavelength absorption (Fig. 3.13a). While the polymer was p-type doped, the intensity of two π–π* transition peaks decreased and two new absorption peaks arouse at around 700 and 1280 nm. During the formation of the new bands, intensity of π–π* transitions did not diminish completely. As a result a pale green color was observed as the color of oxidized state. Also, a pale gray color was observed along stepwise oxidation process. To report the colors of polymer in neutral and oxidized states, colorimetry studies were performed using CIE L*a*b* color space as shown in Figure 3.13b.

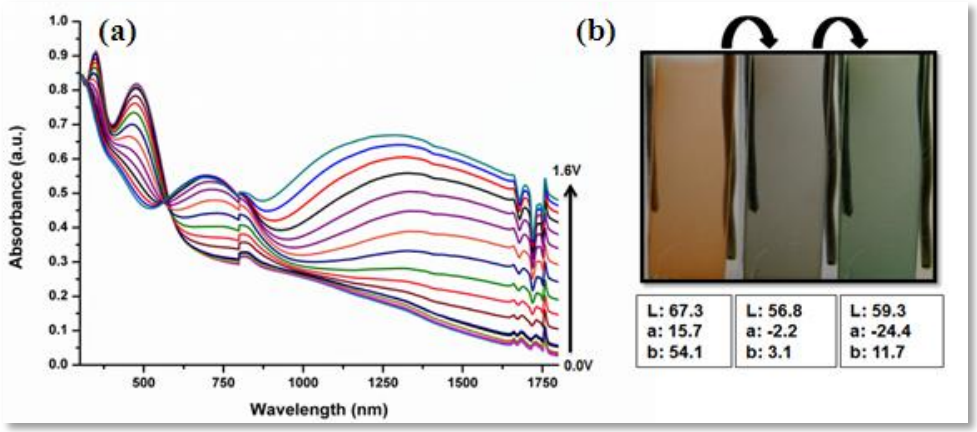

Figure 3. 21 a) Electronic absorption spectra for PBIBA upon p doping between 0.0 V and 1.6 V in a monomer free solution **b)** Colors of PIBA at its neutral (0.0 V) and different oxidized states.

For an electrochromic polymer, optical contrast, response time and stability invisible and NIR regions are important properties. In order to investigate these properties, polymer film were investigated at specific wavelengths between its neutral and oxidized states. For this purpose a square-wave potential step method was applied while optical spectroscopy was monitored. To obtain the switching time, the time difference between the fully reduced and oxidized states was calculated. The optical contrast for polymer was measured as the transmittance difference (ΔT %) between

the neutral and oxidized states and calculated as 21 % at 480 nm and 29 % at 710nm. The switching times were calculated as 0.6 s and 2.7 s at 480 and 710 nm, respectively and summarized in Fig. 3.14.

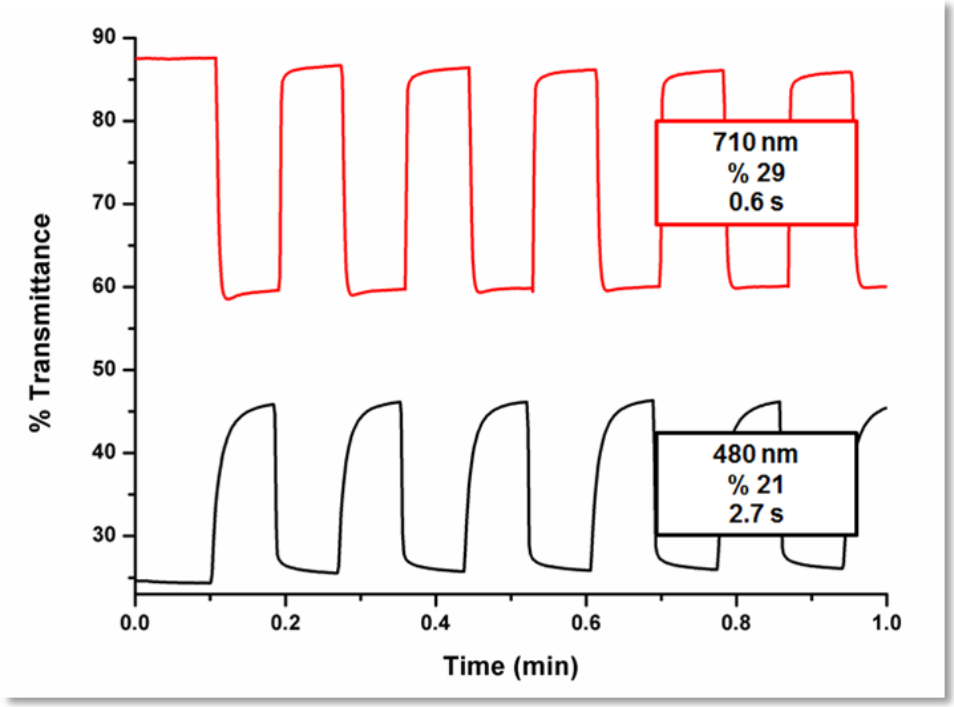

Figure 3. 22 Change of % transmittance and switching time of the polymer at 480 and 710 nm.

3.2.4 Optimization Studies for Biosensors (PBIBA, Au-modified PBIBA and SWCNT-modified PBIBA)

3.2.4.1 Effect of Polymer Thickness on the Surface

Conducting polymers known as good transducers are also convenient bioconjugation matrices thanks to their easy structural modification for enzyme immobilization in biosensor applications [151]. During the immobilization process, film thickness

(related with the scan number of electropolymerization) is of great importance in terms of morphology and biosensor response. A thick film on the bare graphite electrode may hinder the electron transfer resulting in a longer response time. However, low polymer thickness affects the number of functional groups covalently attached to enzyme. Therefore some of the biomolecules on the polymer generated electrode may not be stabilized according to weak interaction with surface and easily leach during the amperometric measurements [175]. In order to determine desired polymer thickness, corresponding monomer was electropolymerized on different graphite rods with different scan numbers varying between 10 (0.35 mC, 7.75 nm) and 60 (20.76 mC, 46.52 nm) cycles. A certain amount of GOx was covalently attached on the surface using equal amounts of GA solution. According to these results, 20 cycles polymerization (0.70 mC, 15.50 nm) was chosen as the optimum scan number for the desired biosensor.

The same optimization studies were repeated for the AuNRs- modified biosensors at the same conditions. After the graphite electrodes were coated with PBIBA polymer, the surface was modified with the AuNRs solution and let for evaporation at room temperature. SWCNT-modified electrodes were prepared in a different pathway for scan rate optimization studies. To increase the electrode electroactivity before electropolymerization and provide SWCNT stability on the surface, graphite electrode was firstly modified with SWCNT solution by drop casting method. Thanks to the deposition ability of carbon nanotubes on the graphite surface, electropolymerization of monomer was successfully achieved without losing SWCNT from the surface [176]. After the modification of the surfaces, the same amount of GOx enzyme was immobilized on the modified surfaces with the help of the same amount of GA. Then, amperometric measurements were performed in sodium acetate buffer (50 mM, pH 5.5) for 0.4 mM glucose. According to responses, 20 cycles of polymerization was determined as the optimum scan number for modified surfaces (Figure 3.15).

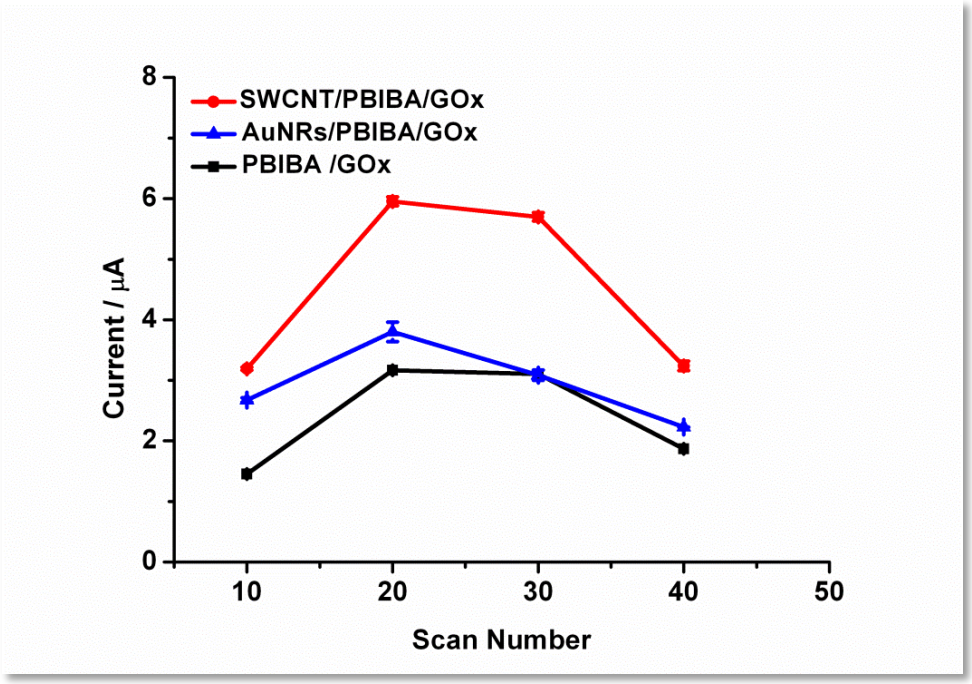

Figure 3. 23 Effect of scan number during electropolymerization on the biosensor responses (in sodium acetate buffer, 50 mM, pH 5.5, 25 C, -0.7 V).
Error bars show standard deviations.

3.2.4.2 Effect of Biomolecule Amount

The optimum enzyme amount should be determined to enhance the biosensor performance. If the required value of enzyme amount cannot be efficiently attached to the immobilization matrix, the excess amount of biomolecule can leach to the buffer solution throughout the measurements. Whereas, low amounts of enzyme on the surfaces can cause a decrease in amperometric response. To optimize the enzyme amount on the surface, working electrodes were coated with polymer using the optimum number of cycles. Then, new sensors with different amounts of GOx (25.0 U, 50.0 U, 85.0 U and 120.0U in 50 mM sodium acetate buffer) were constructed in the presence of glutaraldehyde. For the same glucose concentration highest response was observed with 50.0 U GOx for all biosensors (Fig. 3.16).

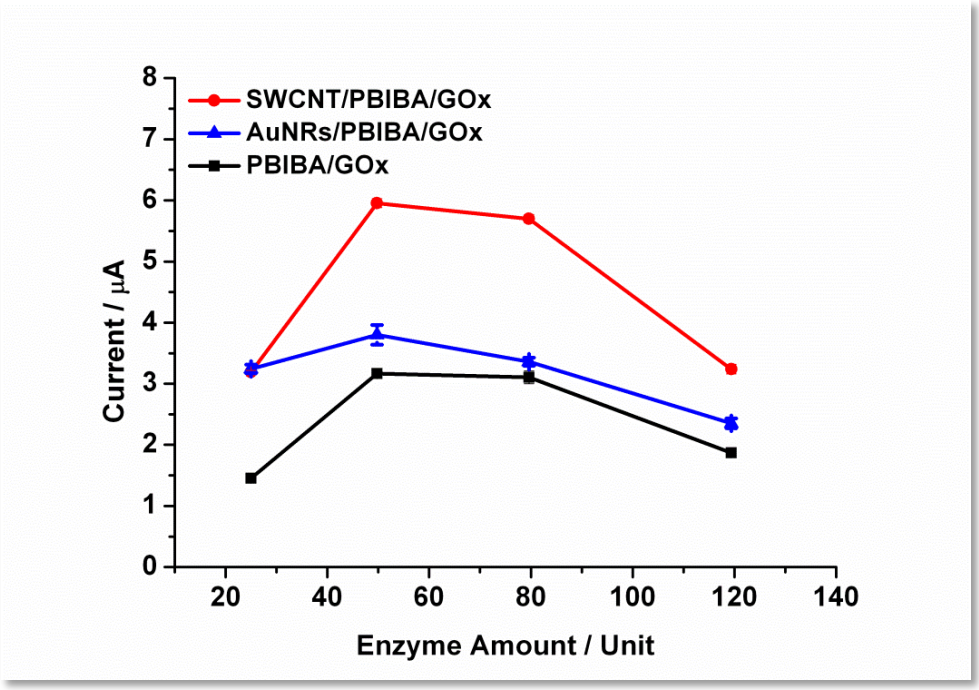

Figure 3. 24 Effect of loaded GOx amounts on biosensors responses (in sodium acetate buffer, 50 mM, pH 5.5, 25 C, -0.7 V). Error bars show standard deviations.

3.2.4.3 Effect of Crosslinker (GA) Amount

Enzyme immobilization is the most crucial step in a biosensor construction. In providing the stability of enzyme on the surface, glutaraldehyde (GA) is a mostly used reagent for crosslinking [177]. However, at high concentrations of GA, this bifunctional agent may affect enzyme activity resulting in a decrease in current response [178]. GA effect on the biosensors performances were investigated by measuring the current response in 50 mM sodium acetate buffer (pH = 5.5). For this purpose, different amounts of GA (0.05 %, 0.1 %, 0.5 % and 1.2 %) were used for each biosensor. As a result, 0.1 % GA amount was found to be suitable for the highest current response in this study (Fig. 3.17).

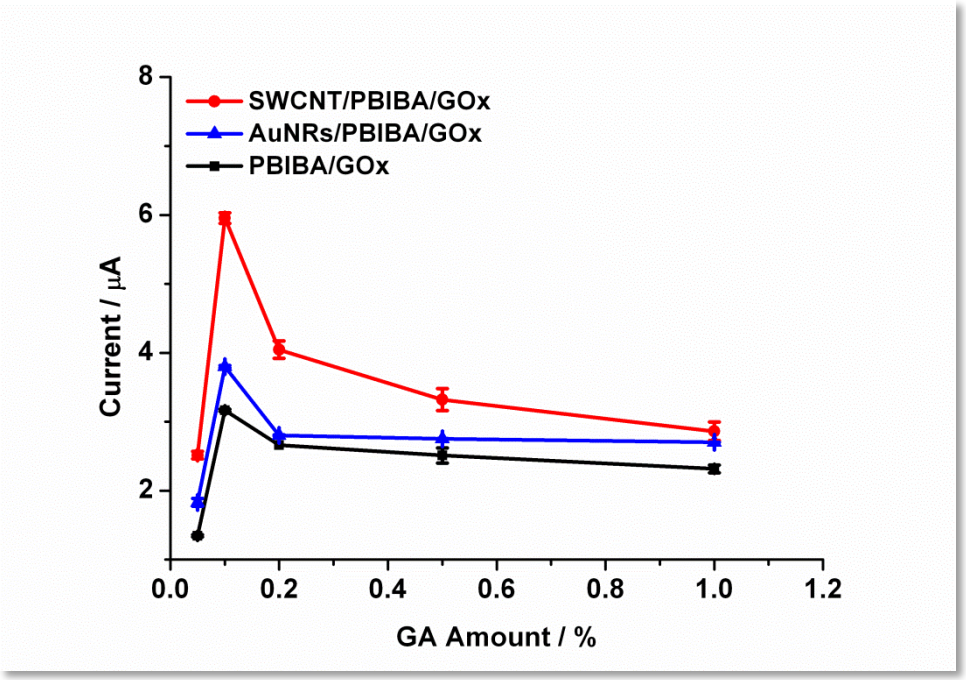

Figure 3. 25 Effect of gluteraldehyde (GA) amount on biosensors responses (in sodium acetate buffer, 50 mM, pH 5.5, 25 C, -0.7 V).
Error bars show standard deviations.

3.2.4.4 Effect of pH

One of the essential parameters in biosensing studies is pH which causes enzyme denaturation in extreme values than the optimum one. To proceed with the measurements in optimum enzyme activity, working pH range should be determined. Optimization studies were carried out in different pH values varying between 4.5 and 7.5 (50 mM sodium acetate buffer at 4.5; 5.0; 5.5 and 50 mM phosphate buffer at 6.0; 6.5, 7.0; 7.5, 25 ^{o}C). According to the results in accordance with the current responses, the value of 5.5 was determined as the optimum pH for each biosensor (Fig. 3.18).

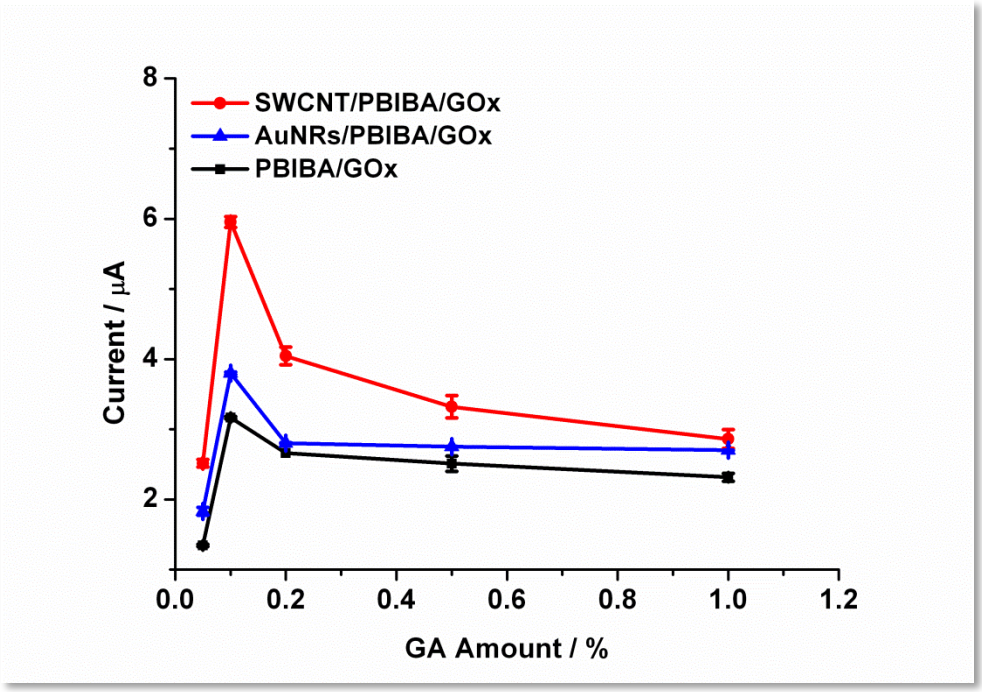

Figure 3. 26 Effect of pH on biosensors responses (in sodium acetate buffer, 50 mM, pH 5.5, 25 C, -0.7 V). Error bars show standard deviations.

3.2.5 Surface Characterization of Constructed Biosensors

3.2.5.1 X-Ray Photoelectron Spectroscopy (XPS)

Surface characterization of polymer coated and biomolecule immobilized electrodes was done via X-ray photoelectron spectroscopy (XPS). According to XPS results, the linkage formation between free amine groups of enzyme and aldehyde group of polymer was detected. The carbon and nitrogen signals were resolved using a fitting program as depicted in Figures 3.19 and 3.20. Polymer exhibits signals related to aromatic bonds (aromatic carbons and C-S in thiophene unit at 284.6 eV and 284.4 eV, respectively), C=N group (285.4 eV), C-N and characteristic C=O group in aldehyde unit (286.5 eV and 287.8 eV, respectively) (Fig. 3.19a) [179-180]. It is possible to obtain information regarding this perfect attachment through investigating

N1s spectra of the polymer. As illustrated in these spectra, the signals centered at 399.2 eV and 400.6 eV were assigned to =N- group and amine group in imidazole unit, respectively (Fig. 3.19b) [181].

In protein immobilized surface, absence of aldehyde signal and an increase in the intensity of C=N- signal prove bond formation between enzyme and polymer surface. Thus, the biomolecule was covalently attached to the polymer as expected (Fig. 3.20a). Hence relative increase in the intensities of N1s of =N- and N-H peaks are attributed to new imine bonds and to new terminal amine groups of enzyme (Fig. 3.20b). Through these results, immobilization of biomolecule on polymer coated surface was successfully achieved.

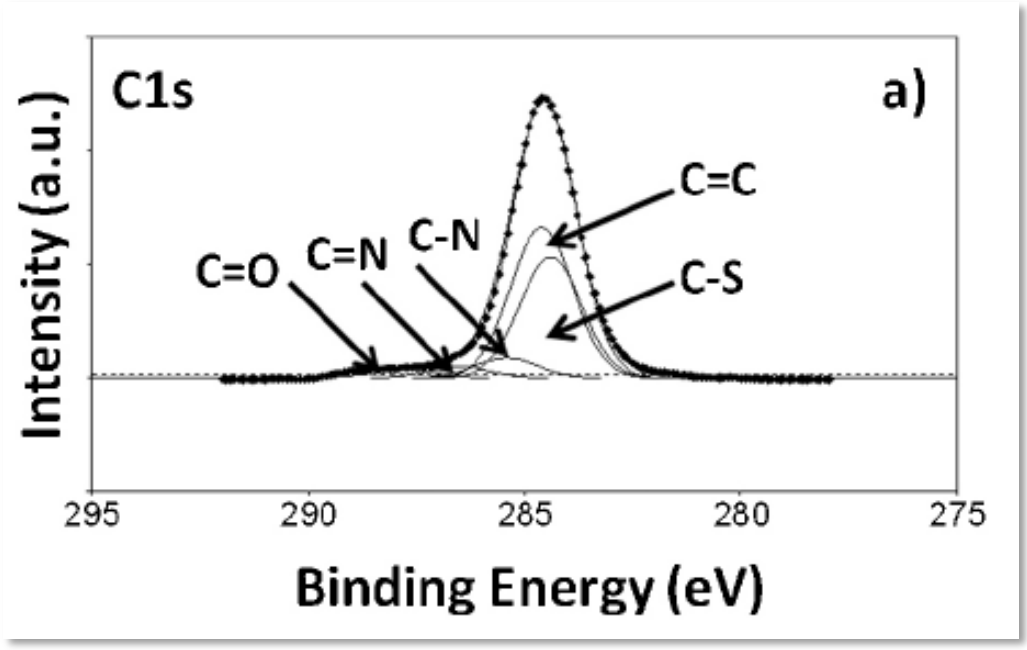

Figure 3. 27 (a) C1s and **(b)** N1s XPS spectra of the polymer surface.

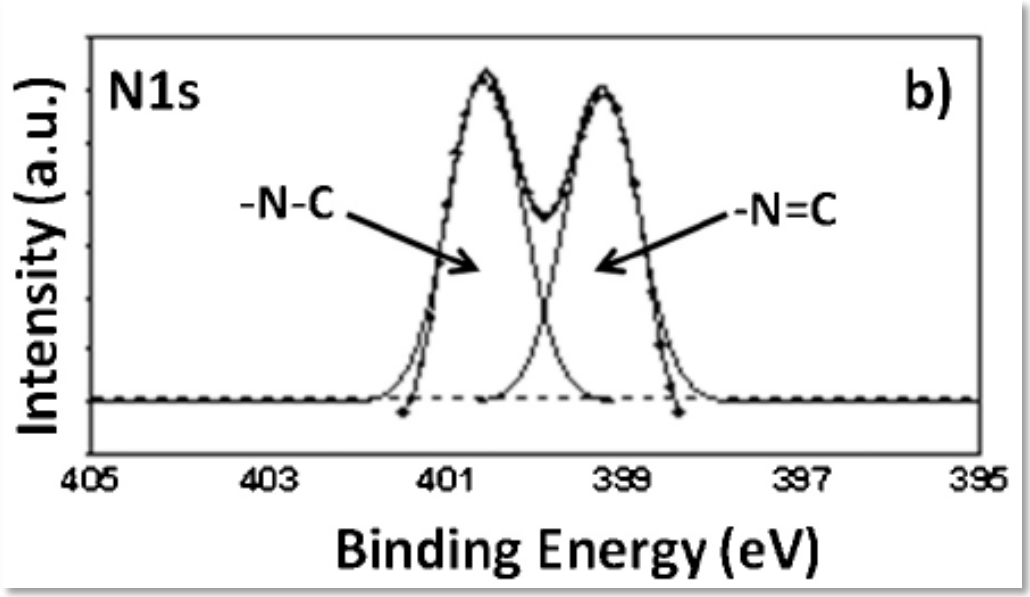

Figure 3. 28 (continued) (a) C1s and **(b)** N1s XPS spectra of the polymer surface.

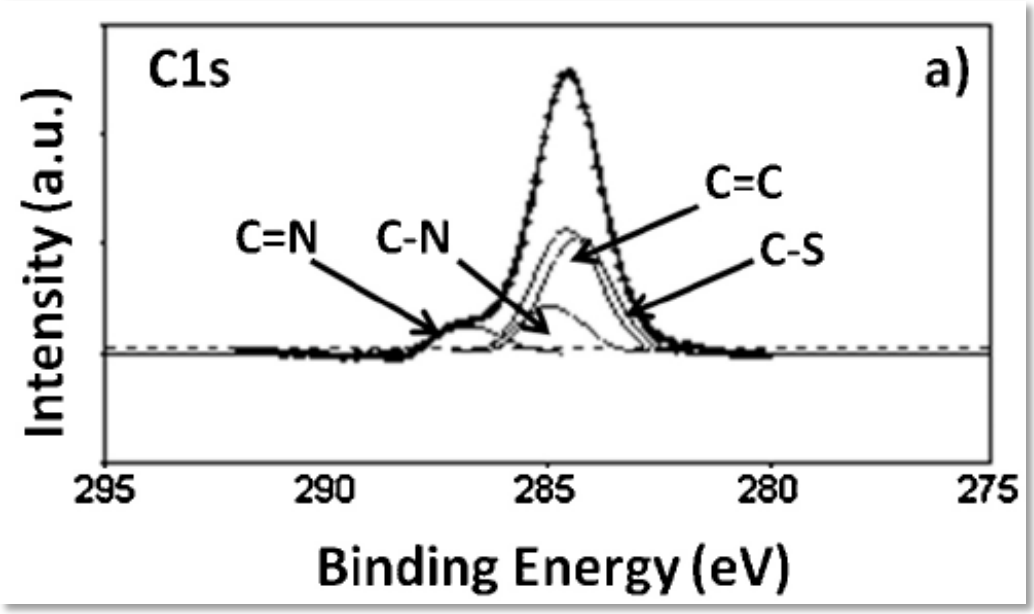

Figure 3. 29 (a) C1s and **(b)** N1s XPS spectra of the polymer surface.

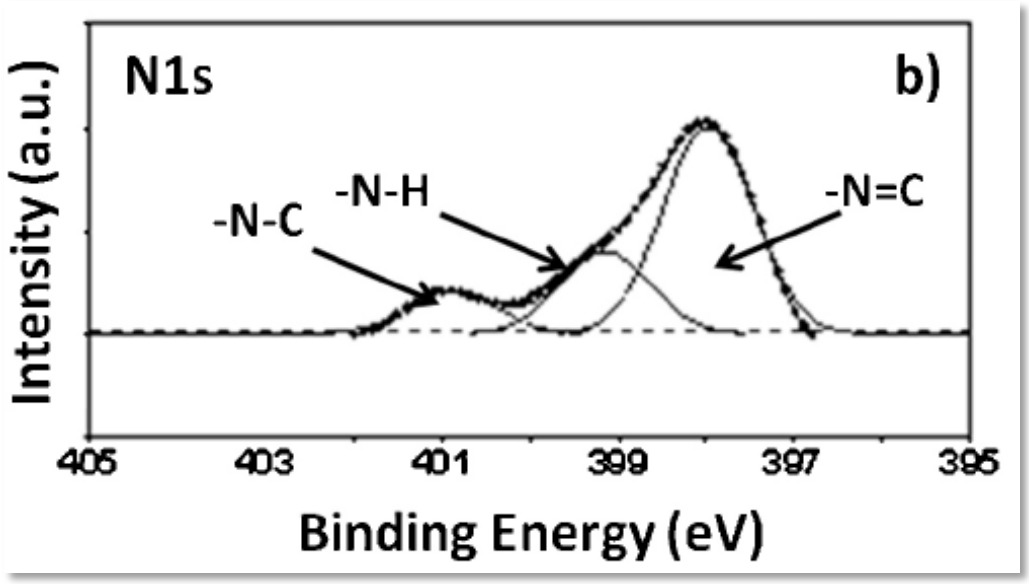

Figure 3. 30 (continued) (a) C1s and **(b)** N1s XPS spectra of the polymer surface.

3.2.5.2 Transmission Electron Microscopy (TEM)

Surface characteristics were investigated using TEM. Figure 3.21 images show polymer coated surface (Fig. 3.21a) and GOx immobilized on polymer matrix (Fig. 3.21b). It is clearly seen that polymer was coated successfully with a uniform and ragged morphology on the surface. Due to small molecular size of the polymer, the surface features of this layer are naive than the one where biomolecule was attached. Contrary to polymer image, bulky and huge enzyme molecules crosslinked by GA completely covers the surface in a uniform and indented manner. Comparing these images, biomolecule and GA attached surface can be depicted as well-organized in terms of surface area to interact with the substrate.

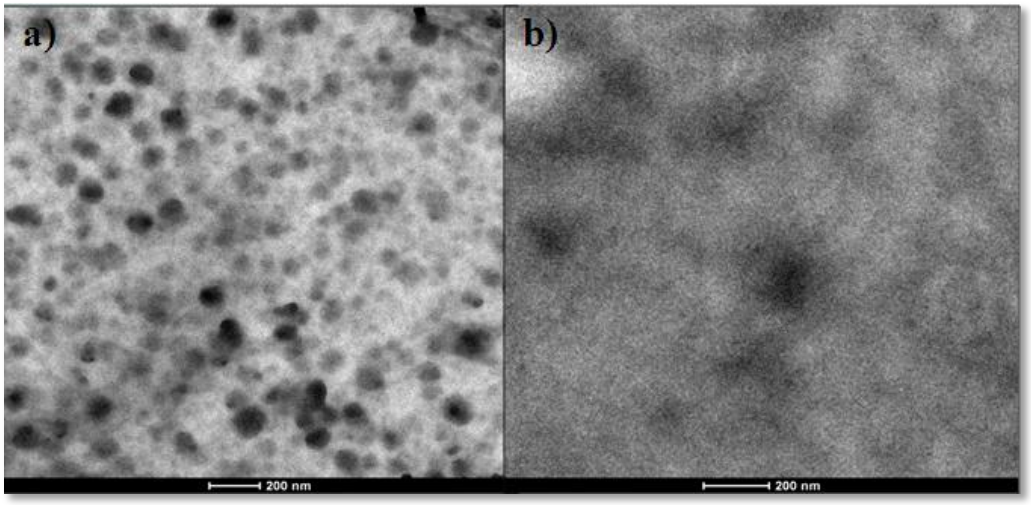

Figure 3. 21 TEM images of polymer **(a)** before and **(b)** after biomolecule immobilization under optimized conditions.

Likewise conducting polymer surface, characteristics of AuNRs modified and enzyme immobilized surfaces were examined by TEM (Fig. 3.22a-b). During construction of AuNRs modified biosensor, bare graphite electrode was coated with PBIBA polymer and this surface was modified with AuNRs by drop casting method. Figure 3.22a illustrates that AuNRs are spread over the polymer coating. Even though these gold nano particles have aggregation, they generally align to form a line like a nanowire on polymer surface. Polymer coating can also reinforce AuNRs orientation on the surface depending electronic interactions between polymer structure and gold nano particles. After GOx immobilization, nano scale modified surface is completely coated with enzyme (Fig. 3.22b). With the help of AuNRs modification, the electron transfer properties of polymer surface are enhanced depending on the high electron conductivity of gold nano particles and with an increase in efficient surface area for enzyme immobilization. In Figure 3.22b, it is clearly observed that GOx immobilized AuNRs are interconnected with branch structures which provide uniform distribution of nano particles and a wide network for electron transfer. Furthermore, they are entrapped on polymer coating through the robust interactions between GOx and polymer like covalent binding and π- π

stacking. Thus, the nano particle leaching from the surface is prevented.

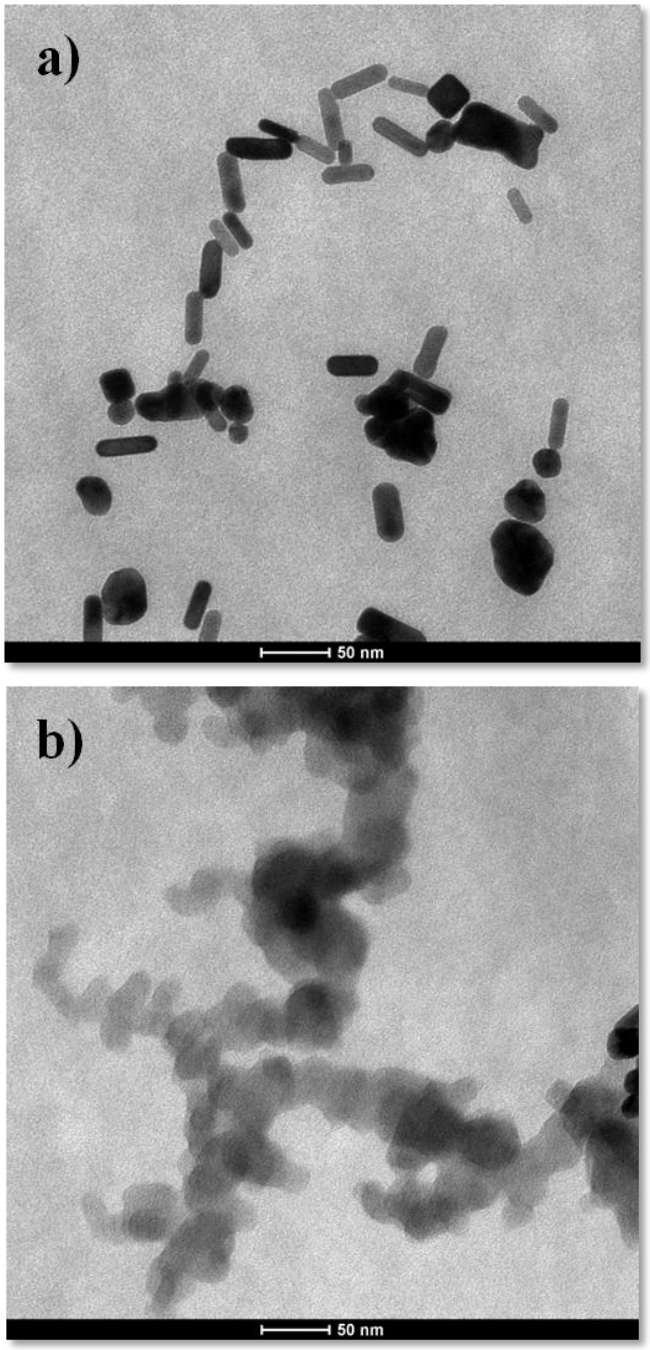

Figure 3. 22 TEM images of AuNRs modified polymer surfaces **(a)** before and **(b)** after biomolecule immobilization.

Figure 3.23 illustrates the SWCNT modified PBIBA and GOx immobilized surfaces. During the SWCNT modified biosensor fabrication, bare graphite electrode was modified with SWCNTs and subsequently, PBIBA was coated on this surface with electrochemically methods. Even so the nano tubes are embedded under polymer coating; they can be clearly observed as fibrous structures in Figure 3.23a. Hence the nano tubes penetrate properly through the polymer film, the electroactivity of immobilization matrix is enhanced substantially. Moreover, such a surface design leads to an increase in active area which has a crucial role on covalent attachment of GOx, depending on high surface to volume ratios of nanotubes. After GOx immobilization, the surface characteristics are changed drastically and well adhered enzyme coating was observed due to tough covalent binding with the functional groups of polymer coating and other electronic interactions including carbon nanotubes, polymer and enzyme molecules. Figure 3.23b shows that the protein molecules are well organized on the surface to allowing efficient interactions between substrates.

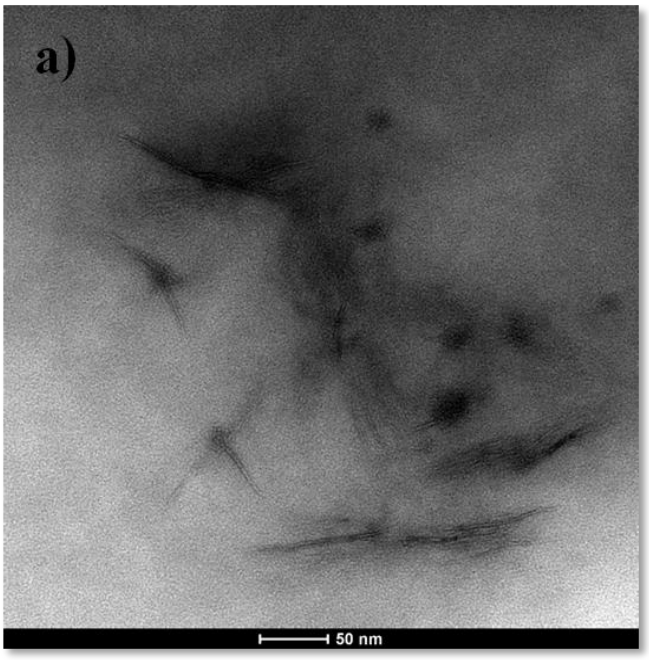

Figure 3. 23 TEM images of SWCNT modified polymer surfaces **(a)** before and **(b)** after biomolecule immobilization.

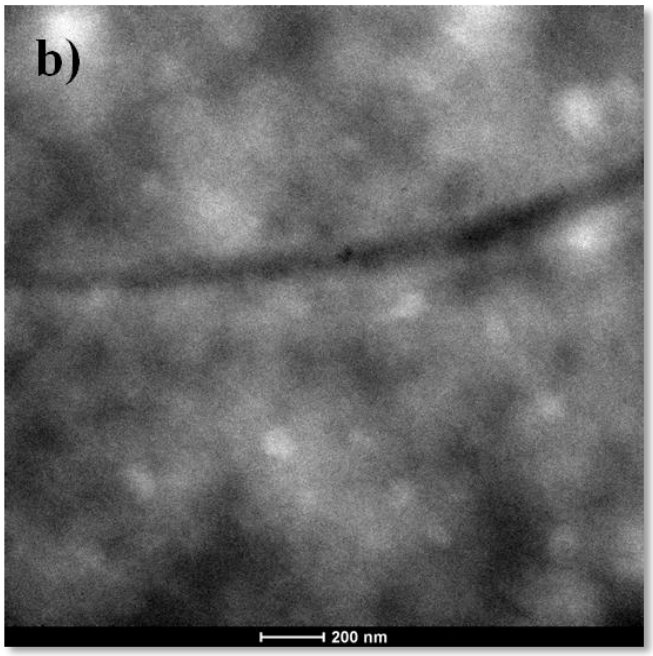

Figure 3. 23 (continued) TEM images of SWCNT modified polymer surfaces **(a)** before and **(b)** after biomolecule immobilization.

3.2.5.3 Contact Angle Measurements

As another surface characterization technique, contact angle determination was used for identifying the hydrophilic or hydrophobic properties of corresponding surfaces. On the basis of the measurements the surface characteristics of each layer were determined using 1.0 ±0.1 μL distilled water for each coating. The volume of water dripped on the surface is one of the important parameters affecting the contact angle. Thus, the volume of water should be possibly same to obtain a comprehension about the differences of each surface at a constant temperature. In this context, bare graphite electrode surface was tested and contact angle of this surface was detected as 114.69º ± 1.06 which is consistent with the hydrophobic property of graphite. After PBIBA coating of graphite electrode, hydrophilic character was observed due to aldehyde groups. Although polymers are generally known as hydrophobic

materials, aldehyde containing films show hydrophilic character [182]. Contact angle of PBIBA coated surface was determined as 46.65º ± 1.69 and this lower value can be correlated with -C=O and -O-C=O groups in structures.

In generally, pristine carbon nano tubes have hydrophobic or super hydrophobic properties [183-185]. However this property varies according to the material used in combination [186-188]. In addition, the contact angle values show a wide range for similar systems. As an example, CNT-PEG interfaces have different values varying between 25 and 73º in literature [188]. In this study, SWCNT-PBIBA system represents mildly hydrophilic character with 53.58 º ± 1.30 contact angle. As most of SWCNT on the graphite electrode is coated with PBIBA polymer during electropolymerization, PBIBA dominates the surface characteristics. Thus, contact angle value is closer to PBIBA than SWCNT surface. After GOx immobilization, the hydrophilic character of the surface is enhanced depending on increasing in acidic property on surface and contact angle value proves that with the value of 33.53º ± 0.33.

Contact angles of water on different gold surfaces are reported as between 56 and 77 degrees at 25 ºC in the literature [189-190]. In this study, the surface characterization of gold nano rod modified platform was tested and contact angle was determined as 54.11º ±0.72. During the preparation of matrix, AuNRs are spread over the PBIBA coating. Therefore, modified surface is affected by PBIBA and AuNRs and the value of contact angle is expected between polymer and nano particles ones. The addition of GOx and GA to the immobilization matrix provides a bit more hydrophilic character with the value of contact angle 51.14º ± 0.73.

3.2.6 Analytical Characterization

The electroanalytic characterization of biosensors was performed using amperometric detection technique. Since oxygen consumption during the enzymatic

redox reaction was achieved at −0.7 V constant potential, current responses versus time values were recorded at this potential. The calibration curves including varying glucose concentration versus current was established for optimum electrodes (Fig. 6). Kinetic parameters were calculated from the Lineweaver–Burk plot at constant temperature and pH 5.5 as summarized in Table 1. The apparent Michaelis-Menten constant, K_m^{app}, represents the enzyme-substrate affinity and this value was reported for free glucose oxidase as 33 mM [191]. It was observed that optimum electrode has very low K_m^{app} value (0.94 mM) and high I_{max} (10.91 μA) for PBIBA based biosensor. These parameters reveal that enzyme has high affinity to its substrate. The linearity range of generated non-modified polymer based biosensor was determined as 0.02–1.2 mM with 0.996 correlation coefficient constant (Fig. 6).

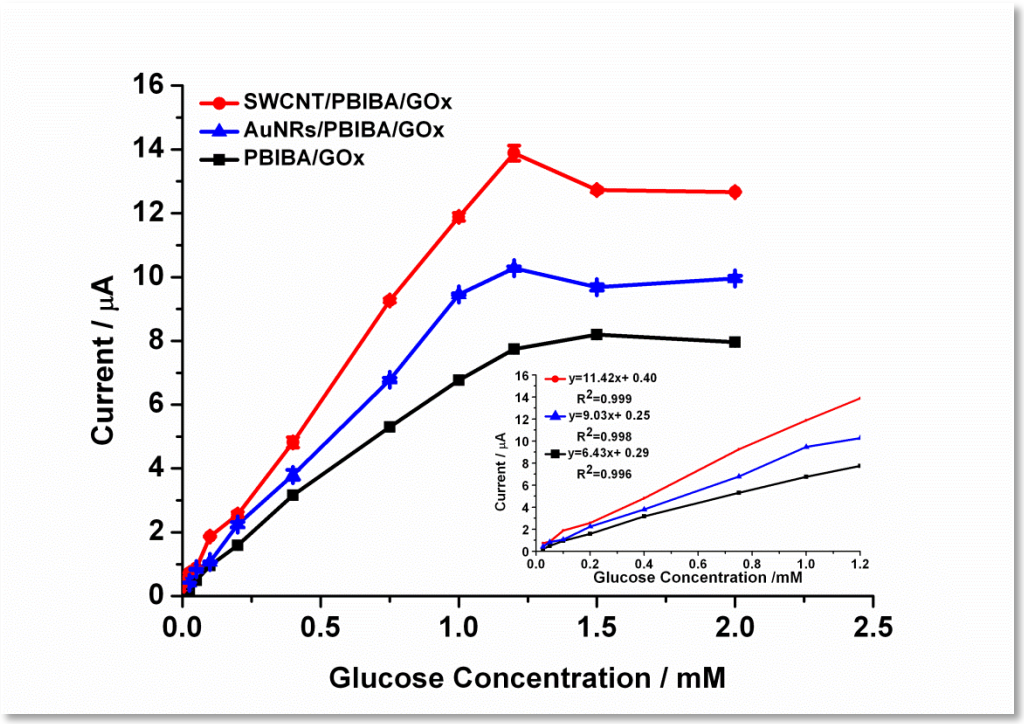

Figure 3.24 Calibration curve for glucose and linear range (inset) (in sodium acetate buffer, 50 mM, pH 5.5, 25 ºC, -0.7 V). Error bars show standard deviations (SD) of three measurements.

Besides non-modified immobilization platform, gold and carbon nano tube modified surface performances were investigated to understand effect of these nano particles on detection systems. For designed AuNRs and CNTs modified biosensors K_m^{app} values were calculated as 0.49 and 1.04 mM, respectively. Considering the immobilized enzymes, AuNRs modified biosensor shows the highest affinity to glucose comparing the CNTs modified and non-modified PBIBA biosensors due to K_m^{app} values. Owing to high electron transfer ability of AuNRs, drastic enhancement in maximum current density, I_{max}, for corresponding biosensor was observed and calculated as 13.95 μA. The AuNRs were conveniently deployed between polymer platform and GOx molecules as a conductive intermediate layer which has high electronic interactions with both of the surfaces. Thus, limit of detection (LOD) value decreased to 1.59 μM in comparison with non-modified biosensor. In addition, linear range of the glucose detection was expanded to 12.5 μM-1.2 mM.

Considering SWCNTs modified biosensor, I_{max} drastically increased to nearly 2 fold compare to that of non-modified biosensor one. This increment in current responses suggests the effect of surface morphology on biosensing performance. In this 3D biosensing design, nano tubes are completely coated by polymer layer and lead to enhance efficient polymer surface area on electrode. Hence a higher amount of GOx (attached to conductive matrix) allows more substrate interaction. In this manner, the biosensor has the lowest LOD value with 1.26 μM compared to other ones and linear range is extended to 6.25 μM-1.2 mM.

Table 3.3 Comparison of the designed biosensors with other glucose sensing examples in the literature (**NR:** Not Reported, **TW:** This Work).

Immobilization Matrix	Limit of Detection	K_m^{app} (mM)	I_{max} (μA)	Reference
PANI/PIP	0.01 mM	11.9	**NR**	**[192]**
Au/PDA/Fe_3O_4	6.50 μM	1.67	**NR**	**[193]**
OOPPy/AuNPs	0.50 mM	**NR**	**NR**	**[194]**
AuNP/(FcSH+Cyst) /PAMAM	0.6 mM	**NR**	**NR**	**[195]**
Poly(1,2-DAB)/CNT PBmodified	0.10 mM	**NR**	**NR**	**[196]**
Poly(2-hydroxyethyl methacrylate)/PPy	25.00 μM	43.7	19.42	**[197]**
PBIBA	2.29 μM	0.94	10.91	**TW**
PBIBA/AuNRs	1.59 μM	0.49	13.95	**TW**
PBIBA/SWCNTs	1.26 μM	1.04	16.45	**TW**

Furthermore, shelf life and operational stability studies were carried out for each optimized biosensor (in 50 mM sodium acetate buffer, pH 5.5, 25 °C, −0.7 V). To determine the operational stability, repeated measurements for 0.4 mM glucose at optimum ambient conditions were recorded where no decrease was observed for 61, 68 and 70 consecutive measurements of non-modified, AuNRs and SWCNTs modified biosensors, respectively. Moreover, optimum sensors were daily tested for 0.4 mM glucose concentration. Between each sequential measurement, biosensor was stored at +4 °C in buffer solution to protect the enzyme from the environmental conditions. The shelf life of biosensors was examined for 28, 34 and 40 days (non-modified, AuNRs and SWCNTs modified biosensors, respectively); no activity loss

was observed. Since nano particles provide improvement in mechanical strength property of the surfaces and larger enzyme loading through the matrices *via* covalent attachment, operational stability and shelf life of biosensors are extended due to the surface modifications.

3.2.7 Sample Applications

To obtain high accuracy results for sample applications, the responses of constructed biosensors in real sample containing interferents should be determined. In order to define the selectivity of biosensor to glucose, real samples containing several electro active species such as ascorbic acid, oxalic acid and urea were examined. For this purpose, these agents were added into the buffer solution (50 mM sodium acetate buffer, pH 5.5, 25 °C) in different concentrations (0.1 M and 0.01 M) in the course of amperometric measurements at −0.7 V. However, no interfering effect was observed at given working conditions.

3.2.7.1 Sample Application of Non-Modified PBIBA Based Biosensor

Corresponding biosensor was also tested for human blood serum samples. Preliminary detection of glucose amount in such samples was carried out with a reference method in a local health center. Then optimized electrode was tested using human blood serums instead of glucose. The glucose concentration was calculated in serum samples via amperometric measurements (50 mM sodium acetate buffer, pH 5.5, 25 °C, −0.7 V). All human blood sample experiments were approved by ethical committee. These results are compared in Table 3.4. According to comparative study results, corresponding biosensor is appropriate for use in real samples.

Table 3.4 Glucose analysis in real serum samples

Sample	Hospital data(mM)	Designed Biosensor(mM)	Relative error (%)
1	0.183	0.185	1.11
2	0.180	0.184	2.22
3	0.178	0.176	1.12
4	0.174	0.171	1.72
5	0.168	0.170	1.19
6	0.162	0.163	0.61
7	0.155	0.159	2.58

3.2.7.2 Sample Applications of Modified Biosensors

To investigate the reliability of designed biosensors, several beverages were used to determine their glucose contents. For this purpose, each modified biosensor was tested with no dilution of beverages and results were compared with the spectroscopic ones (Table 3.5). Corresponding results prove that there is no significant difference between the two methods; hence constructed biosensors show high reliability in real samples.

Table 3.5 Glucose analysis with various beverages

Samples	Spectroscopic (mol/L)	AuNRs modified (mol/L)	SWCNTs modified (mol/L)
E® Lemonade	0.035	0.030	0.042
L® Ice Tea	0.023	0.024	0.028
T® Peach Tea	0.024	0.022	0.021
C® Orange Juice	0.048	0.036	0.047
C® Lemon Juice	0.022	0.024	0.021
L® Pomegranate Juice	0.030	0.028	0.038

CHAPTER 4

4. CONCLUSION

In this study, it is mainly aimed to generate conducting polymer based new immobilization matrices for glucose detection. For this purpose two conjugated polymers were used as transducer layers on graphite electrodes. Since these polymers were designed for protein immobilization, carboxylic acid and aldehyde group containing polymers were chosen to provide covalent attachment of GOx as a model enzyme. In addition, the polymer platforms were modified with different particles such as amino acid, PAMAM derivatives, SWCNT and AuNRs to investigate the effect of these particles on biosensor performance.

Three novel immobilization matrices were developed using SNS-anchored carboxylic acid polymer. Conductive surface was modified with Lys amino acid, PAMAM G2 and PAMAM G4 molecules to examine the effect of functional group amount in terms of getting robust covalent attachment and morphology. The analytical characterization results prove that increasing in amount of amine group in polymer, which provides the covalent attachment of enzyme to the surface, leads to adhering larger amount of protein molecules on polymer surface. Herewith, PAMAM G4 modified biosensor indicates robust and highly active enzyme with the highest operational stability and the longest shelf life. Besides the long term stability, this biosensor showed the highest affinity to substrate with the highest current responses. Furthermore, these novel platform surfaces were investigated via XPS and AFM to explain the surface characteristics. Constructed biosensors were also tested with the determination of different glucose concentrations in real serum samples and the compatible results with the exact values were obtained in promising response times.

As another immobilization matrix, aldehyde functionalized biocompatible benzimidazole containing polymer was designed and successfully synthesized for

glucose detection. The electrochemically polymerized PBIBA performed well as an immobilization matrix for the covalent attachment of GOx. PBIBA was also modified with AuNRs and SWCNTs to enhance the electron transfer ability and amount of enzyme on the surface. Thus, three novel immobilization platforms were improved for amperometric glucose detection and biosensor performance of each matrix were compared to each other. According to analytical results, SWCNTs modified biosensor showed the highest I_{max} value with the longest shelf life and highest operational stability. These results can be explained with the high surface to volume ratio of CNTs allowing more robust covalent binding of GOx in larger amount. The strong mechanical properties of CNTs assist to enhance stability. With the high electronic conductivity of gold, AuNRs modified glucose biosensor indicates higher I_{max} value than non-modified PBIBA biosensor. The covalent attachments between PBIBA and enzyme molecules were confirmed by XPS and TEM studies. Moreover, these three biosensors were tested for real samples and exhibited compatible results.

All fabricated biosensors in this study shown remarkable analytic results for glucose detection. Furthermore, generated immobilization matrices are quite promising for other biosensor applications with their low LOD and high stability values proving the strong protein attachment and good permeability of the surface. As further investigations, these immobilization platforms can be studied with other protein molecules for different substrates or other biotechnological developments.

REFERENCES

[1] H. Letheby, *J. Chem. Soc.*, **1862**, 15, 161.

[2] V. V. Walatka, M. M. Labes, J. H. Perlstein, *Phys. Rew. Lett.*, **1973**, 31, 113.

[3] P. M. Shumbula, MS Thesis, University of the Western Cape, **2005**.

[4] C. K. Chiang, C. R. Fincher, Jr., Y. W. Park, A. J. Heeger, H. Shirakawa, E. J. Louis, S. C. Gau, A. G. MacDiarmid, *Phys. Rev. Lett.*, **1977**, 39,1098.

[5] H. Shirakawa, E. J. Louis, A. G. MacDiarmid, C. K. Chiang, A. J. Heeger, *J. Chem. Soc., Chem. Commun*., **1977**, 579.

[6] C. K. Chiang, M. A. Druy, S. C. Gau, A. J. Heeger, E. J. Louis, A. G. MacDiarmid, Y. W. Park, H. Shirakawa, *J. Am. Chem. Soc.*, **1978**, 100, 1013.

[7] A.F. Diaz, K.K. Kanazawa, In: J.S. Miller (Ed.), *Ext. Linear Chain Compd.*, vol. 3, Plenum Press, New York, 1982, p. 417.

[8] A. F. Diaz, K. K. Kanazawa, G. P. Gardini, *J. Chem. Soc., Chem. Commun.*, **1979**, 635.

[9] K. Lee, A. J. Heeger, *Synth. Met.*, **1997**, 84, 715.

[10] J.H. Burroughes, D.D.C. Bradley, A.R. Brown, R.N. Marks, K. MacKay, R.H. Friend, P.L. Burn, A.B. Holmes, *Nature*, **1990**, 347, 539.

[11] A. Desbene-Monvernay, P.-C.Lacaze, J.-E. Dubois, *J. Electroanal. Chem.*, **1981**, 129, 229.

[12] A. J. Heeger, *J. Phys. Chem. B*, **2001**, 105, 8475.

[13] P. J. Nigrey, A. G. MacDiarmid, and A. J. Heeger, *Chem. Commun.*, **1979**, 96, 594.

[14] D. M. de Leeuw, M. M. J. Simenon, A. R. Brown, R. E. F. Einerhand, *Synth. Met.*, **1997**, 87, 53.

[15] C. J. DuBois, K. A. Abboud, J. R. Reynolds, *J. Phys. Chem. B*, **2004**, 108, 8550.

[16] A. D. Child, J. R. Reynolds, *J. Chem. Soc., Chem. Commun*, **1991**, 1779.

[17] R. Hoffmann, *Angew. Chem Int Ed*., **1987**, 26, 846.

[18] J. J. Apperloo, R. A. J. Janssen, M. M. Nielsen, K. Bechgaard, *Adv. Mater*., **2000**,12, 1594.

[19] K. Shimamura, F.E. Karasz, J.A.Hirsch, J.C. Chien, *Macromol. Chem. Rapid Commun.*, **1981**, 2, 443.

[20] D. Kumar, R.C. Sharma, *Eur. Polym. J.*, **1998**, 34, 1053.

[21] P. J. Nigrey, A. G. MacDiarmid, A. J. Heeger, *J. Chem. Soc,. Chem. Commun.*, **1979**, 594.

[22] V. M. Niemi, P. Knuuttila, J. E. Österholm, *Polymer*, **1992**, 7, 1559.

[23] I. F. Perepichka, D. F. Perepichka, H. Meng, F. Wudl, *Adv. Mater.*, **2005**, 17, 2281.

[24] T. Olinga, B. François, *Synth. Met.*, **1995**, 69, 297.

[25] A. Malinauskas, *Polymer*, **2001**, 42, 3957.

[26] T. Yamamoto, K. Sanechika, A. Yamamoto, *J. Polym. Sci., Polym. Lett.* **1980**, 18, 9.

[27] J. W-P Lin, P. L, Dudek, *J. Polym Sci. Polym. Chem. Edit.*, **1980**, 18 (9), 2869.

[28] M. Kosugi, Y. Shimizu, T. Migita, *Chem. Lett.*, **1977**, 1423.

[29] M. Kosugi, Y. Shimizu, T. Migita,. *J. Organomet. Chem.*, **1977**, 129.

[30] M. Kosugi, Y. Shimizu, T. Migita., *Chem. Lett.*, **1977**, 301.

[31] D. Milstein, J. K. Stille, *J. Am. Chem. So*c., 1978, 100, 3636.

[32] E. A. Meijere, F. Diederich, Metal-Catalyzed Cross-Coupling Reactions, Wiley-VCH, Weinheim, **2004**, 2.

[33] J. Roncali, *Chem Rev.*, **1992**, 92, 711.

[34] N. Gupta, S. Sharma, I. A. Mir, D. Kumar, *J. Sci. Ind. Res.*, 2006, 65, 549.

[35] K.G. Thompson, B.C. Benicewicz, *Polym. Prepr.*, **2000**, 41(2), 1731.

[36] A. Kupniewska, S. Biallozor, *Adv. Eng. Sci. Sect. A*, **2007**, 1, 33.

[37] X. H. Wang, J.L. Lu, Y. Chen, J. Li, F.S. Wang, *Adv. Eng. Sci. Sect. A*, **2007**, 1, 45.

[38] S. Celebi, D. Baran, A. Balan, L. Toppare, *Electrochim. Acta*, **2010**, 55, 2373.

[39] I. Schwendeman, R. Hickman, G. Sonmez, P. Schottland, K. Zong, D. M. Welsh, J. R. Reynolds, *Chem. Mater.*, **2002**, 14, 3118.

[40] G. Sonmez, H. B. Sonmez, C. K. F. Shen, F. Wudl, *Adv. Mater.*, **2004**, 16, 1905.

[41] G. Sonmez, F. Wudl, *J. Mater. Chem.*, **2005**, 15, 20.

[42] R. H. Friend, R. W. Gymer, A. B. Holmes, J.H. Burroughes, R. N. Marks, C. Taliani, D. C. Bradley, D. A. Dos Santos, J. L. Brédas, M. Lögdlund, W.R. Salaneck, *Nature*, **1999**, 397, 121.

[43] X. Liu, L. Chen, H. Liu, G. Yang, P. Zhang, D. Ha, S. Wang , L. Jiang, *NPG Asia Mater.*, **2013**, 5, 63.

[44] R. Wadhwa, C. F. Lagenaur, X. T. Cui, *J. Controlled Release*, **2006**, 110, 531.

[45] A. Ramanavicius, Y. Oztekin, Z. Balevicius, A. Kausaite-Mikstimiene, V. Krikstolaityte, I. Baleviciute, V. Ratautaite, A. Ramanaviciene, *Procedia Eng.*, **2012,** 47, 825.

[46] B. Guoa, L. Glavasa, A.-C. Albertsson, *Prog. Polym Sci.*, **2013**, 38, 1263.

[47] M. Gerard, A. Chaubey, B. D. Malhotra, *Biosens. and Bioelectron.*, **2002**, 17, 345.

[48] T. Vo-Dinh, B. Cullum, *J. Anal. Chem.*, **2000**, 366, 540.

[49] J. Wang, X. J. Zhang, M. Parakash, *Anal. Chim. Acta*, **1999**, 395, 11.

[50] P. Sarkar, I. E. Tothill, S. J. Setford, A. P. Turner, *Analyst*, **1999**, 124, 865.

[51] J. Z. Zhang, B. Li, G. B. Xu, G. J. Cheng, S. J. Dong, *Analyst*, **1999**, 124, 699.

[52] L.C. Jr. Clark, C. Lyons, Ann. *NY Acad. Sci*., **1962**, 102, 29.

[53] D. J. Harrison, R. B. F. Turner, H. P. Baltes, *Anal. Chem.*, **1988**, 60, 2002.

[54] G. G. Guilbault, G. J. Lubrano, *Anal. Chim. Acta*, **1973**, 64 (3), 439.

[55] Y. Shimizu, K. Morita, *Anal. Chem.*, **1990**, 62 (14), 1498 .

[56] Z. Wang, S. Liu, P. Wu, C. Cai, *Anal. Chem.*, **2009**, 81, 1638.

[57] S. F. Peteu, D. Emerson, R. M. Worden, *Biosens. Bioelectron*., **1996**, 11, 1059.

[58] L. Doretti, D. Ferrara, *Biosens. Bioelectron*., **1996**, 11, 365.

[59] J.J. Kulys, G. J. S. Svirmickas, *Anal. Chim. Acta*, **1979**, 109 (1), 55.

[60] J.J. Kulys, G. J. S. Svirmickas, *Anal. Chim. Acta*, **1980**, 117, 115.

[61] A. G. Cass, G. Davis, G. D. Francis, H. A. O. Hill, W. J. Aston, I. J. Higgins, E. V. Plotkin, L. D. L. Scott, A. P. F. Turner, *Anal. Chem.*, **1984**, 56 (4), 667.

[62] N. C. Foulds, C. R. Lowe, *Anal. Chem.*,**1988**, 60, 2473.

[63] Y. Kajiya, R. Tsuda, H. Yoneyama, *J. Electroanal. Chem.*,**1991**, 301 (1 – 2), 155.

[64**]** H. A. O. Hill, G. S. Sanghera, *Mediated Amperometric Enzyme Electrodes in Biosensors: A Practical Approach* (ed. A.E.G. Cass), **1990**, Oxford University Press, London , pp. 19 – 46.

[65] P. N. Bartlett, P. Tebbutt, R. G. Whitaker, *Prog. React. Kinet.*, **1991**, 16 (2), 55.

[66] W. Schuhmann, H. Wohlschläger, R. Lammert, S.-L. Schmidt, U. Löffler, H.-D. Wiemhöfer, W. Göpel, *Sens. Actuators B*, **1990**, B1, 571.

[67] Z. P. Tang, R. F. Louie, J. H. Lee, D. M. Lee, E. E. Miller, G. J. Kost, *Crit. Care Med.*, **2001**, 29 (5), 1062.

[68] R. F. Louie, Z. P. Tang, D. V. Sutton, J. H. Lee, G. J. Kost, *Arc. Pathol. Lab. Med.*, **2000**, 124 (2), 257.

[69] G. J. Kost, T. H. Nguyen, Z. P. Tang, *Arc. Pathol. Lab. Med*, **2000**, 124 (8), 1128.

[70] E. H. Yoo, S. Y. Lee, *Sensors*, **2010**, 10 (5), 4558.

[71] P. N. Bartlett, V. Q. Bradford, R. G. Whitaker, *Talanta*, **1991**, 38 (1), 57.

[72] J. E. Frew, H. A. O. Hill, *E. J. Biochem.*, **1988**, 172, 261.

[73] F. A. Armstrong, *Curr. Opin. Chem. Biol.*, **2005**, 9 (2), 110.

[74] S. R. Betso, M. H. Klapper, L. B. Anderson, *J. Am. Chem. Soc.*, **1972**, 94 (23), 8197.

[75] H. O. Finklea, S. Avery, M. Lynch, T. Furtsch, *Langmuir*, **1987**, 3 (3), 409.

[76] E. Sabatini, I. Rubinstein, R. Maoz, J. Sagiv, *J. Electroanal. Chem.*, **1987**, 219 (1–2), 365.

[77] H. O. Finklea, *Encyclopedia of Analytical Chemistry* (ed. R.A. Meyers), John Wiley & Sons, Inc., New York, **2000**, pp. 10090 – 10115.

[78] J. N. Richardson, S. R. Peck, L. S. Curtin, L. M. Tender, R. H. Terril, M. T. Carter, R. W. Murray, G. K. Rowe, S. E. Creager, *J. Phys. Chem.*, **1995**, 99 (2), 766.

[79] J. J. Gooding, D. B. Hibbert, *TrAC, Trends in Anal. Chem.*, **1999**, 18 (8), 525.

[80] I. Willner, E. Katz, *Ang. Chem. Int. Ed.*, **2000**, 39 (7), 1180.

[81]G. Wittstock, W. Schuhmann, *Anal. Chem*, **1997**, 69 (24), 5059.

[82] T. Wilhelm, G. Wittstock, *Microchim. Acta*, **2000**, 133 (1-4), 1.

[83] T. Wilhelm, G. Wittstock, *Electrochim. Acta*, **2001**, 47 (1-2), 275.

[84] I. Willner, E. Katz, *Ang. Chem. Int. Ed.*, **2000**, 39 (7), 1180.

[85] E. Katz, I. Willner, *Ang. Chem. Int. Ed.*, **2004**, 43 (45), 6042.

[86] C. H. Wong, G. M. Whitesides, *Tetrahedron Org. Chem. Ser.*, **1994**, 12, 41.

[87] J. M. Guisan, *Immobilization of Enzymes and Cells*, **2010**, Human Press. Inc., Totowa, New Jersey, pp. 1-3.

[88] M. Trevan, *Techniques of Immobilization. In: Immobilized Enzymes. An Introduction and Applications in Biotechnology*, **1980,** Wiley, Chichester-New York, pp. 1-9.

[89] K. Buchholz, J. Klein, *Characterization of Immobilized Biocatalysts. In: Methods in Enzymology*, **1987**, Academic Press, London, pp. 3-30.

[90] A. Sassolas, L. J. Blum, B D. Leca-bouvier, *Biotechnol. Adv.*, **2012**, 30, 489.

[91] S. Zhang, G. Wright, Y. Yang, **2000**, *Biosens. Bioelectron.*, 15 (5 – 6), 273.

[92] S. F. White, A. P. F. Turner, *Part 1: Mediated Amperometric Biosensors. In Handbook of Biosensors and Electronic Noses: Medicine, Food and Environment*, **1997**, (ed. E. Kress - Rogers), CRC Press , Boca Raton, FL, USA , pp. 227 – 244.

[93] E. Barendrecht, *J. App. Electrochem.*, **1990**, 20 (2), 175.

[94] P. W. Stoecker, A. M. Yacynych, *Selective Electrode Reviews*, **1990**, 12, 137.

[95]S. Tombelli, M. Mascini, *Comb. Chem. High Throughput Screening*, **2010**, 13 (7), 641.

[96] D. Shan, C. Mousty, S. Cosnier, *Anal. Chem.*, **2004**, 76, 178.

[97] L. Xu, Y. Zhu, L. Tang, X. Yang, C. Li, *Electroanal*., **2007,** 19, 717.

[98] J. Wang, L. Wang, J. Di, Y. Tu, *Talanta*, **2009**, 77, 1454.

[99] F. B. Emre, F. Ekiz, A. Balan, S. Emre, S. Timur, L. Toppare, *Sens. Actuators B*, **2011**, 158, 117.

[100] R. A. Messing, *Adsorption and Inorganic Bridge Formations. In: Methods Enzymology*, **1976**, (Mosbach, K. ed.), Academic Press, New York, pp. 148-169.

[101] J. Woodward *Immobilized Enzymes: Adsorption and Covalent Coupling. In: Immobilized Cells and Enzymes: A Practical Approach,* **1985**, (Woodward J. ed.), IRL, Oxford, UK, pp. 3-7.

[102] S. Borgmann, G. Hartwich, A. Schulte, W. Schuhmann, *Perspectives in Bioanalysis*, **2005**, 1, 599.

[103] Ö. Türkarslan, S. Kıralp Kayahan, L. Toppare, *J. Solid State Electrochem*., **2009,** 13, 657.

[104] P. Bernfeld, J. Wan, *Science*, **1963**, 142, 678.

[105] D. Dinelli, W. Marconi, F. Morisi, *Fiber-Entrapped Enzymes. In: Methods in Enzymology*, (K. Mosbach ed.), **1976**, Academic Press, New York, NY, pp. 227-243.

[106] D. T. Wadiack, R. D. Carbonell, *Biotechnol. Bioeng.*, **17**, 1157.

[107] S. Cosnier, *Electroanalysis*, **2005**, 17, 1701.

[108] S. Kıralp, L. Toppare Y. Yagcı, *Int. J. Biol. Macromol.*, **2003**, 33, 37.

[109] H. B. Yıldız, S. Kıralp, L. Toppare, Y. Yagcı, *Int. J. Biol. Macromol.,* **2005**, 37, 174.

[110] P. Mailley, E. A. Cummmings, S. Mailley, S. Cosnier, B. R. Eggins, E. McAdams, *Bioelectrochemistry*, **2004**, 63, 291.

[111] J. C. Vidal, E. Garcia, J. R. Castillo, *Biosens. Bioelectron.*, **1998**, 13, 371.

[112] S. Reiter, K. Habermuller, W. Schuhmann, *Sens. Actuators B*, **2001**, 79, 150.

[113] W. Trettnak, I. Lionti, M. Mascini, *Electroanalysis*, **1993**, 5, 753.

[114] N. Kizilyar, U. Akbulut, L. Toppare, M. Y. Ozden, Y. Yagci, *Synth. Met.*, **1999**, 104, 45.

[115] A. Ramanavicius, K. Habermuller, E. Csoregi, V. Laurinavicius, W. Schuhmann, *Anal. Chem.*, **1999**, 71, 3581.

[116] B. R. Eggings, *Biosensors an Introduction*, JohhWiley and Sons, **1996**, B.G. Teubner Pub., U.S.A.,

[117] P. W. Carr, L. D. Bowers, *Immobilized Enzymes in Analytical and Clinical Chemistry*, **1980**, John Wiley & Sons, Inc. New York.

[118] B. G. Milagres, G. D. Neto, L. T. Kubato, H. Yamanaka, *Anal. Chim. Acta*, **1997**, 347, 35.

[119] A. Chaubey, M. Gerard, R. Singhal, V. S. Singh, B. D. Malhotra, *Electrochim. Acta*, **2000**, 46, 723.

[120] F. A. Mac Ardle, K. C. Persaud, *Analyst*, **1993**, 118, 419.

[121] P. W. Carr, L. D. Bowers, *Immobilized Enzymes in Analytical and Clinical Chemistry*. **1980**, New York: John Wiley and Sons.

[122] J. Porath, R. Axen, *Immobilization of Enzymes to Agar, Agarose and Sephadex Supports. In: Methods in Enzymology*, (K. Mosbach ed.), **1976**, Academic Press, New York, NY, pp. 19-45.

[123] M. Wilchek, T. Miron, *Anal. Biochem.*, **1982**, 126, 433.

[124] J. Drobnick, W. Labsky, H. Kudlvasrova, V. Saudek, F. Svec, *Biotechnol. Bioeng.*, **1982**, 24, 487.

[125] W. H. Scouten, *A Surway of Enzyme Coupling Techniques. In : Methods in Enzymology*, **1987**, (K. Mosbach ed.), Academic Press, london, pp. 30-65.

[126] C. A. White, J. F. Kennedy, *Enzymes Microb. Technol.*, **1980**, 2, 82.

[127] R. Solna, P. Skladal, *Electroanal.*, **2005**, 17, 2137.

[128] X. Yang, L. Hua, H. Gong, S. Ngin Tan, *Anal. Chim. Acta*, **2003,** 478, 67.

[129] R. F. Tylor, *Commercially Avaliable Supports for Protein Immobilization. In: Protein Immobilization. Fundamentals and Applications.*, **1991**, (R. F. Tylor ed.), Marcel Dekker, New York, NY, pp. 139.

[130] L. Xia, Z, Wei, M, Wan, *J. Colloid Interf. Sci*, **2010,** 341, 1.

[131] V. Leskovac, S. Trivic, G. Wohlfahrt, J. Kandra, D. Pericin, *Int. J. Biochem. Cell B.*, **2005,** 37,731.

[132] D. Pan, J. Chen, S. Yao, W. Tao, L. Nie, *Anal. Sci.*, **2005**, 21, 367.

[133] F. Qu, M. Yang, J. Jiang, G. Shen, R. Yu, *Anal. Biochem.*, **2005**, 344, 108.

[134] C. Vedrine, S. Fabiano, C. Tran-Minh, *Talanta,* **2003**, 59, 535.

[135] A. Curulli, F. Valentini, S. Orlanducci, M.L. Terranova, G. Palleschi, *Biosens. Bioelectron.*, 2004, 20, 1223.

[136] H. Cai, Y. Xu, P.-G. He, Y.-Z. Fang, *Electroanalysis*, **2003**, 15, 1864.

[137] S. Singh, P.R. Solanki, M.K. Pandey, B.D. Malhotra, *Sens. Actuators B*, **2006**,

115, 534.

[138] O. Ngamna, A. Morrin, S.E. Moulton, A.J. Killrad, M.R. Smyth, G.G. Wallace, *Synth. Met.*, **2005**, 153, 185.

[139] M. Trojanowicz, T. K. V. Krawczyk, *Microchim. Acta*, **1995**, 121 (1-4), 167.

[140] T. Ikeda, S. Miyaoka, S. Ozawa, F. Matsushita, D. Kobayashi, M. Senda, *Ana.l Sci.*, **1991**, 7, 1443.

[141] K. Habermüller, M. Mosbach, W. Schuhmann, *Fresenius' J. Anal. Chem.*, **2000**, 366 (6-7), 560.

[142] S. Cosnier, *Biosens. Bioelectron*., **1999**, 14, 443.

[143] M. Holzinger, L. Bouffier, R. Villalonga, S. Cosnier, *Biosens. Bioelectron*., **2009**, 24, 1134.

[144] S. Cosnier, *Anal. Bioanal. Chem.*, **2003**, 377, 139.

[145] S. Cosnier, *Anal. Lett.*, **2007**, 22, 1260.

[146] K. Grennan, A. J. Killard, M. R. Smith, *Electroanalysis*, **2005**, 17, 1360.

[147] D. Shan, C. Mousty, S. Cosnier, *Anal. Chem.*, **2004**, 76, 178.

[148] E. S. Mclamore, A. Diggs, P. Calvo Marzal, J. Shi, J. J. Blakeslee, W. A. Peer, A. S. Murphy, D. M. Porterfield, *The Plant Journal*, **2010**, 63 (6), 1004.

[149] E. S. Mclamore, J. Shi, D. Jaroch, J. C. Claussen, A. Uchida, Y. Jiang, W. Zhang, S. S. Donkin, M. K. Banks, K. K. Buhmann, D. Teegarden, J. L. Rickus, D. M. Poterfield, *Biosens. Bioelectron.*, **2011**, 26 (5), 2237.

[150] J. Shi, E. S. Mclamore, D. Jaroch, J. C. Claussen, J. L. Rickus, D. M. Poterfield, *Anal. Biochem.*, **2010**, 411, 185.

[151] S. Demirci, F. B. Emre, F. Ekiz, F. Oğuzkaya, S. Timur, C. Tanyeli, L. Toppare, *Analyst*, **2012**, 137, 4254.

[152] S. D. Uzun, N. A. Unlu, M. Sendur, F. E. Kanik, S. Timur, L. Toppare, *Colloids Surf. B*, **2013**, 112, 74.

[153] F. Ekiz, F. Oğuzkaya, M. Akin, S. Timur, C. Tanyeli and L. Toppare, *J. Mater. Chem.*, 2011, 21, 12337–12343.

[154] H. Akpınar, A. Balan, D. Baran, E.K. Unver, L. Toppare, *Polymer*, **2010**, 51, 6123.

[155] K. Zhu, V.N. Vukotic, S.J. Loeb, *Angew. Chem. Int. Ed.*, **2012**, 51, 2168.

[156] S.S. Zhu, T.M. Swager, *J. Am. Chem. Soc.*, **1997**, 119, 12568.

[157] D. Kozanoglu, D. H. Apaydin, A. Cirpan, E. N. Esenturk, *Org. Electron.*, **2013**, 14, 1720.

[158] F. Liao, X.-Y. Zhu, Y.-M. Wang, Y.-P. Zuo, *J. Biochem. Biophys. Methods*, **2005**, 62, 13.

[159] P. Hapiot, P. Audebert, K. Monnier, J.- Pernautt, P. Garcia, *Chem. Mater.*, **1994**, 6, 1549.

[160] P. Audebert, J. Catel, G. Coustumer, V. Duchenet, P. Hapiot, *J. Phys. Chem.*, **1995**, 99, 11923.

[161] L. Betancor, F. Lopez-Gallego, A. Hidalgo, N. Alonso-Morales, D. Gellamora-Ortiz and J. M. Guisan, *J. Biotechnol.*, **2006**, 121, 284.

[162] F. Lopez-Gallego, L. Betancor, A. Hidalgo, N. Alonso, G. Fernandez-Lorente, J. M. Guisan and R. Fernandez-Lafuente, *Enzyme Microb. Technol.*, **2005**, 37, 750.

[163] D. Jung, M. Paradiso, M. Hartmann, *J. Mater. Sci.*, **2009**, 44, 6747.

[164] L. A. R. Tylor, T. L. Martin, P. Wagner, *Langmuir*, **2001**, 17, 7313.

[165] N. Li, X. Wei, Z. Mei, X. Xiong, S. Chen, M. Ye, S. Ding, *Carbohydr. Res.*, **2011**, 346, 1721.

[166] M. Akin, M. Yuksel, C. Geyik, D. Odaci, A. Bluma, T. Höpfner, S. Beutel, T. Scheper and S. Timur, *Biotechnol. Prog.*, **2009**, 26, 896.

[167] D.Pan, J.Chen, S.Yao,W.TaoandL.Nie, *Anal. Sci.*, **2005**, 21, 367.

[168] J.-C. Vidal, E. Garcia and J. R. Castillo, *Biosens. Bioelectron.*, **1998**, 13, 371.

[169] X. Pang, P. Imine, I. A Zhitomirsky and A. Adronov, *J. Mater. Chem.*, **2012**, 22, 9147.

[170] J. Manso, M. L. Mena, P. Y. Sedeno and J. Pingarron, *J. Electroanal. Chem.*, **2007**, 603, 1.

[171] Y. Xian, Y. Hu, F. Liu, Y. Xian, H. Wang and L. Jin, *Biosens. Bioelectron.*, **2006**, 21, 1996.

[172] M. Yuksel, M. Akin, C. Geyik, D. Odaci Demirkol, C. Ozdemir, A. Bluma, T. Höpfner, S. Beutel, S. Timur, T. Scheper, *Biotechnol. Prog.*, **2011**, 27, 530.

[173] A.C. Ozercaglayan, M. Sendur, N. Akbasoglu, D.H. Apaydin, A. Cirpan, L. Toppare, *Electrochim. Acta*, **2012,** 67, 224.

[174] G. Sonmez, H. Meng, Q. Zhang, F. Wudl, *Adv. Funct. Mater.*, **2003**, 13, 726.

[175] S. Cosnier, *Appl. Biochem. Biotechnol.*, **2000**, 89, 127.

[176] M. J. Sims, N. V. Rees, E. J. F. Dickinson, R. G. Campton, *Sens. Actuators B*, **2010**, 144, 153.

[177] M.D. Gouda, M.A. Kumar, M.S. Thakur, N.G. Karanth, *Biosens. Bioelectron.*, **2002**, 17, 503.

[178] V. Singh, M. Zharnikov, A. Gulino, T. Gupta, *J. Mater. Chem.*, **2011**, 21, 10602.

[179] Y. Wang, Z. Shi, J. Fang, H. Xu, J. Yin,, *Carbon*, **2011**, 49, 1199.

[180] W. Ai, W. Zhou, Z. Du, Y. Du, H. Zhang, X. Jia, L. Xie, M. Yi, T. Yu, W. Huang, *J. Mat. Chem.*, **2012**, 22, 23439.

[181] M.Y. Hua, H.C. Chen, R.Y. Tsai, Y.C. Lin, L. Wang, *Anal. Chim. Acta*, **2011**, 693, 114.

[182] X. Gong, H. J. Griesser, *Plasmas Polym.*, **1997**, 2 (4), 261.

[183] K. S. Lau, J. Bico, K. B. K. Teo, M. Chhowalla, G. A. J. Amaratunga, W. I. Milne, G. H. McKinley, K. K. Gleason, *Nano Lett*., **2003**, 3 (12), 1701.

[184] Y. Mao, C. L. Chen, Y. Zhang, *Appl Phys A*, **2013**, 111, 757.

[185] M. Pavese, S. Musso, S. Bianco, M. Giorcelli, N. Pugno, *J. Phys.: Condens. Matter*, **2008**, 20, 474206.

[186] L. Xu, Z. Fang, P. Song, M. Peng, *Appl. Surf. Sci.*, **2010**, 256, 6447.

[187] E. Pajootan, M. Arami, *Electrochim. Acta*, **2013**, 112, 505.

[188] M. Rahmat, P. Hubert, *Composites Sci. Technol.*, **2011**, 72, 72.

[189] P.J. van Zwol, G. Palasantzas, J. Th. M. De Hosson, *Physical Rev.*, **2008**, 78, 31606.

[190] K. L. Osborne, *"Temperature Dependence of The Contact Angle of Waater on Graphite, Silicon and Gold"*, Master Thesis, Worcester Polytechnic Institute, April **2009**, 57-59.

[191] B. E. P. Swoboda, V. Massey, *J. Biol. Chem.*, **1965**, 240, 2209.

[192] H. Xue, Z. Shen,Y. Li, *Synth. Met.*, **2001**,124, 345.

[193] H. P. Peng, R. P. Liang, L. Zhang, J. D. Qui, *Biosens. Bioelectron.*, **2013**, 42, 293.

[194] B. Haghighi, M. A. Tabrizi, *Colloids Surf. B*, **2013**, 103, 566.

[195] M. Karadag, C. Geyik, D. O. Demirkol, F. N. Ertas, S. Timur, *Mat. Sci. Eng. C*, **2013**, 33, 634.

[196] A. Curulli, F. Valentini, S. Orlanduci, M. L. Terranova, G. Palleschi, *Biosens. Bioelectron.*, **2004**, 20, 1223.

[197] S. Brahim, D. Narinesingh, A. G. Elie, *Biosens. Bioelectron.*, **2002**, 17, 53.

APPENDIX A

NMR DATA

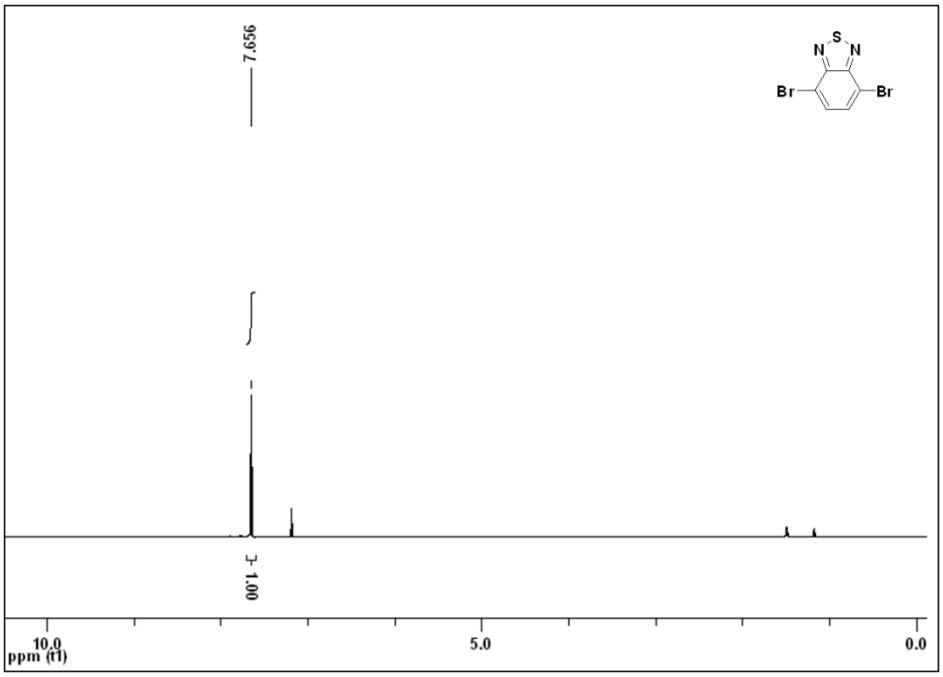

Figure A.1 ^{1}H-NMR spectrum of 4,7-dibromobenzothiadiazole **(4)**

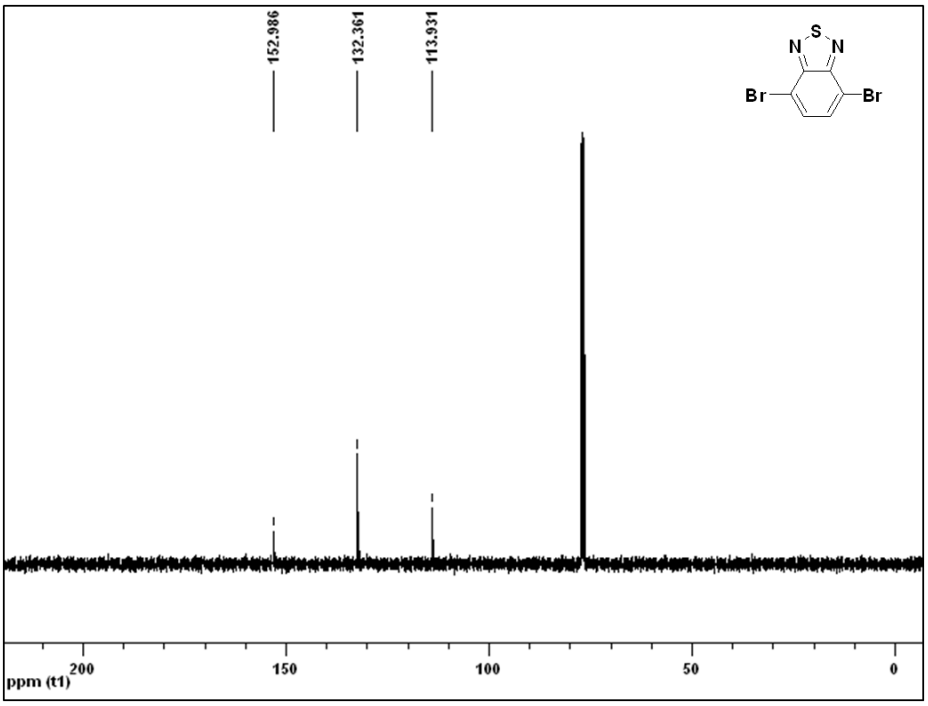

Figure A.2 ^{13}C-NMR spectrum of 4,7-dibromobenzothiadiazole **(4)**

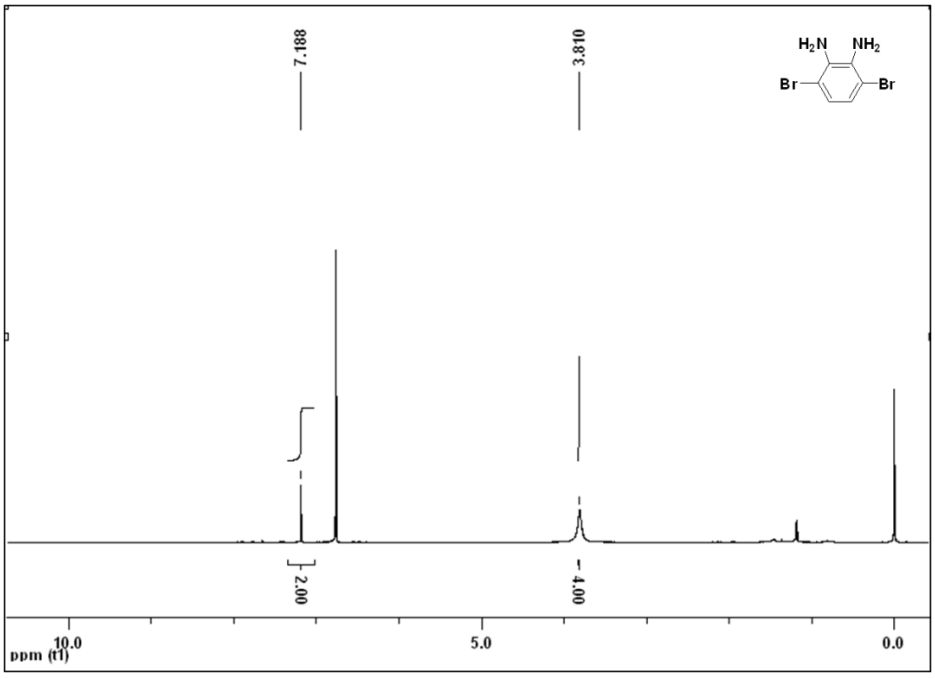

Figure A.3 ^{1}H-NMR spectrum of 3,6-dibromo-1,2-phenylenediamine **(5)**

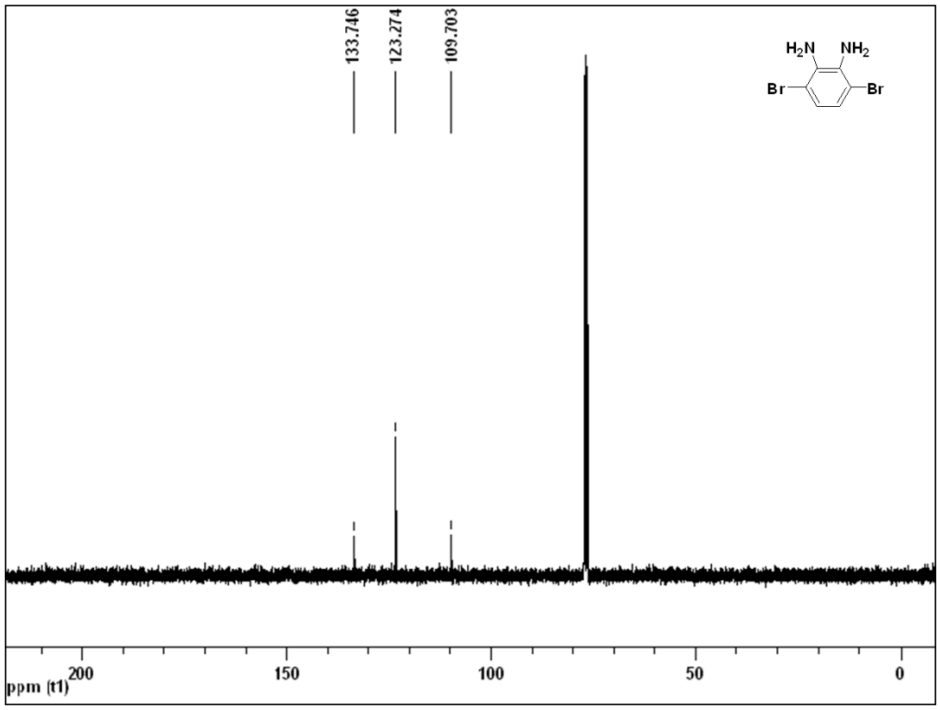

Figure A.4 ^{13}C-NMR spectrum of 3,6-dibromo-1,2-phenylenediamine **(5)**

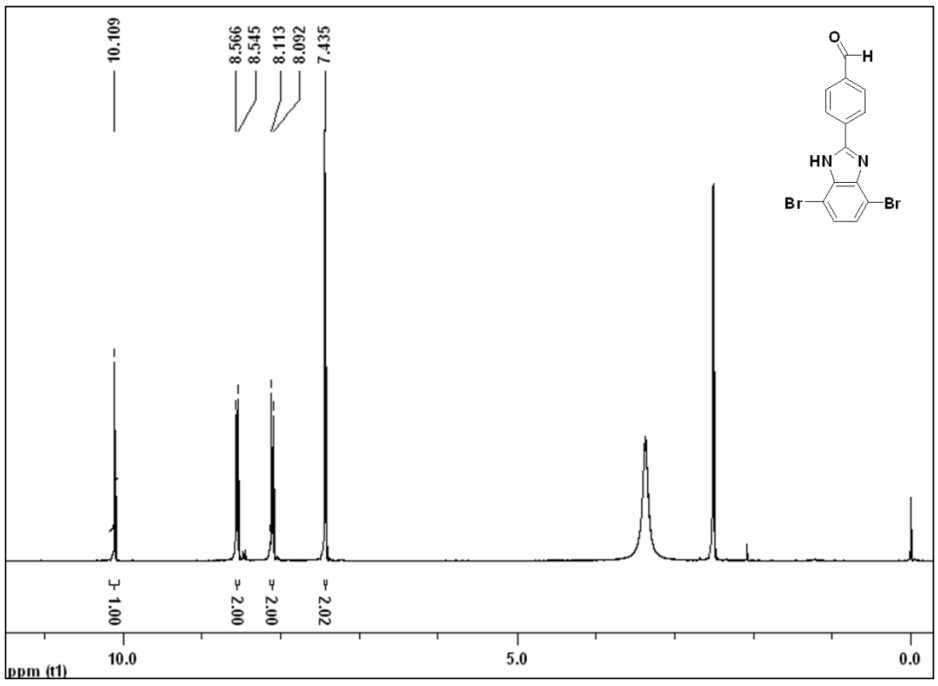

Figure A.5 ^{1}H-NMR spectrum of 4-(4,7-dibromo-1*H*-benzo[*d*]imidazol-2-yl)benzaldehyde **(6)**

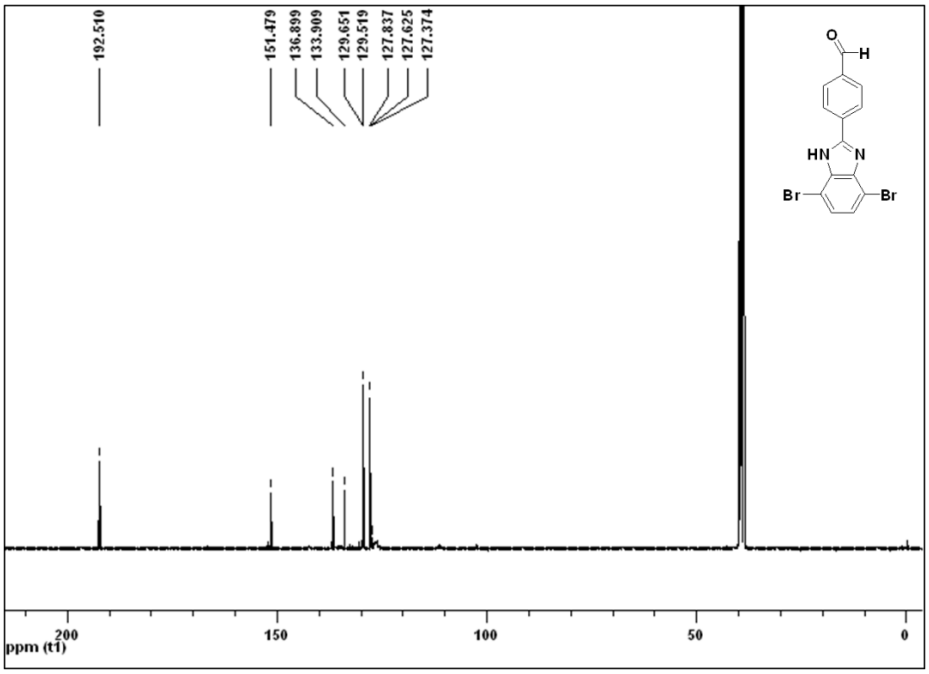

Figure A.6 ^{13}C-NMR spectrum of 4-(4,7-dibromo-1*H*-benzo[*d*]imidazol -2-yl)benzaldehyde **(6)**

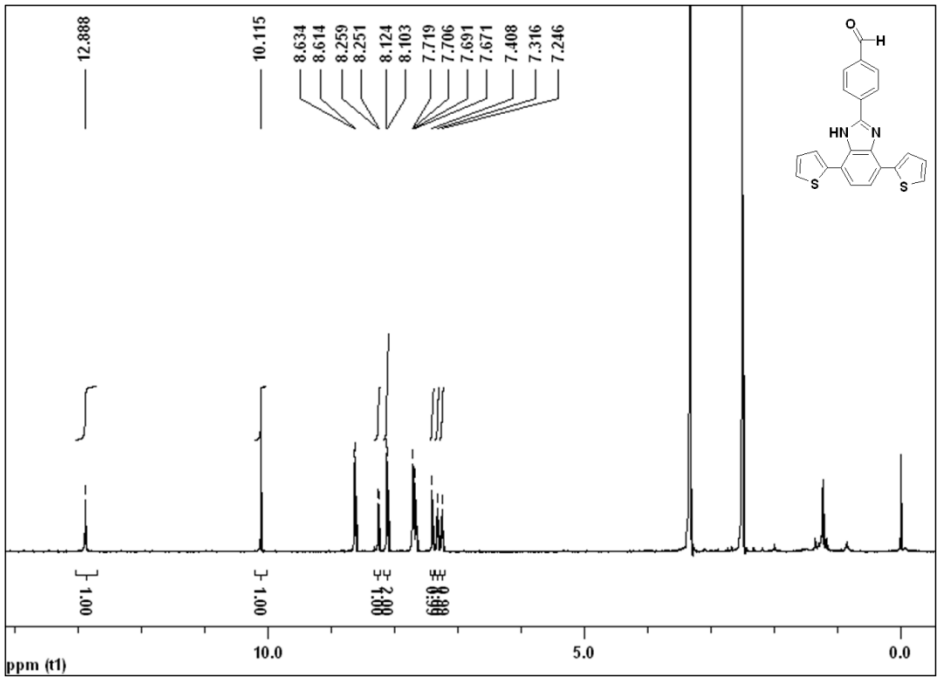

Figure A.7 ^{1}H-NMR spectrum of 4-(4,7-di(thiophen-2-yl)-1*H*-benzo[*d*]imidazol-2-yl)benzaldehyde **(BIBA)**

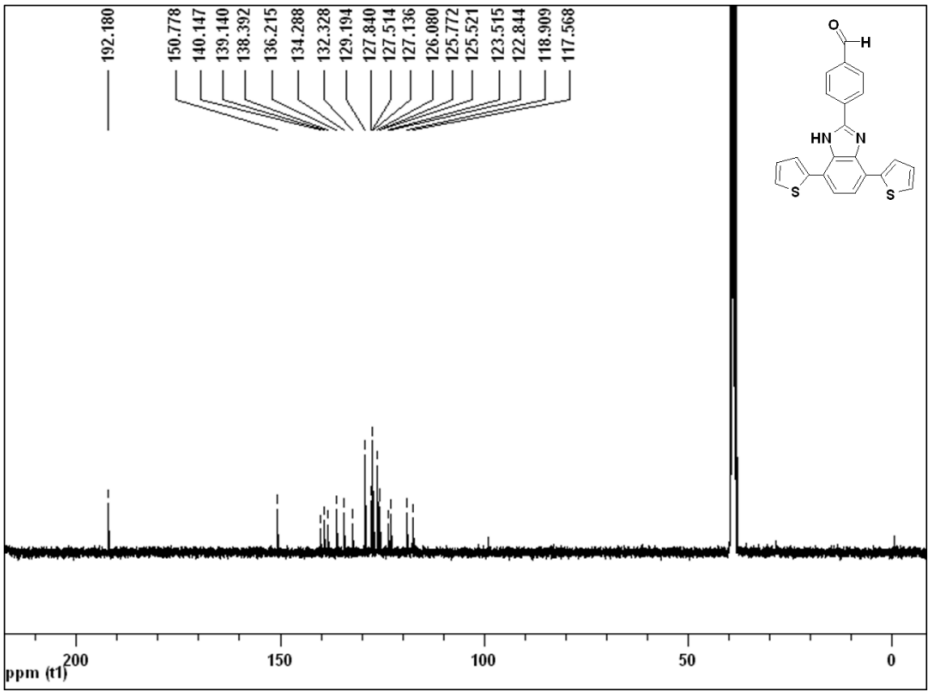

Figure A.8 ^{13}C-NMR spectrum of 4-(4,7-di(thiophen-2-yl)-1*H*-benzo[*d*]imidazol-2-yl)benzaldehyde **(BIBA)**

CURRICULUM VITAE

PERSONAL INFORMATION

Surname, Name: Demirci Uzun, Sema

Nationality: Turkish

Date and Place of Birth: 13 May 1982, İzmir

email: demircisema@gmail.com

EDUCATION

Degree	Institution	Year of Graduation
MS	METU Chemistry Department	2009
MS	Dokuz Eylül University Science & Mathematics Education	2006
BS	Ege University Chemistry Department	2004

PUBLICATIONS

1. Stereoselective synthesis of optically active dihydrofurans and dihydropyrans via ring closes metathesis reaction. M. Çayir, **S. Demirci**, S. Sezer, C. Tanyeli, *Tetrahedron: Asymmetry*, 2011, 22, 1161-1168.

2. Functionalization of poly-SNS-anchored carboxylic acid with Lys and PAMAM: surface modifications for biomolecule immobilization/stabilization

and bio-sensing applications. **S. Demirci**, F. B. Emre, F. Ekiz, F. Oğuzkaya, S. Timur, C. Tanyeli, L. Toppare, *Analyst*, 2012,137, 4254-4261.

3. Synthesis of a novel benzimidazole containing polymer and its biosensor applications. **S. D. Uzun**, N. A. Ünlü, M. Şendur, F. E. Kanik, S. Timur, L. Toppare. *Colloids and Surfaces B: Biointerfaces*, 2013, 112, 74-80.

4. Development of an efficient immobilization matrix based on a conducting polymer and functionalized multiwall carbon nanotubes: synthesis and its application to ethanol biosensors. S. Söylemez, F. E. Kanik, **S. D. Uzun**, S. O. Hacioglu, L. Toppare, *J. Mater. Chem.* B, 2014, 2, 511-521.